

Medizinische Fakultät
der
Universität Duisburg-Essen

Aus dem Zentrum für Kinder- und Jugendmedizin
Klinik für Kinderheilkunde III

YB-1: Functional Analysis of a Potential Serum Marker for Neuroblastoma

Inaugural-Dissertation
zur
Erlangung des Doktorgrades der Naturwissenschaften in der Medizin
durch die Medizinische Fakultät
der Universität Duisburg-Essen

Vorgelegt von
Stephanie Christine Degen
aus Karlsruhe
2012

Dekan: Herr Univ.-Prof. Dr. med. J. Buer
1. Gutachter: Frau Univ.-Prof. Dr. med. A. Eggert
2. Gutachter: Herr Priv.-Doz. Dr. rer. nat. L. Klein-Hitpass

Tag der mündlichen Prüfung: 11. Oktober 2012

Table of Contents

1.	Introduction	5
1.1.	Neuroblastoma	5
1.1.1.	History and Epidemiology	5
1.1.2.	Clinical Presentation and Diagnosis	5
1.1.3.	Histopathology and Staging	7
1.1.4.	Biological and Genetic Factors	8
1.1.5.	Risk Stratification and Therapy	10
1.1.6.	Relapse and Resistance in NB	12
1.2.	DNA Repair Mechanisms and Development of Resistance	13
1.3.	The Y-box Binding Protein 1 (YB-1)	16
1.3.1.	Structure of YB-1	16
1.3.2.	Functions of YB-1	17
1.3.3.	YB-1 and Cancer	19
1.3.4.	YB-1, Cytostatics and Resistance	20
1.3.5.	YB-1 and Repair	21
1.3.6.	YB-1 and Apoptosis	22
1.3.7.	YB-1 and MYCN	23
1.3.8.	YB-1 Secretion	23
1.4.	Project Design and Aim	24
2.	Materials	25
2.1.	Chemicals	25
2.2.	Plasticware	28
2.3.	Technical Equipment	29
3.	Methods	30
3.1.	Cell Culture	30
3.2.	MTT Cell Viability Assay	31
3.3.	RNA Extraction and cDNA Synthesis	32
3.4.	Polymerase Chain Reaction	32
3.5.	Separation and Detection of Nucleic Acids	33
3.6.	Real-time PCR	33
3.7.	Transient Knockdown of YB-1 by RNAi	34
3.8.	Preparation of Protein Lysates from Cultured Cells	35
3.9.	Preparation of Medium Conditioned by Neuroblastoma Cell Cultures	35
3.10.	Crosslinking of Proteins in Conditioned Medium	36
3.11.	Western Blotting	36
3.12.	Co- Immunoprecipitation	37
3.13.	YB- 1 Reverse ELISA	38
3.14.	Quantification of Double-Strand Breaks via gamma-H2AX	38

3.15.	Immunocytochemistry	39
3.16.	Adduct Ak	40
3.17.	ChIP-Chip Analysis	41
3.18.	Acquisition of Serum samples	42
3.19.	Fetal Brain Array	42
3.20.	Statistical Analysis	43
4	Results	44
4.1.	Using Autoantibodies in Neuroblastoma Patient Serum to Identify Tumor Markers	44
4.1.1.	Autoantibodies were detected in NB patient sera via a protein array	44
4.1.2.	The GPI protein is present in conditioned media of neuroblastoma cells	46
4.1.3.	YB-1 is expressed in neuroblastoma cells	48
4.1.4.	Use of a reverse ELISA to detect and quantify YB-1 autoantibodies in patient serum	49
4.1.5.	YB-1 is present in medium conditioned by NB cell lines	55
4.2.	Association of YB-1 with known Neuroblastoma Marker Proteins	56
4.2.1.	YB-1 is associated with TrkA expression in the SY5Y cell line	56
4.2.2.	MYCN activates expression of YB-1 and promoter binding analysis confirms that both MYCN and c-Myc bind can the YB-1 promoter and activate transcription	57
4.3.	Influence of YB1 on Proliferation	60
4.3.1.	Downregulation of YB-1 reduces cell viability	60
4.4.	Association of YB- 1 with Repair and the Development of Resistance in NB	63
4.4.1.	YB-1 is involved in the repair of double-strand breaks in NB	63
4.4.2.	The effect of YB-1 downregulation on DNA adduct formation	64
4.4.3.	YB-1 localization in response to cisplatin	65
4.4.4.	Cisplatin treatment increases YB-1 expression	66
4.4.5.	YB-1 binds to various repair proteins	67
5.	Discussion	69
6.	Summary	80
7.	References	81
8.	Appendix	94
8.1.	List of Abbreviations	94
8.2.	List of Figures	95
8.3.	List of Tables	95
8.4.	Supplementary Data for Binding Analysis	96
9.	Acknowledgements	98
10.	Curriculum vitae	99

1. INTRODUCTION

1.1. NEUROBLASTOMA

1.1.1. HISTORY AND EPIDEMIOLOGY

Much research has been done on neuroblastoma (NB) since its discovery about 150 years ago. NB was originally described by Virchow in 1864, but thought it to be a glioma at that time (Virchow 1864-65). NB was linked to the sympathetic ganglia in 1891, and Herxheimer was able to stain NB fibrils with special neural silver stain in 1914, providing further evidence for its origin (Marchand 1891; Herxheimer 1914). Current thinking is that NB derives from primitive sympathetic neural precursor cells. This is based on the localization of NB in the adrenal gland or along the spinal cord in association with sympathetic ganglia and the neuroblastic phenotype of NB (Hoehner et al. 1996).

NB is the second most common childhood cancer after leukemia in Germany, and is the most common solid extracranial pediatric tumor with an incidence of 1.1 cases in 100,000 children under 15 years of age (Gadner H. 2005; Krebsgesellschaft 2010). The median age at diagnosis is 18 months; with approximately 40 % of patients diagnosed by 1 year of age, 75 % by 4 years and 98 % by 10 years of age (Goodman 1999; Brodeur GM 2006).

1.1.2. CLINICAL PRESENTATION AND DIAGNOSIS

NB has been called the “great mimicker” because it can appear in many different variations, related to the site of the primary tumor, metastatic disease and metabolic tumor by-products. While children with localized disease are usually asymptomatic, patients with disseminated NB are very sick and may have systemic manifestations, including unexplained fevers, weight loss, anorexia, failure to thrive, general malaise, irritability and bone pain. Tumors can develop anywhere along the sympathetic nervous system, but most (65 %) primary tumors occur within the abdomen, with at least half of these arising in the adrenal medulla. Other common sites include the neck, chest and pelvis (Brodeur GM 2006). Around 40 % of patients show a localized stage of disease. These tumors are often clinically asymptomatic and often incidentally diagnosed in routine screenings such as ultrasound diagnosis or chest radiographs. Cervical masses are sometimes associated with a Horner syndrome, which can be the first and/or only manifestation (Mahoney et al. 2006). Elevated blood pressure due to excess catecholamine concentrations occurs in some, but not all, patients

(Wargalla-Plate et al. 1995). About half of all NB patients are diagnosed with metastatic disease. NB has a tendency to metastasize to the orbita bone, which leads to periorbital ecchymoses (raccoon eyes) or proptosis, as classical signs for disseminated NB. Metastasis to bone and bone marrow occurs and can result in bone pain, limping or irritability. Bone marrow replacement and symptoms of marrow failure can also occur (Quinn et al. 1979). Taken together, NB presents itself in many heterogeneous ways, creating a diagnostic challenge.

Laboratory diagnostics are powerful tools to detect NB and provide further evidence for NB if it is suspected. Patients can present with elevated erythrocyte sedimentation rates, normochromic anemia or unspecific elevation of lactate dehydrogenase or ferritin levels in serum. Higher levels of these proteins may indicate rapid tumor growth and/or large tumor burden, and are rather used for follow-up and risk stratification than for diagnosis (Hann et al. 1985). Specific tumor markers for NB are elevated levels of catecholamine metabolites, such homovanillic acid and vanillylmandelic acid, in the urine. Large NB screening programs in the 1980s were based on detection of these tumor-derived catecholamines in spot urine samples, since it was believed that aggressive and biologically unfavorable disease stages evolved from more localized, biologically favorable tumors in infants. Since infants with NB were known to have a better outcome than children over 1 year of age at diagnosis, early detection was hypothesized to be capable of improving survival of NB patients. Studies in Japan showed that NB was detectable via urine screening at 6 months of age, and early results suggested that preclinical detection led to improved survival (Sawada et al. 1984). However, subsequent reports from mass screening programs in Canada and Germany showed that screening did not reduce mortality. The incidence of NB increased in both of the screened populations, but almost all detected tumors showed favorable biological features and lower stages of disease (Schilling et al. 2002; Woods et al. 2002), indicating that the increased prevalence and incidence was due to NB detection in patients, whose tumors would have regressed or matured without developing symptomatic disease and without requiring therapeutic intervention (Brodeur et al. 2001). The cost of screening and the unchanged mortality rates argued against the usefulness of mass screening for NB in infants. Other serum markers of NB exist, such as neuron specific enolase (NSE), a cytoplasmic protein associated with neural cells. Survival was shown to be worse for patients with advanced disease and high serum NSE (Zeltzer et al. 1986). The GD2 protein is a disialoganglioside present on the surface of most NB cells, and increased levels have been detected in the plasma of NB patients (Mujoo et al. 1987). Gangliosides that are shed by tumor cells might be important in accelerating tumor progression. Since laboratory diagnostics are non-invasive, easy to perform and relatively inexpensive, they are not only important for NB diagnosis, but would be useful for stratification of high stage disease as novel markers become available.

Once NB is diagnosed, the staging and follow-up routine require other diagnostic tools. Ultrasound, MRI and meta-iodobenzylguanidine scintigraphy are used to define dissemination of the primary tumor and lymph node status. Bone marrow aspiration at four sites is used to exclude bone marrow infiltration, and spinal fluid is analyzed for tumor cells as well. If metastases are suspected, technetium imaging can be used (Leitlinie Hämatologie 2008). The choice of diagnostic tools depends on the stage of disease and available equipment, with the goal of achieving a complete picture of the current status of disease.

1.1.3. HISTOPATHOLOGY AND STAGING

Due to the heterogeneous presentation of NB, a good staging schema is important to prevent over- or undertreatment. However, including all features in one classification schema is a challenge. In 1984, Shimada and colleagues proposed a classification schema, relating the histopathological features of the tumor to its clinical behavior. Tumors are classified as favorable or unfavorable, depending on the degree of neuroblast differentiation, Schwannian stroma content, mitosis-karyorrhexis index (MKI) and age at diagnosis (Shimada et al. 1984). In subsequent studies, the Shimada system was then modified into the International Neuroblastoma Pathology Classification (INPC) which also takes the age of the patient into consideration (Shimada et al. 1999), and is now internationally recognized. The most important clinical variables in predicting patient outcome are the stage of disease as defined by the International Neuroblastoma Staging System (INSS). The INSS was developed by Evans in 1971 and was modified in 1993 by Brodeur (Evans et al. 1971; Brodeur et al. 1993). Five stages of disease are described by the INSS. Stage 1 defines a localized tumor, confined to the area of origin which is macroscopically resectable and only infiltrates lymph nodes in direct proximity. Stage 2a describes a unilateral tumor with incomplete gross resection where identifiable ipsilateral and contralateral lymph nodes are free of tumor material. Stage 2b describes a unilateral tumor that could be completely or incompletely resected, where ipsilateral lymph nodes are positive for tumor but contralateral lymph nodes are free of tumor material. Stage 3 tumors infiltrate across the midline with or without regional lymph node involvement, are unilateral tumors with contralateral lymph node involvement or are midline tumors with bilateral lymph node involvement. Stage 4 describes a dissemination of the tumor to distant lymph nodes, bone marrow, bone, liver, or other organs except as defined by Stage 4S, which is limited to children under 1 year of age by definition and makes up about 5 % of NB cases. Patients show small localized primary tumors, similar to stages 1 or 2, but have metastases in the liver, skin or bone marrow, but never in the bone. A unique feature of this stage is that the tumor almost always spontaneously regresses or differentiates. Survival of patients with 4S NB is, therefore, up to 90 % (Nickerson et al. 2000). Different NB stages are treated with different protocols, making correct

staging essential. This diversity in the disease and its implication for patient treatment has spawned much research into biological and genetic factors of the tumors that could be diagnostically or prognostically helpful.

1.1.4. BIOLOGICAL AND GENETIC FACTORS

1.1.4.1. Genomics of neuroblastoma

Although NB usually occurs sporadically, 1 % to 2 % of patients have a family history of the disease. Familial neuroblastoma is inherited in an autosomal-dominant Mendelian fashion with incomplete penetrance. Affected children from these families differ from those with sporadic disease. They are often diagnosed at an earlier age and/or have multiple primary tumors (Maris et al. 1999), supporting the presence of germline mutations in one allele of tumor suppressor genes as a cause for familial NB. Knudson and Strong proposed that a new germinal mutation in a predisposition gene may account for the initiation of tumorigenesis in up to 22 % of nonfamilial cases, and that this predisposition follows an autosomal-dominant pattern of inheritance (Knudson et al. 1972). Various genetic alterations affecting NB are known, the most important of which are described below.

MYCN amplification

The genetic aberration most consistently associated with poor outcome in NB is the genomic amplification of *MYCN*. It was initially observed that some NBs showed double-minute chromatin bodies or homogeneously staining regions (HSRs), both cytogenetic manifestations of gene amplification. Identification of a novel MYC-related oncogene, *MYCN*, in the amplified region was published in 1983 (Schwab et al. 1983). *MYCN* is amplified in approximately 20 % of primary tumors, and is strongly correlated with advanced disease stage and treatment failure. Even in infants and patients with lower disease stages is *MYCN* amplification associated with poor outcome (Brodeur et al. 1984). *MYCN* is a member of the MYC family, and encodes a nuclear protein with a basic helix-loop-helix (bHLH) domain, which is normally expressed during neurogenesis and required for organogenesis (Knoepfler et al. 2002). MYC oncoproteins are transcription factors that can cause deregulation of growth and proliferation when overexpressed. Reasons for the association of *MYCN* amplification with a more aggressive phenotype are still unclear, but the *MYCN* protein is also overexpressed in *MYCN*-amplified tumors. *MYCN* forms a heterodimer with the MAX protein, and this protein complex functions as a transcriptional activator. In the absence of *MYCN*, MAX forms a homodimer that is then transcriptionally repressive. Some *MYCN* targets include *ODC*, *MCM7* and *MRP1*, and activation of these genes leads to progression through the G1 phase of the cell cycle. Although the *MYCN* protein has a short half-life, the extremely high

steady-state levels in amplified tumor cells probably ensure that cells proceed through the cell cycle and do not enter G0 (Brodeur 2003). Due to the strong association with poor outcome, identification of *MYCN* amplification in a tumor of any stage classifies the patient as high-risk.

1p deletion

Deletions of the short arm of chromosome 1 (1p) are present in 25–35 % of neuroblastomas. These deletions correlate with *MYCN* amplification and also with advanced disease stage. The independent prognostic significance of 1p loss of heterozygosity (LOH) has been controversial, but Maris et al. showed that allelic loss at 1p36 predicts for disease progression but not decreased overall survival probability (Maris et al. 2000).

11q deletion

Allelic loss of 11q is detected in 35–45 % of primary NB, making it the most common deletion in NB, to date. *MYCN*-amplified tumors rarely have 11q deletions, but 11q deletions are strongly associated with 3p deletions, another high-risk feature (Plantaz et al. 2001).

Trisomy of 17q

Another karyotypic abnormality in NBs, is a gain of 1–3 additional copies of 17q. This occurs in more than half of all NBs, and is often a result of unbalanced translocation with chromosome 1 or 11. Trisomy of 17q has also been correlated with a more aggressive disease phenotype (Bown et al. 1999).

DNA index

Although most tumors have karyotypes in the diploid range, tumors from patients with lower disease stages are often hyperdiploid or near-triploid. Kaneko et al., showed the association of good patient prognosis with near-triploid tumors in infants with untreated NB (Kaneko et al. 1987). Ploidy is less prognostically significant in patients over 2 years of age. This is probably because hyperdiploid and near-triploid tumors from infants generally have whole chromosome gains without structural rearrangements, whereas these tumors in older patients have several additional structural rearrangements (Look et al. 1991).

1.1.4.2. Biological factors involved in molecular pathogenesis of neuroblastoma

Neurotrophin receptors and their ligands are important regulators of survival, growth, and differentiation of neural cells. Receptors are encoded by the *NTRK1*, *NTRK2*, and *NTRK3* genes for TrkA, TrkB, and TrkC, respectively, which are activated by the ligands NGF, BDNF and neurotrophin-3. Biologically favorable NBs express high levels of TrkA, and high *NTRK1*

expression strongly correlates with patient survival and younger age, while aggressive, MYCN-amplified NBs express little or no *NTRK1* (Nakagawara et al. 1993). TrkA also promotes growth inhibition and neuronal differentiation when expressed in the human NB cell line, SH-SY5Y, which has a single copy of *MYCN* (Eggert et al. 2000). TrkB and BDNF expression are associated with NBs that show MYCN amplification and are classified as high-risk tumors (Nakagawara et al. 1994). A hypothetical model based on these observations was devised for the genetic origin of neuroblastoma (Fig.1).

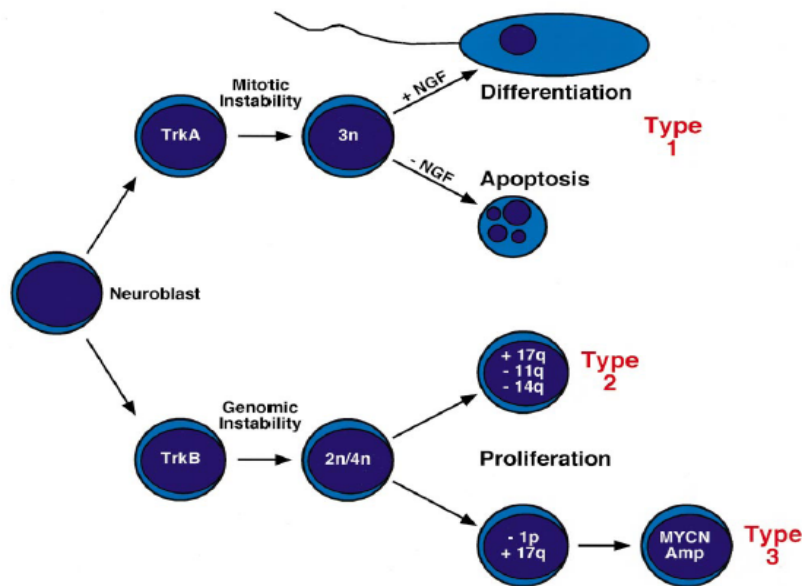


Fig. 1: Hypothetical model of the genetic origin of neuroblastoma. Mutations in undifferentiated neuroblasts cause tumorigenesis, and the degree of neuroblastic differentiation at the time of the mutation determines neurotrophin expression pattern. TrkA-expressing tumors are more likely to have errors in mitotic recombination, resulting in whole chromosome gains. They are called “type 1 tumors”, are often near triploid (3n) and can differentiate in response to NGF or undergo programmed cell death in the absence of NGF. TrkB-expressing tumors (“type 2 tumors”) show more genomic instability, with structural chromosomal alterations. They often have unbalanced gain of distal 17q material, loss of 11q and/or 14q material and are often without 1p deletion and MYCN amplification. Tumors with 1p loss (by unbalanced translocation or other mechanisms) often contain MYCN amplification (type 3 tumors). Thus, inactivation of a 1p gene may be a prerequisite for MYCN amplification (Maris et al. 1999)

1.1.5. RISK STRATIFICATION AND THERAPY

Risk assessment for NB patients depends on several clinical and biological features and the INSS stage of disease. To countermand the great variability in risk assessment worldwide, a working group developed the International Neuroblastoma Risk Group (INRG) classification system in 2005. It is based on clinical criteria and tumor imaging and includes age, histological category, grade of tumor differentiation, DNA ploidy and status of the *MYCN* oncogene and chromosome

11q. The extent of locoregional disease is determined by the absence or presence of image-defined risk factors (L1 and L2, respectively). Stage M is used for widely disseminated disease, and MS describes metastatic NB limited to skin, liver and bone marrow, without cortical bone involvement in children up to 18 months with L1 or L2 primary tumors. An overview of the INRG Consensus Pretreatment Classification schema is shown in Fig. 2. This schema is currently used to classify the patient into a defined pretreatment risk group, and allows risk-adapted therapy (Ambros et al. 2009; Cohn et al. 2009). Current studies also include novel biomarkers to investigate their prognostic significance and consider their inclusion in future classifications systems. Co-amplification of several genes, including *DDXI*, *NAG*, and *ALK*, with *MYCN* has been observed in NBs and HER2 expression is also suspected to be a marker for positive prognostic significance in NB (Izycka-Swieszewska et al 2010; Ambros et al. 2009). Although only few biomarkers are included in the current classification systems, high-throughput and high-coverage genetic and expression profiling of NBs has the power to deliver new markers for defining risk groups more precisely and indicating targeted therapies.

INRG Stage	Age (months)	Histologic Category	Grade of Tumor Differentiation	MYCN	11q Aberration	Ploidy	Pretreatment Risk Group
L1/L2		GN maturing; GNB intermixed					A Very low
L1		Any, except GN maturing or GNB intermixed		NA			B Very low
				Amp			K High
L2	< 18	Any, except GN maturing or GNB intermixed		NA	No		D Low
					Yes		G Intermediate
			Differentiating	NA	No		E Low
					Yes		
	≥ 18	GNB nodular; neuroblastoma	Poorly differentiated or undifferentiated	NA			H Intermediate
				Amp			N High
M	< 18			NA		Hyperdiploid	F Low
	< 12			NA		Diploid	I Intermediate
	12 to < 18			NA		Diploid	J Intermediate
	< 18			Amp			O High
	≥ 18						P High
MS					No		C Very low
	< 18			NA	Yes		Q High
				Amp			R High

Fig. 2: International Neuroblastoma Risk Group (INRG) Consensus Pretreatment Classification schema (taken from Cohn et al. 2009). GN, ganglioneuroma; GNB, ganglioneuroblastoma; Amp, amplified; NA, not amplified; L1, localized tumor confined to one body compartment and with absence of image-defined risk factors (IDRFs); L2, locoregional tumor with presence of one or more IDRFs; M, distant metastatic disease (except stage MS); MS, metastatic disease confined to skin, liver and/or bone marrow in children < 18 months of age; EFS, event-free survival.

Treatment of neuroblastoma is heterogenous and depends on various factors defining the specific risk group of the patient. Low-stage tumors are usually localized, and are surgically removed without chemotherapy. Moderate chemotherapy is only applied in these cases for patients who

experience tumor progression or relapse. Stage 4S tumors may regress spontaneously, and are often only observed without any treatment. Mild chemotherapy may be applied in cases where other organs are affected to induce regression. Treatment of high-risk patients requires maximum therapy, which may include surgical removal of the tumor, chemotherapy and/or radiotherapy as well as bone marrow transplantation (Matthay et al. 1999). Treatment with retinoic acid to induce tumor differentiation of residual tumor cells that are resistant to cytotoxic agents may be included as an additional therapeutic option after transplantation or chemotherapy (Matthay et al. 1999).

Chemotherapy consists of combinations of multiple cytostatic agents, and is applied within controlled studies and according to a protocol, depending on the stage of disease. Treatment protocols may include combinations of alkylating agents (such as ifosfamide, dacarbazine), anthracyclines (adriamycin), etoposide, melphalan, cisplatin and vinca alkaloids (vincristine, vindesine). Duration of therapy may be up to two years, depending on the stage of disease (Hämatologie 2008). All of these agents are prone to induce resistance in tumor cells over time (Kotchetkov et al. 2003; Raguz et al. 2008; Boegsted et al. 2011), especially in progressive disease, which remains a problem in therapy. While low-risk NB patients have good overall survival, cure rates for tumors of INSS stages 3 and 4 are only 13–38 % (Chan et al. 1997). This poor patient survival and the danger of developing resistance underscore the need for a more targeted therapeutic approach to more effectively treat high-risk patients

1.1.6. RELAPSE AND RESISTANCE IN NB

One of the main treatment problems of NB is the particular tendency of NB cells to develop resistance to cytostatic agents. Tumor cells from relapse patients have been shown to have increased resistance to standard cytostatic treatment in comparison to control cells (Keshelava et al. 1997). Different mechanisms including elevated efflux, prohibiting accumulation of the toxins in the cell, have been shown to be involved in the development of resistance. The best known mechanism of multidrug resistance involves increased expression of the adenosine triphosphate-dependent efflux pump, P-glycoprotein. The *PGY1* gene (previously named *MDR1*) at chromosome 7q21.1 encodes the ubiquitously expressed P-glycoprotein. Chan et al. reported that P-glycoprotein expression was restricted to advanced-stage tumors and correlated with a poor response to chemotherapy, but other groups were unable to confirm these findings (Chan et al. 1991; Dhooze et al. 1997). *PGY1* mRNA expression was reported to be inversely correlated with *MYCN* mRNA expression in NBs, and appeared to be restricted to normal stromal cells in the primary tumors. Chemoresistance in widespread NB is therefore less likely to be associated with P-glycoprotein expression (Favrot et al. 1991; Nakagawara et al. 1991). MRP (multidrug resistance-related

protein) encodes another multidrug resistance-associated protein. Norris et al. showed that *MRP* gene expression in primary NBs was strongly correlated with *MYCN* oncogene amplification and poor outcome (Norris et al. 1996). The presence of E-box consensus sequences in the MRP promoter region supports potential transcriptional regulation by MYCN (Zhu et al. 1994). High telomerase activity can also immortalize cancer cells. This reverse transcriptase extends the telomere ends of chromosomes, enabling cells to overcome cell death. High telomerase activity was reported in NB cases and was correlated with *MYCN* amplification and unfavorable patient prognosis (Hiyama et al. 1995). These reports show that resistance can develop via several mechanisms in NB.

1.2. DNA REPAIR MECHANISMS AND DEVELOPMENT OF RESISTANCE

Enhanced repair protects cellular DNA from damage and can also promote resistance in cancer cells. Five major repair mechanisms have been described to date: nucleotide excision repair (NER), mismatch repair (MMR), double-strand break repair, base excision repair (BER) and direct repair. Major forms of DNA damage include single-strand breaks, double-strand breaks, base alteration, hydrolytic depurination, hydrolytic deamination of cytosine and 5-methylcytosine bases, formation of covalent adducts as well as oxidative damage to the bases or phosphodiester backbone. The vast majorities of these lesions are repaired by BER, NER and MMR (Norbury et al. 2001).

Nucleotide excision repair

NER is a highly conserved DNA repair pathway for lesions which alter the helical structure of the DNA molecule, thus, interfering with replication and transcription. It has been proposed as the key pathway involved in mediating resistance or sensitivity to platinating chemotherapeutic agents (Rabik et al. 2007). Cisplatin was the first platinating agent approved for cancer treatment and is still a part of the standard multimodal treatment protocol for NB. Cisplatin and its analog, carboplatin, work by binding to DNA and forming DNA adducts. These adducts lead to intrastrand or interstrand cross-links, which disrupt the structure of DNA molecules, causing steric changes in the helix (Rabik et al. 2007). The distorted DNA structure inhibits replication and transcription, and, if not repaired, leads to cell death via apoptosis (Boeckman et al. 2005). Important steps in this repair mechanism include the recognition of DNA damage and demarcation of the affected area, followed by the formation of a complex to unwind the damaged portion and excise it. The excised area is then re-synthesized and ligated to maintain the complete DNA molecule. The excision repair cross-complementation group 1 (ERCC1) protein plays a key role in NER. ERCC1 dimerizes with xeroderma pigmentosum complementation group F, and the resulting complex is required for the excision of damaged DNA (Martin et al. 2008). Since cisplatin is used in NB treatment,

modifications of the NER pathway that lead to enhanced repair capacity might be involved in the development of resistance.

Mismatch repair

MMR is a strand-specific repair pathway that follows a stepwise process, initiated by recognition of DNA damage (Kunkel et al. 2005). MMR proteins are called Mut proteins. They recognize mismatched or unmatched DNA base pairs or insertion-deletion loops, and initiate the assembly of a protein complex that excises the affected area. DNA is then resynthesized by DNA polymerase. Without intact MMR, unrepaired areas of DNA accumulate when unrepaired base pair mismatches are replicated during DNA synthesis, and repeats are formed due to slippage of the synthetic complex at these areas, leading to microsatellite instability. A functional MMR system is required for the detection of damaged DNA created by cisplatin or carboplatin (Aebi et al. 1996). Platinating chemotherapeutic agents interfere with normal MMR activity and prevent the completion of repair, which then leads to DNA damage and apoptosis. When MMR is deficient, cells can continue to proliferate in spite of DNA damage caused by platinating agents, and are thus resistant. MMR, as well as NER, is important for repairing cisplatin-induced damage, and therefore, might be involved in development of resistance against this drug. The recognition of cisplatin-induced DNA damage via MMR has been reported to be important for cisplatin-mediated cytotoxicity (Sedletska et al. 2007). Cisplatin treatment has been reported to enhance the interaction between the MLH1 MMR protein, the PMS2 (postmeiotic segregation increased 2) protein and p7, triggering apoptosis in mismatch repair-proficient cells (Shimodaira et al. 2003). However, the repair function of MMR proteins has been shown to be uncoupled from their involvement in cisplatin-induced cell death (Basu et al. 2010). Taken together, these findings suggest that MMR is involved in repairing cisplatin adducts.

Double-strand break repair

Double-strand breaks (DSBs) are induced by a variety of genotoxic agents, such as ionizing radiation or cytotoxic agents, but are also frequently generated during normal cellular processes such as DNA replication (Cahill et al. 2006). Two main mechanisms are involved in DSB repair: nonhomologous end joining (NHEJ) and the homologous recombination (HR). HR is predominantly utilized by bacteria and lower eukaryotes, while NHEJ predominates in higher eukaryotes, especially in cells of complex multicellular organisms, such as mammals (Fattah et al. 2010)

Nonhomologous end joining

The term was coined in 1996 by Moore and Haber because the break ends are directly ligated without requiring a homologous template (Moore et al. 1996). At least seven proteins are required

for NHEJ: Ku70, Ku86, the DNA-dependent protein kinase catalytic subunit DNA-PKcs, Artemis, X-ray cross complementing 4 (XRCC4), XRCC4-like factor (XLF) and DNA ligase IV (LIGIV). Ku proteins were named based on protein gel mobilities (actually 70 kDa and 83 kDa) of autoantigenic proteins from a scleroderma patient with the initials, “K.U.”. Ku86 is also referred to as Ku80 (Lieber 2010). Ku70 and Ku86 form a basket-shaped heterodimer (Ku) that slides onto the DNA ends, translocates inwards and binds to broken DNA ends. Ku protects the ends from exonucleolytic attack and recruits DNA-PKcs, a phosphoinositol-3-like family serine/threonine protein kinase. Together, Ku70, Ku86 and DNA-PKcs form the trimeric DNA-dependent protein kinase complex and the assembly of this complex on the ends of double-stranded DNA activates the kinase activity of DNA-PKcs. DNA-PKcs, in turn, phosphorylates and activates the artemis nuclease, which facilitates “clean up” of the ends. Finally, ligation of the broken ends is catalyzed by the trimeric LIGIV complex, which consists of a catalytic core (DNA LIGIV) and its two accessory factors, XLF and XRCC4 (Fattah et al. 2010). The role of NHEJ in repair of ionizing radiation-induced double-strand breaks is well established (Lieber 2010), but is also connected to cisplatin-induced lesions, since cisplatin sensitizes the cells to ionizing radiation via inhibition of NHEJ (Boeckman et al. 2005).

Base excision repair

BER repairs damaged DNA throughout the cell cycle and is primarily responsible for removing small base lesions that do not distort the helix. While the related NER pathway repairs bulky helix-distorting lesions, BER is important for removing damaged bases that could otherwise cause mutations by mispairing or lead to DNA breaks during replication. BER is initiated by DNA glycosylases that recognize and remove damaged or incorrect bases, forming apurinic/apyridinic (AP) sites, which are then cleaved by an AP endonuclease. The resulting single-strand break can then be repaired by short-patch replacing of a single nucleotide or long-patch BER, where 2-10 new nucleotides are synthesized (Liu et al. 2007).

Direct repair

Another way to remove mutations is via direct reversal of the lesion. No template is needed, since the type of damage is specific for each of the four bases. Pyrimidine dimers formed by UV irradiation, resulting in an abnormal covalent bond between the adjacent pyrimidine bases can be repaired in this way. The photolyase enzyme directly reverses this damage (Sancar 2003). Another example is the methylation of guanine, which can be directly reversed by the O-6 methylguanine-DNA methyltransferase (Sassanfar et al. 1991).

1.3. THE Y-BOX BINDING PROTEIN 1 (YB-1)

1.3.1. STRUCTURE OF YB-1

YB-1 was first described in 1988 as a transcription factor that binds to the Y-box of MHC class II promoters (Didier et al. 1988), and belongs to the family of "cold-shock domain" (CSD) proteins. Cold-shock proteins are expressed in bacteria for protection against low temperatures, the most-primitive stress that organisms can be exposed to (Jones et al. 1994; Jurchott et al. 2003). In eukaryotes, 40 % of the nucleic acid-binding region of the CSD protein family is homologous to the bacterial cold shock protein. Eukaryotic Y-box-binding proteins are not known to be involved in the cold-shock response, however, they are thought to play a role in a wide variety of environmental stress reactions (Kohno et al. 2003). Proteins that contain CSDs belong to the most evolutionarily conserved family of nucleic acid-binding proteins known among bacteria, plants and animals. Based on their broad DNA/RNA-binding properties, a myriad of cellular functions have been ascribed to CSD proteins.

The YB-1 gene is located on chromosome 1p34 and contains 8 exons spanning 19 kb (Toh et al. 1998). Several transcription initiation sites have been identified, and the 5' UTR of the major initiation site is extremely long and thought to be involved in regulating gene expression. The YB-1 mRNA contains approximately 1.5 kb, and encodes a 43 kDa protein with 324 amino acids. Homology searches reveal five pseudo genes present on chromosomes 3, 7, 9, 14 and 15 (Kohno et al. 2003). YB-1 is also known as dbpB. A number of closely related genes have been identified, including dbpA and dbpC (Fig. 3). The sizes of exons 2, 3 and 4 are well conserved within these three genes, and codon splitting within the CSD is also similar (Kudo et al. 1995; Tekur et al. 1999).

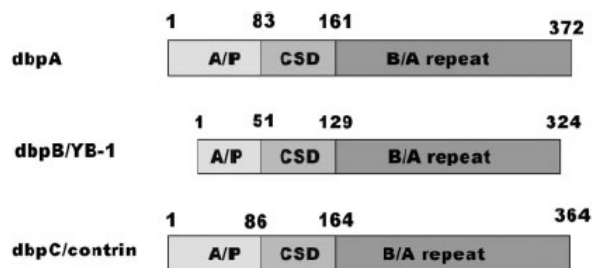


Fig. 3: Schematic representation of the structure of Y-box binding proteins A/P = alanine/proline-rich region, CSD = cold-shock domain, B/A = base/acid repeats (taken from Kohno et al., 2003).

YB-1 proteins contain three domains: A variable N-terminal domain region (aa 1-50), the highly conserved cold-shock domain (CSD, aa 51-129) and a C-terminal domain (130-C) (Wolffe 1994). The N-terminal domain is rich in alanine and proline residues and is thought to be a transactivation

domain (Kohno et al. 2003). The CSD is one of the most evolutionary conserved nucleic acid-binding protein domain between bacteria and eukaryotes identified (Wolffe 1994). It comprises a five-stranded β -barrel and belongs to the β -sheet RNA-binding protein group with conserved RNP motifs (Graumann et al. 1996). It binds RNA as well as double-stranded and single-stranded DNA (Wu et al. 2007). The structure of the C-terminal domain varies significantly in different organisms, these structural alterations may have been necessary for the evolution from poikilotherms to homoiotherms, and may be involved in the pleiotropic functions of Y-box-binding proteins (Kohno et al. 2003). The C-terminus is thought to be involved in protein–protein interactions since it contains alternate regions of basic or acidic amino acids, each of about 30 amino acids in length, termed charged zipper or B/A repeats (Wu et al. 2007). This domain has also been shown to have a strong affinity for single-stranded DNA/RNA *in vitro*, and is most probably involved in nucleic acid binding (Izumi et al. 2001). Both a noncanonical nuclear localization signal and a cytoplasmic retention site within the C-terminal region of YB-1, which control cellular localization, allowing YB-1 to shuttle between the cytoplasm and nucleus (Kohno et al. 2003). The CSD also reportedly co-operates with the C-terminus to facilitate nuclear trafficking (Jurchott et al. 2003). Taken together, each domain has unique features and is involved in multiple functions of YB-1, as summarized in Fig.4.

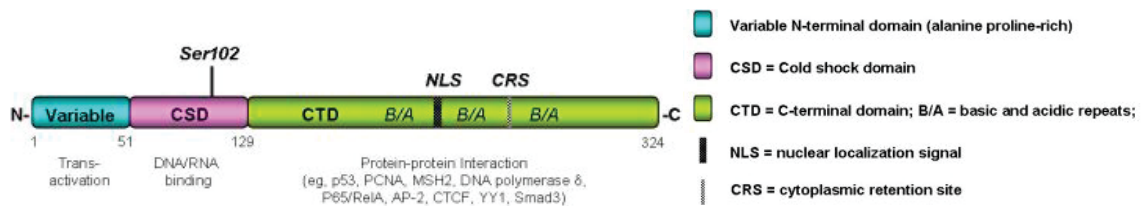


Fig. 4: Schematic diagram of the functional domains of YB-1. YB-1 contains an N-terminal domain, a cold-shock domain (CSD) and a C-terminal domain (CTD). The N-terminal domain is thought to be involved in transactivation. The CSD is important for RNA/DNA binding. Most of the characterized protein-protein interactions occur with regions within the CTD. The CSD and CTD also work together to facilitate nuclear trafficking. The CTD contains a nuclear localization signal (NLS) and a cytoplasmic retention signal (CRS). (Adapted from Wu et al. 2007).

1.3.2. FUNCTIONS OF YB-1

YB-1 is involved in numerous functions at all levels of the cell. It is expressed throughout embryogenesis and is one protein regulating cell proliferation. It is involved in early mouse development, homozygous knockout of YB-1 in mice leads to impaired neural tube closure and is embryonically lethal. Mice exhibit exencephaly with abnormal patterns of cell proliferation within the neuroepithelium (Uchiumi et al. 2006). The level of YB-1 expression is closely correlated with the level of cell proliferation (Lu et al. 2005). YB-1 is also induced in response to mitogenic stimuli

in various cell types, such as in T cells following cytokine stimulation (Sabath et al. 1990) as well as in endothelial cells (Stenina et al. 2000).

YB- functionality is controlled by the abundance, location and phosphorylation status of the protein within the cell. Cellular translocation of YB-1 greatly influences its function, and correlates with specific characteristics of tumors. In the cytoplasm, YB-1 regulates mRNA stability and translational regulation (Evdokimova et al. 2001; Fukuda et al. 2004), while in the nucleus, it regulates transcription of genes containing the Y-box promoter element (Kohn et al. 2003). YB-1 is mainly localized in the cytoplasm, but treatment of cells with anticancer drugs, hyperthermia or UV radiation has been shown to result in protein translocation to the nucleus (Koike et al. 1997; Stein et al. 2001). This translocation may, at least in some cells, be dependent on the status of the p53 tumor suppressor protein, since Zhang et al., showed that nuclear translocation of YB-1 after cisplatin treatment or adenoviral infection required wild-type p53 (Zhang et al. 2003). Nuclear translocation has also been shown to be cell cycle regulated, with YB-1 protein accumulating in the nucleus during G1/S phase (Jurchott et al. 2003). YB-1 cellular abundance is at least partly regulated via proteosomal degradation. The F-Box protein 33 and RB binding protein 6 (RBBP6) are among the proteins targeting YB-1 for proteosomal degradation via polyubiquitination (Lutz et al. 2006; Chibi et al. 2008). Initially, it was thought that nuclear translocation of YB-1 in response to genotoxic stress required sequence-specific endoproteolytic cleavage (Sorokin et al. 2005). But in 2009 Cohen et al. showed that only the larger form of YB-1 exists, and that the smaller protein band observed on western blots and thought to be YB-1, was an artifact of antibody cross-reactivity (Cohen et al. 2009). The C-terminal tail of YB-1 contains multiple phosphorylation sites that allow regulation of YB-1 functions (Kohn et al. 2003). Akt/PKB is a serine/threonine kinase that promotes tumor cell growth by phosphorylating transcription factors and cell cycle proteins, and activated Akt phosphorylates Ser102 of YB-1 (Sutherland et al. 2005). Phosphorylation of YB-1 regulates nuclear translocation (Basaki et al. 2006), activates cap-independent translation (Evdokimova et al. 2009) and reduces binding to the mRNA cap (Bader et al. 2008). Phosphorylated YB-1 also upregulates PI3K activity, which is known to lead to transformation through the ras pathway (Astanehe et al. 2009), and is required for transcriptional activation of growth-enhancing genes, such as EGFR (Wu et al. 2006).

The consensus binding site for YB-1 was defined as 5'-CTGATTGG-3', a sequence motif known as the Y-box, which contains an inverted CCAAT box sequence (Didier et al. 1988). This motif is present in the promoter regions of many eukaryotic genes, such as growth-associated genes, the major histocompatibility complex class II (MHC II) genes or the *PGY1* gene (Wolffe et al. 1994).

YB-1 regulates gene expression via three different mechanisms. (Swamynathan et al. 1998). Interaction of YB-1 with the Y-box consensus motif is known to either activate or repress gene expression (Ohga et al. 1998). Additionally YB-1 is involved in translational control (Evdokimova et al. 2001; Gaudreault et al. 2004). YB-1 directly activates transcription of a number of genes. It binds to the inverted CCAAT box and enhances transcription of cell cycle proteins (Jurchott et al. 2003) and several genes, involved in replication, such as topoisomerase II or DNA polymerase α and δ (Shibao et al. 1999; En-Nia et al. 2005). A recent report for breast cancer cells also claims that YB-1 activates genes, linked to cancer stem cells such as CD44 and CD49f (To et al. 2010). YB-1 has been shown to mediate repression of genes involved in cell death regulation, including p53 (Lasham et al. 2003), genes coding for structural proteins (Higashi et al. 2003) or metabolic proteins (Chen et al. 2009). In addition to transcriptional regulation, YB-1 is also implicated in translational control. It positively regulates translation of Myc oncoproteins via an alternative method, using internal ribosome entry segments (IRES). YB-1 also interacts with and stabilizes mRNA in a sequence non-specific, but cap-dependent manner (Evdokimova et al. 2001). Binding of YB-1 displaces the initiation factors eIF4E (eukaryotic translation initiation factor 4E) and eIF4G and thereby causes translational silencing of the bound mRNA (Evdokimova et al. 2001). Microarray analysis revealed, that YB-1 interacts with and silences a large set of mRNAs, among them mRNA's coding for cyclins and members of the mitogen-activated protein kinase cascade (Evdokimova et al. 2006). YB-1 has also been shown to preferentially bind to RNA containing 8-oxoguanine, suggesting it can detect damaged RNA molecules (Hayakawa et al. 2002). Taken together, YB-1 participates in controlling expression at several levels, localized in either the nuclear or cytoplasmic compartments. The involvement of YB-1 in the control of so many different types of proteins highlights its significance in cellular functions, and underpins its involvement in the central processes of cancer progression.

1.3.3. YB-1 AND CANCER

YB-1 has been linked with many malignancies including colorectal carcinomas (Shibao et al. 1999), breast cancer (Bargou et al. 1997), prostate cancer (Gimenez-Bonafe et al. 2004), osteosarcoma (Oda et al. 2003), ovarian cancer (Kamura et al. 1999), melanoma (Schitteck et al. 2007) and lung cancer (Shibahara et al. 2001). Especially the role of YB-1 in breast cancer has been intensively researched. YB-1 directly induced transcription of the human epidermal growth factor receptor (her-2) and its dimerization partner, EGFR, and targeting YB-1 via siRNA drugs induced apoptosis in breast cancer cells with her-2 amplifications (Lee et al. 2008). Transgenic mice overexpressing YB-1 in a breast-specific manner were highly prone to developing tumors, and the tumor cells were genetically unstable (Bergmann et al. 2005). Janz et al., showed that YB-1

expression correlated with breast cancer aggressiveness in patients not treated with postoperative chemotherapy. At 5 years following surgical removal of the primary tumor, patients whose tumors expressed low levels of YB-1 remained free of disease, whereas 30 % of patients with tumors strongly expressing YB-1 had experienced relapses (Janz et al. 2002). Much less is known about the role of YB-1 in childhood cancers. YB-1 overexpression has been described for pediatric glioblastoma, (Faury et al. 2007) and YB-1 expression was recently assessed in a small cohort of 36 NBs via immunohistochemistry (Wachowiak et al. 2010). YB-1 expression was detected in 35 of 37 (94.6 %) NBs, but YB-1 expression did not correlate with survival, risk factors or tumor stage. YB-1 expression in other tumor compartments has also associated it with angiogenesis. The endothelial cells of brain tumor microvasculature and microvessels in the desmoplastic region surrounding multiple solid tumors expressed high levels of YB-1. YB-1 knockdown was also shown to inhibit the growth of human umbilical vein endothelial cells in culture (Takahashi et al. 2010). Elevated expression of YB-1 is observed in the tumor cells and tumor vasculature of many tumor types and YB-1 overexpression can be clearly linked to a more aggressive form in some of these malignancies.

Nuclear localization of YB-1 has been associated with indicators of more aggressive cancer subtypes. Nuclear localization of YB-1 was associated with *PGYI* expression in breast carcinomas (Bargou et al. 1997), sarcomas (Oda et al. 2003) diffuse large B cell lymphomas (Xu et al. 2009) and ovarian carcinomas (Kamura et al. 1999). Nuclear YB-1 expression correlated with high levels of proliferation, drug resistance and poor patient prognosis (Jurchott et al. 2003; Homer et al. 2005; Sutherland et al. 2005). Nuclear YB-1 was associated with poor prognosis of patients with non-small cell lung cancer (Shibahara et al. 2001) and sarcomas (Oda et al. 2003). A recent study also linked nuclear YB-1 expression in human breast cancer cells closely to progesterone receptor negativity and categorized this as a strong adverse survival factor (Dahl et al. 2009). Nuclear expression of YB-1 in diffuse large B cell lymphomas was significantly correlated with clinical stage, bone marrow involvement, extra nodal involvement and poor response to chemotherapy (Xu et al. 2009). Patients with ovarian carcinomas expressing higher nuclear YB-1 concentration had poorer prognoses, with shorter relapse-free periods (Kamura et al. 1999).

1.3.4. YB-1, CYTOSTATICS AND RESISTANCE

High YB-1 expression is associated with poor patient outcome in various cancers. One study reported that 66 % of patients with breast cancer whose tumors expressed high levels of YB-1 experienced relapses within 5 years of completing treatment, whereas, no patient experienced relapse whose tumor expressed low YB-1 levels (Janz et al. 2002). This high rate of relapse may

reflect an advantage for cells with elevated YB-1 expression on development of resistance to drugs used during initial patient treatment. Ohga et al., discovered back in 1996 that knockdown of YB-1 sensitized cells to cisplatin, mitomycin C and UV radiation, but not to vincristine, doxorubicin, camptothecin or etoposide (Ohga et al. 1996). In 2004, Shibahara et al., showed that mouse embryonic stem cells expressing heterozygous YB-1 were hypersensitive to cisplatin and mitomycin C (Shibahara et al. 2004). These findings suggest that YB-1 has a protective capacity against cytotoxic effects of DNA damaging agents. YB-1 binds preferentially to cisplatin-modified DNA and interacts with proliferating cell nuclear antigen 1 (PCNA), which may mean that YB-1 can function as a recognition protein for DNA damaged by platinating compounds, such as cisplatin (Ise et al. 1999). Total expression as well as nuclear localization of YB-1 have been associated with a functional response to DNA-damaging agents. Expression profiling revealed that, among others, YB-1 was upregulated in fibrosarcoma cells resistant to a diverse group of DNA-interactive agents, including cytarabine, etoposide or doxorubicin (Levenson et al. 2000). Global expression profiles from breast cancer cell lines contained YB-1 in several chemoresistance signatures (Guay et al. 2008). The importance of nuclear localization in predicting development of drug resistance has been described for several cancer entities, including breast cancers, ovarian cancers, and synovial sarcomas (Janz et al. 2002; Oda et al. 2003). Basaki et al. described the role of Akt-mediated activation of YB-1, which is required for nuclear translocation, in acquisition of drug resistance through transcriptional activation of relevant genes and repair of damaged DNA (Basaki et al. 2006).

The *PGY1* gene is important in the development of resistance against cytostatic agents. *PGY1* is an SOS gene, its promoter activity is increased in response to environmental stress including various anticancer agents (Chaudhary et al. 1993), UV radiation (Uchiumi et al. 1993) or heat shock (Miyazaki et al. 1992). Its product, P-glycoprotein, is a 170 kDa transmembrane protein, belonging to the ATP-binding transporter family, that actively effluxes many drugs from cells, and is responsible for tumor cell resistance to a range of anticancer drugs (Kuwano et al. 2004). The *PGY1* promoter also contains a Y-box motif, and YB-1 has been shown to bind to it (Swamynathan et al. 1998) and activate transcription of *PGY1* (Stein et al. 2001; Chattopadhyay et al. 2008). Different reports described that nuclear, but not cytoplasmic, YB-1 correlated with increased *PGY1* expression (Bargou et al. 1997; Fujita et al. 2005).

1.3.5. YB-1 AND REPAIR

YB-1 has been connected with several different repair pathways. It was identified among other protein binding partners of base-excision repair enzymes in a yeast two-hybrid screen in 2001

(Marenstein et al. 2001). Gaudreault et al., showed three years later that purified YB-1 can separate different DNA duplexes containing forked structures or blunt, 5' or 3' recessed ends, and that strand separation activity increases around cisplatin-modified DNA or mismatch-containing DNA duplexes. They showed that YB-1 exhibited exo- and endonucleolytic activities and bound to Ku80, MSH2, WRN and DNApol δ *in vitro*, repair proteins involved in base-excision and mismatch repair (Gaudreault et al. 2004). YB-1 has been shown to bind cisplatin-modified DNA and interact with PCNA, which acts as a processing factor for DNA polymerase δ in eukaryotic cells, implicating its involvement in resynthesis of excised, damaged DNA strands during DNA repair (Ise et al. 1999). YB-1 also interacts with NEIL2, one of the four oxidized base-specific DNA glycosylases, and was reported to stimulate its base-excision activity in human colon carcinoma HCT116 cells (Das et al. 2007). The same report showed that YB-1 interacted with the other NEIL2-associated BER proteins *in vitro*, including DNA ligase III α and DNA polymerase β . It was speculated that YB-1 may be a component of a large multiprotein complex formed by these factors (Das et al. 2007).

1.3.6. YB-1 AND APOPTOSIS

Various connections have been described between YB-1 and p53, a tumor suppressor protein rendered dysfunctional in more than 50 % of all cancers and a cellular gatekeeper halting proliferation in response to cellular stress, and capable of initiating either senescence or apoptosis (reviewed in Suzuki et al. 2011). p53 exhibits growth suppressive properties by transcriptional regulation of gene expression. Genes directed by p53 within the DNA damage response pathway include p21/Waf1/Cip1 (el-Deiry et al. 1993) and bax (Reed et al. 1995). By modulating expression levels of these genes, p53 can induce either cell arrest or apoptosis under genotoxic stress through cell cycle checkpoints to ensure genetic stability. Okamoto described a model of induction of p53 activity after DNA damage implicating it in repair. When DNA damage leads to single-stranded regions, DNA ends, and insertion/deletion mismatches, p53 is recruited to the damaged region via the high binding affinity of its C-terminus for these structures, and interaction with other repair-associated proteins, including RPA, XPB, and XPD, also cause p53 accumulation. Sequence-specific DNA binding activity is then stimulated by short, single-stranded DNA produced in process of NER or by other modification of the C-terminal regulatory domain (Okamoto et al. 2000). YB-1 has also been reported to accumulate in the nucleus under conditions of genotoxic stress and associates with single-stranded, apurinic, or cisplatin-adducted DNA. It was shown in various cell lines after treatment with the antitumor drugs cisplatin, actinomycin D and amsacrine as well as adenovirus infection that wild-type p53 is necessary for YB-1 translocation while mutated p53 protein is defective for nuclear localization. A possible interaction of YB-1 and p53 in

the DNA damage region to mediate repair and activate the specific DNA-binding activity of p53 was proposed in 1997 (Koike et al. 1997). Direct interaction of p53 with YB-1 has been described by different working groups, who showed that YB-1 prevents p53 from inducing apoptosis by selectively inhibiting its transactivation of proapoptotic genes. (Okamoto et al. 2000; Homer et al. 2005). Lasham et al., reported that YB-1 can negatively regulate p53 by reducing its endogenous cellular level in various cell lines of mouse and human origin, thus, reducing activity. This same report showed that nuclear YB-1 was associated with a failure to increase the level of Bax protein in normal mammary epithelial cells after stress activation of p53 (Lasham et al. 2003). From these reports, it appears that YB-1 may be capable of protecting cells from p53-induced apoptosis, thus, assisting tumor cells in escaping death by upregulating and/or translocating YB-1 to the nucleus.

1.3.7. YB-1 AND MYCN

Upregulation of the MYCN protein via either *MYCN* amplification or other mechanisms is an important factor for neuroblastoma aggressiveness, therefore, connections between the MYC protein family and YB-1 could be of importance specifically for neuroblastoma. The MYC family of transcription factors regulate gene transcription via binding to the DNA sequence, CACGTG, called E-box in the gene promoter. The YB-1 promoter contains an E-box motif, making it a potential MYCN target (Wu et al. 2007). The proto-oncogenes, *c-*, *L-*, and *MYCN*, can all be translated via an alternative method where the ribosome is recruited to a complex structural element, termed an internal ribosome entry segment (IRES). YB-1 was shown to positively regulate IRES-mediated translation of *c-*, *L-*, and *MYCN* both *in vivo* and *in vitro* (Cobbold et al. 2008). Another connection can be made through the Twist protein, an E-box-binding transcription factor. Twist is constantly overexpressed in *MYCN*-amplified neuroblastomas as well as in cisplatin-resistant human epidermoid cancer KB and human prostate cancer PC3 cells. Twist was shown to bind the YB-1 promoter and activate transcription (Valsesia-Wittmann et al. 2004; Shiota et al. 2009). Shiota et al. also described the involvement of programmed cell death protein 4 (PDCD4) in this interaction. PDCD4 interacts directly with Twist and leads to reduced cell growth through the downregulation of the Twist1 target gene, YB-1 (Shiota et al. 2009). These observations implicate YB-1 as positive translational regulator of MYC family proteins and as a protein involved in maintaining growth alongside MYC proteins or possibly as an effector.

1.3.8. YB-1 SECRETION

Secretion of a protein from a tumor cell exposes it to the hosts immune system, which could result in autoantibody production under certain circumstances. In 2009, Frye et al. showed that mesangial

and monocytic cells actively secreted YB-1 after inflammatory challenge. Secretion occurred via a nonclassical pathway, by-passing the endoplasmic reticulum and Golgi apparatus in the usual manner of inflammatory mediators, and YB-1 release required ATP-binding cassette transporters and acetylation of two lysine residues in the YB-1 C-terminal domain (Frye et al. 2009). Mitogenic and promigratory effects in inflammation, association with outer cell membrane components as well as interaction with extracellular Notch-3 receptor domains have been described as effects of extracellular YB-1 to date (Rauen et al. 2009). Autoantibodies against YB-1 have also been reported in the serum of patients with primary biliary cirrhosis, which is an autoimmune disease (Yang et al. 2007). These reports establish proof-of-principle that the YB-1 protein can be secreted at least by certain cell types and that it may be autoimmunogenic as a protein in bloodstream.

1.4. PROJECT DESIGN AND AIM

NB is a very heterogeneous disease and early detection as well as consequent patient monitoring and staging of the disease to prevent patient over- or undertreatment is crucial. Although several biological features are currently used for classification, no reliable serum marker protein has been described to date. Marker proteins present in patient blood would provide a less invasive and effective way to monitor disease. Proteins expressed by the tumor can cause formation of autoantibodies. This project aimed to use autoantibodies to identify novel proteins involved in development and progression of NB. Protein array analysis was used as an initial step to compare antibody expression profiles of NB patients with age- and gender-matched healthy children to identify potential tumor-relevant proteins. This group was then narrowed down by choosing proteins represented by clones, which were highly abundant on the array or with specificity for a certain tumor stage. Additionally, reported connections of the target proteins with aspects of cancerogenesis were taken into consideration. The most promising candidate, YB-1, was then investigated in cell culture models for NB for its extra- and intracellular abundance in various NB cell lines as well as a possible correlation of YB-1 protein expression with known markers of NB, such as neurotrophin receptors or NMYC. Since relapse tumors and drug resistance provide a large challenge in the treatment of NB patients, downregulation experiments were used to address a possible role of YB-1 for proliferation and repair mechanisms and to monitor cytostatic-mediated effects on expression as well as cellular distribution via immunofluorescent staining. Co-immunoprecipitation experiments were then used to identify possible repair-associated binding partners of YB-1 in order to gain more insights into the role of YB-1 in NB cells.

2. MATERIALS

2.1. CHEMICALS

Tab. 1: General chemicals

Acetic acid	J.T.Baker, Deventer, Netherlands
Acetone	Merck, Darmstadt, Germany
Albumin ELISA kit	Assaypro, St. Charles, USA
Chloroform	J.T.Baker, Deventer, Netherlands
Coomassie brilliant blue R	Sigma, Deisenhofen, Germany
DMSO	Roth, Karlsruhe, Germany
DTT	Invitrogen, Karlsruhe, Germany
Dulbecco's Phosphate-Buffered Saline	Invitrogen, Karlsruhe, Germany
Ethanol	Sigma, Deisenhofen, Germany
Glycerin	Merck, Darmstadt, Germany
HCl	Merck, Darmstadt, Germany
Hoechst 33342 stain	Sigma, Deisenhofen, Germany
Hydrogen peroxide, 30 %	Roth, Karlsruhe, Germany
Isopropanol	Roth, Karlsruhe, Germany
Isotone	Becton-Dickinson, New York, USA
Methanol	J.T.Baker, Deventer, Netherlands
Mounting medium for fluorescence	Vector, Burlingame, USA
MTT (3-(4,5-Dimethylthiazol-2-yl)-2,5-diphenyltetrazoliumbromide)	Roth, Karlsruhe, Germany
NaCl	Roth, Karlsruhe, Germany
NP-40 (nonyl phenoxypolyethoxylethanol)	Sigma, Deisenhofen, Germany
Paraformaldehyde	Sigma, Deisenhofen, Germany
Pepsin	Roche Diagnostics, Mannheim, Germany
Polyhydroxyethyl starch, 10 %	Fresenius, Bad Homburg, Germany
Sodium acetate	Merck, Darmstadt, Germany
Sodium dodecyl sulfate	Gerbü, Gaiberg, Germany
Sodium- EDTA	Sigma, Deisenhofen, Germany
β -Mercaptoethanol	Sigma, Deisenhofen, Germany
Tris base	Roth, Karlsruhe, Germany
Tris-HCl	Sigma, Deisenhofen, Germany

Triton X-100	Merck, Darmstadt, Germany
Tween 20	Sigma, Deisenhofen, Germany
YB-1 recombinant protein	Biozol, Eching, Germany

Tab. 2: Chemicals for western blotting, ELISA and Co-IP

BioFX TMB Microwell substrate	SurModics, Inc., Eden Prairie, USA
BioFX Stop solution	SurModics, Inc., Eden Prairie, USA
Bradford reagent	Roth, Karlsruhe, Germany
ECL Plus	GE Healthcare, Buckinghamshire, UK
Immunoprecipitation kit	Santa Cruz Biotechnology, Santa Cruz, USA
MOPS (3-(N-morpholino)propanesulfonic acid)	Roth, Karlsruhe, Germany
Nonfat powdered milk	Roth, Karlsruhe, Germany
Nuclear extract kit	Active Motif, Carlsbad, USA
Preclearing matrix F	Santa Cruz Biotechnology, Santa Cruz, USA
Proteinase inhibitor cocktail	Roche Diagnostics, Mannheim, Germany
YB-1 human recombinant protein	Abnova, Taipei City, Taiwan

Tab. 3: Chemicals for cell culture

Amphotericin B	PAA, Pasching, Austria
Bovine serum albumin	Roth, Karlsruhe, Germany
Cisplatin	Neocorp AG, Weilheim, Germany
FCS	Biochrom, Berlin, Germany
Geneticine	Invitrogen, Karlsruhe, Germany
Gentamycin	Hexal, Holzkirchen, Germany
4-hydroxy-tamoxifen	Sigma-Aldrich, Munich, Germany
Hyperfect transfection reagent	Qiagen, Hilden, Germany
Insulin-transferrin-sodium selenite supplement (ITS)	Sigma-Aldrich, Munich, Germany
Methylene blue vital stain	Serva, Heidelberg, Germany
Penicillin / Streptomycin	Invitrogen, Karlsruhe, Germany
RPMI medium	Gibco, Eggenstein, Germany
Trypsin/EDTA	Invitrogen, Karlsruhe, Germany
YB-1 siRNA	Qiagen, Hilden, Germany

Tab. 4: Chemicals for PCR

Agarose	Peqlab, Erlangen, Germany
Dithiothreitol (DTT)	Invitrogen, Karlsruhe, Germany
dNTPs	Bio-Budget, Krefeld, Germany
Go Tag polymerase	Promega, Madison, USA
MgCl ₂ , 25 mM	Promega, Madison, USA
Random primers	Invitrogen, Karlsruhe, Germany
RNAse H	TaKaRa, Otsu, Japan
RNeasy Micro kit	Qiagen, Hilden, Germany
Superscript II reverse transcriptase	Invitrogen, Karlsruhe, Germany
Trizol reagent	Invitrogen, Karlsruhe, Germany

Tab. 5: Primary Antibodies

ERCC1, mouse	Santa Cruz Biotechnology, Santa Cruz, USA
GAPDH, mouse	Santa Cruz Biotechnology, Santa Cruz, USA
GPI, rabbit	Santa Cruz Biotechnology, Santa Cruz, USA
HDAC 5, rabbit	Santa Cruz Biotechnology, Santa Cruz, USA
Histone H3, rabbit	Cell Signaling, Danvers, USA
Ku80, mouse	kindly provided by G. Iliakis, Institute of Medical Radiation Biology
MAZ, rabbit	Santa Cruz Biotechnology, Santa Cruz, USA
MYCN, mouse	Cell Signaling, Danvers, USA
phospho-H2AX (Ser 139), mouse	Millipore, Billerica, USA
Rad51, rabbit	Abcam, Cambridge, USA
Transferrin, rabbit	Stressgen, Hamburg, Germany
XPC, rabbit	Santa Cruz Biotechnology, Santa Cruz, USA
YB-1, mouse	Abnova, Taipei City, Taiwan
YB-1, rabbit	Epitomics, Burlingame, USA
YB-1, rabbit	Abcam, Cambridge, USA

Tab. 6: Secondary Antibodies

biotinylated anti-human, IgG	Jackson ImmunoResearch, Newmarket, UK
Donkey, anti-rabbit IgG-Texas Red	Dako, Glostrup, Denmark
Goat, anti-mouse IgG-Alexa Flour 594	Invitrogen, Karlsruhe, Germany

Goat, anti-rabbit IgG-HRP	Dako, Glostrup, Denmark
Goat, anti-mouse IgG	Dako, Glostrup, Denmark
Rabbit, anti-mouse IgG-HRP	Dako, Glostrup, Denmark
Streptavidin-Biotin HRP Complex	GE Healthcare, Munich, Germany

2.2. PLASTICWARE

Tab. 7: General plasticware

0.5, 1 and 2 ml safe-lock microcentrifuge tubes	Eppendorf, Hamburg, Germany
1-1000 µl filter pipette tips	Starlab, Ahrensburg, Germany
15 and 50 ml polypropylene screw-cap centrifuge tubes	Greiner, Frickenhausen, Germany
5.0 ml combitips	Eppendorf, Hamburg, Germany
Amicon Ultra-15 centrifugal filter units	Millipore, Billerica, USA
Gluthatione-coated 96-well plates	Therma-Scientific, Rockford, USA
Nitrocellulose membrane	Whatman, Kent, UK
Polyacrylamide precast gels (4-12 %)	Invitrogen, Karlsruhe, Germany
Single-use PMMA cuvettes	Roth, Karlsruhe, Germany
Super RX X-Ray film	Fujifilm, Tokyo, Japan
Whatman blotting paper	Whatman, Kent, UK

Tab. 8: Plasticware for cell culture

12-, 24- and 96-well culture plates	Corning, NY, USA
25 cm ² cell culture flasks	Corning, NY, USA
75 cm ² cell culture flasks	Greiner, Frickenhausen, Germany
Cell culture petri plates	Greiner, Frickenhausen, Germany
Cell scrapers	Greiner, Frickenhausen, Germany
Cryopreservation tubes	Simport, Beloeil, Canada
Sterile pipettes for cell culture	Greiner Frickenhausen, Germany

2.3. TECHNICAL EQUIPMENT

Tab. 9: Technical Equipment

Agarose gel chambers	PeqLab, Erlangen, Germany
Autoclave	Systec, Wetztenberg, Germany
Beckman Epics XL FACS	Beckman Coulter, Brea, USA
Biofuge fresco	Kendro, Langenselbold, Germany
Blotting chamber	BioRad, Herts, UK
C 1000 thermal cycler	BioRad, Herts, UK
Coulter counter	Beckman Coulter, Brea, USA
Electrophoresis chambers	Invitrogen, Karlsruhe, Germany
iBlot western blotting system	Invitrogen, Karlsruhe, Germany
KC Junior ELISA reader	Biotek, Bad Friedrichshall, Germany
Leica TCS SP NT confocal microscope	Leica, Wetzlar, Germany
ND-1000 spectrophotometer	Thermo Scientific, Wilmington, USA
Photometer	Eppendorf, Hamburg, Germany
Precision balance	Kern, Balingen, Germany
Step One Plus real-time PCR system	Applied Biosystems, Foster City, USA
Rotixa 50S	Hettich, Mülheim a.d.Ruhr, Germany
Thermoblock	Roth, Karlsruhe, Germany
Transilluminator	Biometra, Göttingen, Germany
UVI Chemi	Biometra, Göttingen, Germany

3. METHODS

3.1. CELL CULTURE

Cell culture was performed under sterile conditions in a laminar flow hood using good sterile technique. Cells were cultivated in an incubator at 37°C, 5 % CO₂ and humidified air. Established neuroblastoma cell lines were cultured in complete medium (RPMI 1640) supplemented with 10 % fetal calf serum (FCS), 100 µg/ml penicillin/streptomycin or gentamycin, and Amphotericin B. Geneticin (G418, 500 µg/ml) was used for selection of stably transfected cells. A cisplatin-resistant subline of SK-N-BE (named SK-N-BEcp here) was kept in complete medium, containing 1.36 µl cisplatin per ml medium to maintain resistance. Medium was changed every 2-4 days, and cultures were passaged upon 80- 100 % confluency.

The following human neuroblastoma cell lines were used in this dissertation research (detailed information can be found in table 10: SK-N-BE as well as the cisplatin-resistant SK-N-BE-cp subline, SH-SY5Y as well as the retrovirally transfected SH-SY5Y subclones stably expressing the TrkA or TrkB neurotrophin receptors (SY5Y-TrkA or SY5Y-TrkB), SK-N-SH-EP as well as the SH-EP-MYCN-ER and Tet-21N subclones, NB69 as well as the retrovirally transfected NB69-TrkA subclone, IMR-5 as well as the retrovirally transfected IMR-5 TrkA subclone, NGP, Kelly, SK-N-SH, WAC2 and SK-N-AS.

Tab. 10: Cell lines used in this dissertation

Cell line	Subclone of	MYCN-amplification	Original reference	Provided by
IMR-5	IMR-32	yes	Tumilowicz et al. 1970	Brodeur
Kelly	--	yes	Schwab et al. 1983	Brodeur
NB69	--	no	Brodeur et al. 1976	Brodeur
NGP	--	yes	Brodeur et al. 1976	Brodeur
SK-N-SH-EP	SK-N-SH	no	Biedler et al. 1973	Westermann
SH-SY5Y	SK-N-SH	no	Biedler et al. 1973	Brodeur
SK-N-BE	--	yes	Seeger et al. 1977	Centre Leon Berard
SK-N-AS	--	no	El-Badry et al. 1989	Brodeur

Brodeur = Garrett Brodeur, Children's Hospital of Philadelphia, USA; Centre Leon Berard, Lyon, France; Westermann = Frank Westermann, DKFZ, Heidelberg, Germany

The SK-N-SH-EP (subsequently named SH-EP) cell line was used for the development of two inducible systems. For the tamoxifen-inducible SH-EP-MYCN-ER cell line, cDNA encoding MYCN fused to an estrogen-responsive domain (ER) was cloned into the pWZL vector and retrovirally transduced into the SH-EP cell line, as described in Schulte et al. 2008. SH-EP-MYCN-ER cells were induced with 200 μ mol tamoxifen (4-OHT) /ml medium for 72 h. The Tet-21/N cell line is a conditional, tetracycline-regulated expression system (Lutz et al. 1996). Treating Tet-21/N cells with 1 μ g tetracycline /ml medium reduced *MYCN* mRNA expression by at least 15-fold.

To passage cell lines, the medium was removed with a pasteur pipette, and trypsin was added to the cell layer (1 ml for a 25 cm² cell culture flask, 2 ml for a 75 cm² cell culture flask) for 3-5 min. Trypsinized cells were mixed with complete medium, transferred into a 15 ml tube and centrifuged at 800 rpm for 5 min at room temperature. The cell pellet was resuspended in complete medium, and cells were seeded into a new flask at a ratio of 1:2 - 1:10, depending on confluency prior to splitting and cell line. After trypsinization, cells were counted using a Coulter Counter (Beckman). The pellet was resuspended in 5-10 ml complete medium, and 100 μ l of the cell suspension was diluted with 9.9 ml isotonic saline solution. The cell number was then calculated, and the cell suspension diluted accordingly for plating.

Cells were stored in liquid nitrogen for extended periods between experiments. In preparation for freezing, cells were trypsinized and centrifuged as described above. The pellet was carefully resuspended in 1-2 ml of 90 % FCS and 10 % DMSO and transferred to a cryopreservation tube. The cell suspension was slowly cooled and kept in the -80°C freezer or in liquid nitrogen until further use. To thaw cells, the cryopreservation tube was quickly warmed to 38 °C and then medium was added dropwise to a final volume of 5 ml. The cell suspension was centrifuged as described above, and cells seeded into a new flask.

3.2. MTT CELL VIABILITY ASSAY

Cell proliferation assays measure the viability and proliferation of cells *in vitro* under the influence of defined external factors. The MTT assay is a colorimetric test, based on the reduction of the yellow tetrazolium salt 3-[4,5-dimethylthiazol-2-yl]-2,5- diphenyltetrazoliumbromide (MTT) to violet formazan crystals via the mitochondrial dehydrogenase in metabolically active cells (Mosmann 1983). Absorption of the formazan crystals is measured spectrophotometrically at 570 nm wavelength against a reference of 630 nm, which MTT does not absorb. Since dehydrogenases are only active in living cells, conversion of MTT can be used as a viability assay. Cells were

cultured in the presence of MTT in a 96-well plate (MTT stock solution consisted of 5 mg MTT in 1 ml PBS and was stored in aliquots at – 20 °C). The supernatant was then removed, cells lysed in 10 % SDS, 5 % acetic acid in DMSO and the 570 nm absorption of the solution was measured on an EM800 ELISA-reader (Bio-Tek Instruments). Every experiment was performed at least in triplicate.

3.3. **RNA EXTRACTION AND cDNA SYNTHESIS**

The Qiagen RNeasy® kit was used to extract total RNA from cells. Cells were lysed in RLT buffer (included in the isolation kit) and homogenized by pipetting. The solution was mixed with 70 % ethanol in a 1:1 ratio and applied to the RNA-extraction column. RNA bound to the silicagel-matrix was washed in several steps and then eluted in RNase-free water. Concentration of purified RNA was measured photometrically using the absorbance at 260 nm, and RNA samples were stored at -80 °C until further use or directly reverse transcribed to cDNA.

For cDNA synthesis, 0.5 - 3 µg total RNA were reverse transcribed using SuperScript II reverse transcriptase (Invitrogen), equimolar mixed deoxyribonucleotide triphosphates (dNTPs) and random hexamer primers. The reaction mix is shown below, and was initially incubated 5 min at 65 °C to break RNA secondary structures.

Reaction volume

6 µl	RNA solution (max. 0.5 µg/µl)
1 µl	10 mM dNTPs
3 µl	random hexamer primer
5 µl	5x buffer
5 µl	25 mM MgCl ₂
2.5 µl	0.1 M DTT
1.25 µl	RNaseOut
1.25 µl	Superscript II RT polymerase

3.4. **POLYMERASE CHAIN REACTION**

The polymerase chain reaction (PCR) is used for the specific *in vitro* amplification of DNA (Mullis et al. 1987; Saiki et al. 1988). A temperature-insensitive polymerase and a gene specific pair of primers are used.

Primer sequences used in this dissertation were:

<u>Primer</u>	<u>forward</u>	<u>reverse</u>
GAPDH	ccacccatggcaaattccatggca	tctagacggcaggtcaggctccacc
YB1	aagtgatggagggtgctgac	tgaccttgggtctcatctcc
ODC1	cccagcgttgacaaataact	cattgaacgtagaggcagca

A final reaction volume of 20 µl included 4 µl 5 x PCR buffer, 1.2 µl 25mM MgCl₂, 0.57 µl 10 mM dNTPs, 1 µl cDNA, 0,1 µl Taq polymerase and dH₂O. The reaction was performed in 25-30 cycles after an initial denaturation period. The specific temperature steps were:

Initial denaturation	95 °C	10'
Denaturation	94 °C	30 ''
Hybridization	x °C	30 ''
DNA synthesis	72 °C	30 ''
	72 °C	10'

3.5. SEPARATION AND DETECTION OF NUCLEIC ACIDS

If nucleic acids pass through a matrix in an electric field, they are separated in proportion to their molecular weight due to their constant charge: mass ratio. The degree of separation is influenced by pore size, depending on the concentration of gel constituent. DNA was separated on 2 % agarose gels as previously described (Sambrook 1989). Electrophoresis was performed using Tris-Acetate-EDTA Buffer (TAE: 0.4 M Tris, 0.01 M EDTA-Na, 0.2 M acetic acid, pH 8.5) as a running buffer, and etidium bromide was incorporated in the gel for DNA detection. Etidium bromide integrates into nucleic acids and is fluorescent under UV light.

3.6. REAL-TIME PCR

Quantitative real-time PCR was performed on the Applied Biosystems Step One Plus™ real-time PCR System. Following the instructions of the manufacturer, the optimal concentration for each primer pair and probe were determined. Negative and positive control templates were included for each PCR reaction. YB-1 cDNA was amplified using the TaqMan® Gene Expression Assay Nr. Hs00898625 (Applied Biosystems).

Components of the real-time PCR reaction mixture were:

TaqMan Fast (20 µl in total)

TaqMan Fast Universal PCR Master Mix 2 x	10 µl
--	-------

Assay on Demand Gene Expression Assay Mix 20 x	1 μ l
cDNA dil. in RNA-free H ₂ O (ca. 100 ng)	9 μ l

Taq SYBR Green (20 μ l in total)

SYBR Green PCR Master Mix 2x	10 μ l
5 pmol forward primer	1 μ l
5 pmol reverse primer	1 μ l
cDNA dil. in RNA-free H ₂ O (ca. 100 ng)	8 μ l

<u>Conditions TaqMan Fast</u>		<u>Conditions SYBR Green</u>	
95 °C	00:20	95 °C	10:00
95 °C	00:01	95 °C	00:15
60 °C	00:20	60 °C	01:00
40 cycles		40 cycles	

Relative concentrations were calculated for each gene by using a standard curve and crossing points. Values for each gene were normalized between samples using the GAPDH housekeeping gene.

3.7. TRANSIENT KNOCKDOWN OF YB-1 BY RNAi

RNA interference (RNAi) describes a mechanism for the highly specific silencing of genes using short double-stranded RNAs directed against YB-1 mRNA, termed silencing RNAs (Mittal 2004). Silencing RNA (siRNA) was directed against YB-1 using the target sequence, 5'-CAG GCG AAG GTT CCC ACC TTA-3', and labeled with Alexa Fluor 488 at the 3' end of the sense stand (Qiagen) to control for transfection efficiency.

Sense: r(GGC GAA GGU UCC CAC CUU A)dTdT
 Antisense : r(UAA GGU GGG AAC CUU CGC C)dTdT

The siRNA was diluted in siRNA suspension buffer (provided by the manufacturer) to a final concentration of 20 μ M and stored at -20°C. Cells were seeded into 96-well plates and transfected when adherent and 60 -70 % confluent. Prior to transfection, 20 pmol siRNA was incubated at 90°C for 1 min, then at 37 °C for 1 h, then diluted in 100 μ l RPMI medium containing 1 μ l Hyperfect (Qiagen) transfection reagent, and incubated for another 30 min at 37 °C. The transfection mix was distributed dropwise into 100 μ l culture medium. Fresh culture medium, replacing the transfection mix, was added after 24 h.

3.8. PREPARATION OF PROTEIN LYSATES FROM CULTURED CELLS

Whole-cell lysates were prepared in RIPA buffer. Medium was removed and cells were washed twice with cold PBS before adding 500 µl RIPA buffer (for a 75 cm² cell culture flask) and incubating the flask 1 min on ice. The lysed cells were concentrated to a corner using a cell scraper then transferred into a 1.5 ml centrifuge tube. The lysate was incubated for 20 min on ice and then centrifuged at 12,000 rpm at 4 °C for 30 min to clear unsolubilized cellular debris from the lysate. The supernatant was transferred into a fresh tube, and 24 µl of Roche Complete™ protease inhibitor cocktail/ml lysate was added to prevent protein degradation by cellular proteases.

RIPA- Buffer

Tris-HCl	50 mM
NaCl	150 mM
NP-40	1 %
Sodium Deoxycholate	0.5 %
SDS	0.1 %

Roche Complete™ protease inhibitor:

1 tablet was dissolved in 3 ml sterile ddH₂O and stored at -20 ° for up to 4 weeks

3.9. PREPARATION OF MEDIUM CONDITIONED BY NEUROBLASTOMA CELL CULTURES

Medium was collected in which NB cell lines had been cultured to detect proteins secreted by the cultured cells. In order to reduce the mitogen background present in fetal calf serum, cell lines were cultured in serum-free, supplemented medium for conditioned medium (CM) collection. Cells were plated at 30-50 % confluency in complete medium. When cultures reached approximately 60 % confluency, the complete medium was removed, cells were washed three times with RPMI medium containing no supplements and RPMI supplemented with 1 % ITS and 0.001 % hydrocortisone was added (15 ml for a 75 cm² cell culture flask). After 72 h, the medium was transferred into a 50 ml centrifuge tube, 24 µl Complete™ proteinase inhibitor cocktail (Roche) was added per ml and the CM was centrifuged at 1000 rpm and 4 °C for 10 min to remove cellular debris. The cleared CM was sterile filtered and stored at -80 °C. CM was concentrated using Amicon Ultra-15 Centrifugal Filter Units (Millipore), centrifuged at 1500-3000 rpm until an approx. 100-fold concentration was achieved. Concentrated CM was transferred into 1.5 ml tubes and stored at -80 °C.

3.10. CROSSLINKING OF PROTEINS IN CONDITIONED MEDIUM

Conditioned medium was prepared as described above and 1 ml was mixed with 5 µl 25 % glutaraldehyde then incubated 5 min at 4 °C. The crosslinking reaction was stopped by adding 100 µl 1M Tris-HCl. Crosslinked CM was either used directly or stored at -80 °C.

3.11. WESTERN BLOTTING

Cells were washed three times with PBS and lysed in cold RIPA buffer containing Complete™ Protease Inhibitor Cocktail (Roche). Protein concentration was measured using the Bradford photometric assay, then lysate containing 5 µg protein was separated in a NuPAGE® BisTRIS 4-12 % polyacrylamide gradient gel (Invitrogen), electroblotted onto a nitrocellulose membrane and blocked with 5 % milk powder in PBS containing 0.02 % Tween-20 (PBS-T). The primary antibody was diluted in the blocking solution and incubated with the membrane for 16 h at 4 °C. After three washes with PBS-T, the blot was incubated with the secondary antibody in blocking solution for 1 h at room temperature. Concentrations varied for the different antibodies, and are listed in the table below. Immune complexes were detected via the light emitted by the reaction of the horseradish-peroxidase enzyme conjugated to the secondary antibody with the Amersham ECL Plus™ Western Blotting Detection Reagent (GE Healthcare), and visualized on either Kodak Medical x-ray film or by the BioDocAnalyze system (Biometra). The GAPDH housekeeping enzyme was analysed on the same immunoblots to allow normalization for target protein amounts between cell lysates. Immune complexes from the target protein detection were removed from the membrane by stripping for 20 min at 65 °C before GAPDH detection.

Tab. 11: Antibodies and corresponding dilutions used in this dissertation project

ERCC1, mouse (Santa Cruz Biotechnology)	1:2000
GAPDH, mouse (Santa Cruz Biotechnology)	1:2000
GPI, rabbit (Santa Cruz Biotechnology)	1:2000
Ku80, mouse (kindly provided by G. Iliakis, Institute of Med. Radiation Biology)	1:200
MYCN, mouse (Cell Signaling)	1:1000
Rad51, rabbit (Abcam)	1:1000
Transferrin, rabbit (Stressgen)	1:4000
XPC, rabbit (Santa Cruz Biotechnology)	1:2000
YB-1, mouse (Abnova)	1:2000
YB-1, rabbit (Epitomics)	1:2000
YB-1, rabbit (Abcam)	1:2000

Goat, anti-rabbit IgG-HRP (Dako)	1:2000
Rabbit, anti-mouse IgG-HRP (Dako)	1:2000
Streptavidin-Biotin HRP Complex (GE Healthcare)	1:2000

MOPS-SDS running buffer (20 x)

MOPS	104.6 g
Tris base	60.6 g
SDS	10.0 g
EDTA	3.0 g
ddH ₂ O	to 500 ml

10 x transfer buffer

Tris base	30.3 g
Glycine	144.0 g
ddH ₂ O	to 1 l

Stripping buffer

Tris-HCl	9.47 g
Tris base	0.289 g
SDS	20.0 g
ddH ₂ O	to 1 l

β-mercaptoethanol was added to a final concentration of 0.7 % immediately before use

3.12. Co- IMMUNOPRECIPITATION

Whole-cell lysates were prepared in RIPA buffer and were precleared by incubation for 16 h at 4 °C with Preclearing Matrix F (ExactaCruz) to remove proteins that unspecifically bind the co-immunoprecipitation matrix. The suspension was then centrifuged to pellet the matrix, and the supernatant was used for co-immunoprecipitation (Co-IP) of YB-1 with binding partners. Formation of the antibody-IP matrix complex was performed according to the manufacturer's instructions. The matrix was mixed with the precleared cell lysate and incubated on a rotary shaker overnight at 4 °C. The complex was pelleted by centrifugation at 10,000 rpm for 30 sec at 4 °C. The supernatant was removed and the matrix washed twice with RIPA and then once with PBS, each washing step was performed for 15 min on a rotary shaker at 4 °C. Proteins bound to the matrix were eluted in 15 µl loading buffer for SDS-PAGE, of which 5 µl was loaded per lane and separated on a NuPAGE® BisTRIS 4-12 % polyacrylamide gradient gel, then the presence of YB-

1, Ku80, Rad51 and XPC was analyzed on western blots. Aliquots of the supernatant at each step were also analyzed by western blotting to establish the co-IP protocol and as controls for the co-IP.

3.13. YB-1 REVERSE ELISA

An ELISA-based detection method was developed to detect autoantibodies against YB-1 in patient sera using immobilized YB-1 protein and photometric quantification of the immune complex. All incubation steps were carried out on a rotary shaker and the indicated temperature. To immobilize YB-1 protein, 30 μ l of a 0.01 μ g/ml solution of recombinant GST-tagged YB-1 protein in 0.05 M Tris-HCl was incubated per well of a glutathione-coated 96-well plate for 16 h at 4 °C to allow binding of the GST-tag to the glutathione-coated surface. Unbound protein was removed in three rounds of washing with 200 μ l PBS-T-05 (PBS containing 0.05 % Tween-20) per well. PBS-T-05 containing 5 % BSA was used to block unspecific binding for 7 h at RT, after which wells were washed twice with 200 μ l PBS-T-05, then 24 μ l blocking solution mixed with 3 μ l patient serum were transferred to the wells and incubated for 16 h at 4 °C. Subsequently, wells were washed once with PBS-T-05 to remove unbound proteins. Biotinylated α -human IgG antibody (Jackson ImmunoResearch) was diluted 1:100,000 in blocking solution, and 40 μ l was added to each well and incubated for 3 h at room temperature. Wells were washed once with 200 μ l PBS-T-05 then 1 μ l of streptavidin-biotin-HRP complex (GE Healthcare) diluted 1:2000 in blocking solution was added to each well and incubated for 1 h at room temperature. Wells were subsequently washed 3 x with PBS-T-05 prior to immune complex detection using 100 μ l BioFX® TMB Microwell Substrate (SurModics, Inc.) per well. The plate was incubated for 10-60 min until sufficient color change occurred, and the reaction was stopped and fixed by adding 100 μ l BioFX® Stop Solution (SurModics, Inc.). The absorbance at 450 nm was measured for the reverse ELISA plate wells. Serum from a healthy adult volunteer was used as a reference to standardize individual experiments and allow comparison across experiments. Control serum was included on every plate, and set to 100 units. For normalization of YB-1 antibody concentrations across different patient serum samples, total protein concentration in the patient sera was either estimated based on the intensity of a defined band from 1 μ l serum separated on NuPAGE® BisTRIS 4-12 % polyacrylamide gradient gels, total protein in the gels were stained with Coomassie Brilliant Blue R, or based on the albumin concentration determined by the AssayMax Human Albumin ELISA Kit (Assaypro).

3.14. QUANTIFICATION OF DOUBLE-STRAND BREAKS VIA GAMMA-H2AX

The histone variant H2AX is phosphorylated at serine 139 in response to DNA double-strand breaks, leading to the formation of γ -H2AX foci at the damaged sites. Phosphorylation is mediated

by activation of the phosphatidylinositol-3-OH-kinase-like family of protein kinases, DNA-PKcs, ATM and ATR, and is used as a connection point for accumulation of central components of the signal cascade initiated by the DNA damage (Rogakou et al. 1998). DNA double-strand breaks were quantified by immunocytochemically staining NB cells for γ -H2AX foci and counting them in a total number of 100 cells per sample. Cells were grown in complete medium on sterile coverslips in a 24-well plate. Transfection with siRNA against YB-1 was performed at 70 % confluency as described above. Medium was changed 24 h after transfection. Cells were then left untreated or irradiated with gamma radiation at 1 Grey 48 h after transfection, depending on the experiment. For γ -H2AX staining, cells were washed with PBS, fixed on coverslips with 4 % paraformaldehyde for 10 min at room temperature, then washed three times with PBS and either stored at 4 °C or processed immediately. All incubations were conducted at room temperature unless otherwise stated. Cells were permeabilized in PBS containing 0.2 % Triton X-100 and 1 % BSA for 10 min on ice, then washed again with PBS containing 1 % BSA for 2 x 5 min and incubated in blocking solution (PBS containing 3 % BSA and 0.2 M glycine) for 1 h. A polyclonal antibody against phospho-H2AX (Ser 139, Millipore) was diluted 1:200 in PBS-T-05 containing 1 % BSA for 1 h. Unspecific antibody binding was removed by a 1 h washing step in PBS-T-05 containing 1 % BSA. Alexa Flour 594-labeled Molecular Probes® anti-mouse IgG (Invitrogen) was diluted 1:2000 in PBS containing 0.5 % goat serum and incubated with the cells for 1 h. Cells were washed twice in PBS, then nuclei were counterstained with a 250 ng/ml DAPI (H33342). After washing another time with PBS, cells were mounted onto microscope slides using Vectashield® Fluorescent Mounting Medium (Vector Laboratories) and stored at 4 °C until observation.

3.15. IMMUNOCYTOCHEMISTRY

Cells were grown in complete medium on sterile coverslips in 24-well plates for YB-1 immunocytochemistry. When cultures reached 60 % confluency, cells were washed with PBS, fixed on coverslips with 4 % paraformaldehyde for 10 min at room temperature, then washed three times with PBS and either stored at 4 °C or processed immediately. All incubations were conducted at room temperature unless otherwise stated. Cells were permeabilized in PBS containing 0.2 % Triton X-100 and 1 % BSA for 10 min on ice then washed twice for 5 min with PBS containing 1 % BSA. A demasking step was performed next to allow better binding of the antibody to intracellular proteins. The coverslips were incubated 5 min in saline-sodium citrate (SSC) buffer in a steam bath, then slowly cooled to room temperature 3 times in succession using fresh SSC buffer each time. To prevent unspecific binding, the coverslips were then incubated in blocking solution for 1 h. The primary antibody targeting YB-1 (Abcam) was diluted 1:100 in PBS-T-05 containing 1 % BSA, and cells were incubated for 1 h. Unspecific antibody binding was removed by a 1 h

washing step in PBS-T-05 containing 1 % BSA before incubation with the secondary antibody, donkey anti-rabbit IgG labeled with Texas Red (Dako), diluted 1:200 in PBS for 1 h. Cells were washed twice in PBS, then nuclei were counterstained in a 250 ng/ml solution of DAPI (H33342) in PBS before washing again once with PBS. Coverslips were mounted onto microscope slides using Vectashield® Fluorescent Mounting Medium (Vector Laboratories) and stored at 4 °C.

20 x Saline-sodium citrate (SSC) buffer

NaCl	175.3 g
Na ₃ Citrate x 2H ₂ O	88.2 g
ddH ₂ O	to 1 l

3.16. ADDUCT AK

SK-N-BE and SK-N-BEcp cells were transfected with siRNA targeting YB-1, then pulse-treated with cisplatin for 4 h (SK-N-BE cells with 12.5 µg/ml and SK-N-BEcp with 17.5 µg/ml) 48 h after transfection, before transferring to fresh medium without cisplatin and an additional 24 h of culture. After trypsinization and washing, cells were pelleted by centrifugation, resuspended in PBS containing 25% starch solution and spotted onto precoated microscopic slides. The following steps were performed in the Institute for Cell Biology, University Hospital Essen (Thomale Group). After air drying the slides, cells were fixed in methanol at –20°C for 12 h and then rehydrated in PBS for 10 min at 25° C. Cellular RNA was digested by RNase treatment (RNase A, 200 µg/ml; RNase T1, 50 U/ml in PBS; 100 µl per slide) for 1 h at 37°C in a humidified chamber. Each of the steps was followed by washing with PBS. Nuclear DNA was partly denatured by mild treatment with alkali (70 mM NaOH, 140 mM NaCl, 40% methanol v/v; 5 min at 0° C) and cellular proteins were removed by a two-step proteolytic procedure: Samples were first digested with prewarmed pepsin (Roche; 200 µg/ml;) for 5 min at 37°C, and then with prewarmed proteinase K (2 µg/ml in 20 mM Tris–HCl, 2 mM CaCl₂, pH 7.5) for 5 min at 37°C. After blocking with casein (1% in PBS) for 30 min at 25°C, slides were incubated with anti-Pt-DNA antibodies (in-house antibody, 0.1 µg/ml in PBS containing 1% casein and 200 µg of sonicated calf thymus DNA/ml; 2 h; 37°C). After washing with 0.05% Tween 20 in PBS for 2 min at 25°C, three-step sandwich immunostaining was performed by subsequent incubation with: (i) FITC-labeled goat anti-rat Ig (Dianova, Hamburg, Germany; 6.5 µg/ml in PBS, 1% casein; 45 min; 37°C), (ii) ALEXA FLUOR 488-labeled rabbit anti-FITC (5 µg/ml in PBS, 1% casein; 45 min at 37°C; Molecular Probes) and (iii) ALEXA FLUOR 488 goat anti-rabbit IgG (5 µg/ml in PBS, 1% casein; 45 min, 37°C; Molecular Probes). Nuclear DNA was counterstained with DAPI (1µg/ml in PBS) for 30 min at 25°C, and cells were mounted in Vectashield mounting medium. Position, area and intensities of

signals from individual cell nuclei were visualized by fluorescence microscopy, and recorded using an image analysis system. Antibody-derived signals were normalized for the actual DNA content of a given cell and expressed as arbitrary fluorescence units (AFU).

3.17. CHIP-CHIP ANALYSIS

Chromatin immunoprecipitation (ChIP) was performed to detect binding of MYCN/cMYC proteins to target gene promoters. ChIP was performed in the laboratory of F. Westermann (DKFZ, Heidelberg), and a shortened version of the original protocol is described here. Cells were treated with 1 % formaldehyde for 10 min at RT to crosslink DNA with bound proteins, then incubated with 125 mM glycine for 5 min to inactivate formaldehyde within the cells. Cells were washed with 5 ml PBS, scraped off and pooled in 2 ml PBS containing protease inhibitors. After pelleting, nuclei were isolated from cells in a step-wise procedure. Cells were flash frozen in nitrogen, incubated in lysis buffer then manually disrupted using a Dounce homogenizer. Nuclei were washed, then sonicated, and DNA amount and fragment size were assessed on 2% agarose gels. For preclearing, chromatin was treated with RNase A and proteinase K, centrifuged at 16,000 g at 4 °C for 10 min, then supernatant was incubated with 200µl 1:1 protein A/protein G-coated sepharose beads. After preclearing, chromatin amount was measured by NanoDrop. ChIP was performed using the precleared chromatin-protein suspension on the magnetic substrate, Dynabeads. Dynabeads were first incubated in 250 µl block solution and 10 µg corresponding antibody overnight at 4 °C on a rolling mixer, then washed 3 times with 1 ml block solution and resuspended in 100 µl block solution. All components for immunoprecipitation were transferred to a pre-cooled 15 ml polyethylene tube, adding the DNA and Dynabeads last. The immunoprecipitation mixture (130 µl 10 % Triton X-100, 26 µl 50x protease inhibitor, 13µl 10% Na-deoxycholate, 131 µl water, 100 µl Dynabeads and 400 µg DNA, adjusted to 1300 µl with LB3) was incubated overnight at 4 °C on a rolling mixer. Dynabeads were washed, residual buffer removed, and 210 µl elution buffer was added then incubated at a 65 °C for 30 min. Dynabeads were centrifuged at 16,000 g for 1 min, and 200 µl of the supernatant was transferred to a new tube. All samples were incubated at 65 °C for at least 6 h for reverse of crosslinking. To dilute the SDS in the elution buffer, 200 µl of TE buffer was added to the samples. DNA was precipitated via phenol–chloroform extraction, washed with 500 µl 80% ethanol and diluted in 12.3 µl ultrapure water then stored at -80 °C. Amplification of the immunoprecipitated DNA is necessary for later microarray analysis, and was performed using the WGA kit (Sigma). Input concentration was quantified by UV absorption and adjusted to 1 ng/µl, whereas, immunoprecipitated DNA was not diluted. Fragmentation buffer at a 10x concentration (1 µl) was added to 10 µl of DNA and incubated at 95 °C for 4 min. To each sample, 2 µl of 1x library preparation buffer and 1 µl of library stabilization solution were added. Samples

were incubated at 95 °C for 2 min, cooled on ice, then 1 µl library preparation enzyme was added before incubating at 16 °C for 20 min, 24 °C for 20 min, 37 °C for 20 min and 75 °C for 5 min. Amplification master mix was added to the reaction (7.5 µl of 10x amplification master mix, 47.5 µl water, 5 µl of WGA DNA Polymerase), vortexed thoroughly, centrifuged and put into the thermocycler (95 °C for 3 min; 14 cycles: 94 °C for 15 s, 65 °C for 5 min). DNA concentration was measured and all samples were normalized to 100 ng/µL. For a 2-color microarray input, the input DNA was labeled with Cy3 and the immunoprecipitated sample with Cy5 fluorescent dyes. Components of the BioPrime CGH labeling kit (Invitrogen) were joined in a 0.5 ml tube and incubated at 95 °C for 5 min (2 µg amplified sample DNA, 35 µl random primer, 20 µl ddH₂O). The mixture was put on ice immediately and 13 µl of the labeling mastermix (8.2 µl 10x dUTP nucleotide mix, 1.5 µl Cy5- or Cy3-dUTP, 1.5 µl Klenow, 1.8 µl ddH₂O) was added. The samples were incubated for 3 h, 37 °C, then 9 µl of stop buffer was added. Labeled fragments were isolated on the columns provided in the kit, according to the manufacture's manual. Cy-label and total DNA yield was measured by NanoDrop. Cy5- and Cy3-labeled samples were combined in a 1.5 ml tube (5 µg input DNA, 5 µg immunoprecipitated DNA, 150 µl ddH₂O). 50 µl Cot-1 DNA (1 mg/ml), 50 µl blocking agent and 250 µl hybridization buffer from the Oligo aCGH/ChIP-on-chip Hybridization Kit (Agilent) were added. The samples were mixed, incubated at 95 °C for 3 min and 37 °C for 30 min, then collected by centrifugation then used to probe the Agilent Human Promoter Microarray. Arrays were incubated in a rotating hybridization oven at 65 °C and 10 rpm for 40 h. The array slide was washed with Oligo aCGH/ChIP-on-chip wash buffers prior to scanning on a GenePix® 4000B scanner (Molecular Devices).

3.18. ACQUISITION OF SERUM SAMPLES

Serum was obtained from NB patients at the time of and for the purpose of diagnosis. All patients were included in German NB trials, for which patient/parent consent was obtained. Retrospectively collected serum was provided by the serum-bank in Göttingen, Germany. Serum from healthy children was obtained from stored samples from being tested for unrelated problems, which were deemed healthy, or before acting as bone marrow donors. Only serum obtained from healthy adult volunteers was obtained solely for the purpose of this study. Controls serum samples were chosen from those available to be age- and gender-matched to those from NB patients.

3.19. FETAL BRAIN ARRAY

The search for autoantibodies in patient serum using the fetal brain protein array was performed by the RZPD institute in Heidelberg, Germany. The protein array contained 4438 proteins, printed in

duplicate onto PVDF membranes. Printed proteins were derived from expression verified, full-length or shorter cDNA clones from a human fetal brain cDNA library. Detection was carried out using either a Cy3- or Cy5-labeled IgM antibody against human IgG. Results of the separate runs were obtained by laser scanning and then compared pair-wise between control and disease sera. The data generated from these screens was analyzed by P2b to identify autoantibodies to possible stage-specific marker proteins in pooled serum. Patient sera were pooled according to their NB stage for array analysis, and each serum pool was composed of serum from 8-10 individual patients.

3.20. STATISTICAL ANALYSIS

Measurement of band intensity on Coomassie brilliant blue R stained gels, ethidium bromide-stained agarose gels containing PCR products and western blots was done using the Biometra BioDocAnalyze software. The GraphPad Prism 5 program was used for statistical analysis, including the calculation of significance for reverse ELISA, TrkA expression in NB cells and quantification of double strand breaks by unpaired two tailed t-test (95 % confidence interval). Data of ELISAs, TrkA expression, proliferation assays, double strand break quantification and YB-1 protein expression following cisplatin treatment is shown as mean with standard deviation.

4 RESULTS

4.1 USING AUTOANTIBODIES IN NEUROBLASTOMA PATIENT SERUM TO IDENTIFY TUMOR MARKERS

4.1.1 Autoantibodies were detected in NB patient sera via a protein array

Differentially expressed proteins by tumor and healthy cells or between cells from NBs of different stages may be indicative of the presence of the tumor or different states of the disease, and could, in certain cases, induce the formation of autoantibodies against the protein by patient's immune system. It has been shown that cancer patients occasionally show immune responses to self-proteins expressed by their tumors (Anderson et al. 2005). Antibody proteins generally have a long half-life in serum, indicating that they should also be highly stable molecules in stored blood and serum samples. Specific antibodies are also relatively easy to measure using current immunologically based methods, making them potentially useful as clinical biomarkers for detection or monitoring of cancer and cancer treatment. More importantly, antibodies can be generated from very slight changes in overall expression of a tumor-related or disease stage-related protein, making them potentially useful for identifying proteins important in these processes. A protein array of 4438 proteins from a human fetal brain cDNA library (Fig. 5a) was used to detect NB-specific or NB stage-specific autoantibodies in pooled patient serum. Array membranes were incubated with pooled sera from patients with stage 1, 4 or 4S NB, or from healthy age- and gender-matched children. When a signal was detected for both duplicate spots of the protein from the same cDNA clone, the protein was designated as being recognized by an autoantibody from that serum pool. The defined order in which clones were spotted onto the membrane allowed subsequent identification of corresponding positive clones via location of the positive binding signal (Fig.5b).

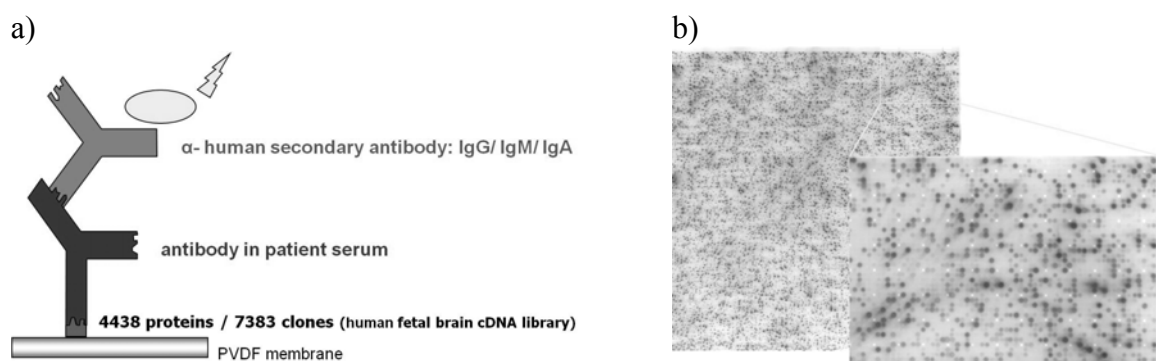


Fig. 5: The fetal brain protein array used for the detection of autoantibodies **a)** Schematic overview of the detection method. **b)** Image of the readout of positive clones from the protein array. Protein array screening was conducted by the *Deutsche Ressourcenzentrum für Genomforschung* (RZPD, Heidelberg).

Positive signals from groups were compared to yield a relative picture for the identification of autoantibodies produced by a specific group. In this pairwise comparison, NB patient groups were compared with each other or to healthy controls. Each pairwise comparison generated a list of clones, whose protein products were bound by patient autoantibodies relative to the group to which it was being compared. These protein targets were ranked according to the significance of the relative difference between the two groups that were compared. Lists were generated, which showed the top 20 clones of the comparisons between specific patient subgroups. Proteins against which autoantibodies were detected for a specific NB stage within a specific pairwise comparison were sorted by function and are shown as pie charts in Fig. 6. Among these were intracellular as well as cell surface proteins. A large fraction of the proteins detected are of unknown function (grey, Fig.6) because either unambiguous sequence data was unavailable for many of the clones on the protein array or the sequence data did not depict a single identifiable protein.

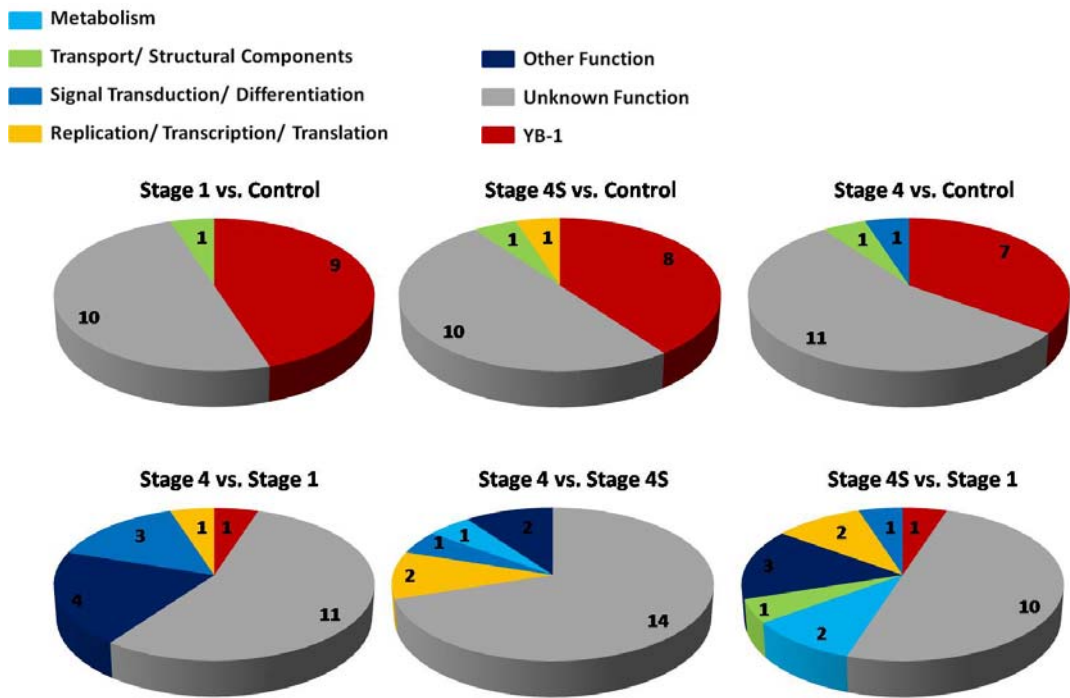


Fig. 6: Graphical breakdown of the 20 most significant targets of autoantibodies detected according to patient subgroup. Protein functions and/or identities were used for the top 20 targets of the pairwise comparison indicated above each pie chart. Data was analyzed in cooperation with M. Zapatka (DKFZ Dept. of Theoretical Bioinformatics, Heidelberg).

Five protein targets of patient autoantibodies were chosen for further investigation (Table 3). Various factors were considered for this decision, including the abundance of positive clones recognized on the protein array or a specificity for a certain tumor stage. Autoantibodies against the MAZ protein were, for example, detected in serum from NB patients but not healthy controls. Reported connections of the target proteins with aspects of cancerogenesis were also taken into

consideration. Autoantibodies to the YB-1 protein were not only detected in serum from patients with stage 1, 4 and 4S NB, but also recognized several independent clones expressing different areas of the YB-1 protein, making it an interesting target for further research.

Table 12: Autoantibody target proteins selected for further investigation

<u>Autoantibody Target Protein</u>	<u>Specifically Detected in Sera from:</u>
Glucose-6-phosphate isomerase (GPI)	stage 1 NB patients
Myc-associated zinc finger protein (MAZ)	all NB patients, compared to healthy controls
Heat-shock protein 90 (Hsp90)	stage 4S NB patients
Histone deacetylase 5 (HDAC5)	stage 4S NB patients
Y-box binding protein 1 (YB-1)	all NB patients, compared to healthy controls

4.1.2 The GPI protein is present in conditioned media of neuroblastoma cells

Glucose-6-phosphate isomerase (GPI) was originally described as a housekeeping enzyme in the Embden-Meyerhof pathway (Watanabe et al. 1996). It was also independently identified as both neuroleukin (NLK) and autocrine motility factor (AMF), extracellular factors that promote tumor progression and metastasis as well as cell migration and invasion (Yanagawa et al. 2004; Torimura et al. 2001). This link makes GPI an interesting target for NB research. Autoantibodies against GPI were detected in pooled sera from stage 1 NB patients on the protein array. This is not the first case where patient autoantibodies against GPI have been detected. They have also been reported in patients with rheumatoid arthritis (Schaller, 2001). In this project, the next step was to check whether GPI was also present in NB sera. Western blot analysis confirmed ubiquitous strong expression of GPI in a panel of NB cell lines frequently used in the laboratory (data not shown), as was expected for a house-keeping enzyme. To assess whether GPI could also be secreted from NB cells, the cell lines were maintained in serum-free medium for three days to reduce proteins from the calf serum, and this conditioned medium was collected and sterile filtered. The conditioned medium was concentrated, then analyzed on western blots. GPI was detected at its predicted size of 63 kDa in conditioned medium from SK-N-BE, IMR5, SY5Y, NGP, NB69 SK-N-AS and Kelly cells (Fig. 7), confirming the extracellular presence of GPI in all tested NB cell culture models. Since neurotrophin receptors play a crucial role in the development of NB, an SH-SY5Y cell model, stably transfected with either TrkA or TrkB was also included in the panel to assess whether neurotrophin receptor overexpression altered extracellular GPI levels. Higher amounts of GPI were detected in conditioned medium from TrkA overexpressing cells, whereas lower amounts of GPI were detected in medium conditioned by TrkB-transfected cells compared to the parental cell line. Since NBs often develop resistance to the chemotherapeutic agent used in therapy, a cisplatin-resistant cell line was also included in the panel to test for a possible correlation of resistance with

extracellular GPI. Higher amounts of GPI were also detected in conditioned medium from cisplatin-resistant SK-N-BE cells, compared to the parental cell line.

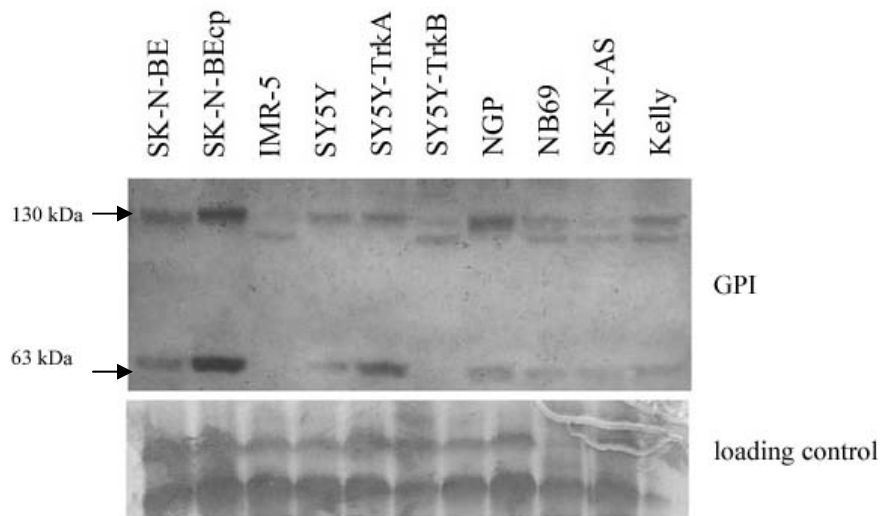


Fig. 7: GPI protein in conditioned media from neuroblastoma cell lines and expression cell models for Trk receptor proteins. The cells were cultured in serum-free medium for three days. The medium was removed, concentrated using Amicon[®] 5 kDa cut-off centrifugal concentration units and GPI protein was analyzed on western blots. Total protein content in the conditioned media was determined on SDS-PAGE via staining with coomassie brilliant blue R and used as a loading control.

In addition to the 63 kDa band, a second band of approximately 130 kDa was detected. GPI is known to dimerize (Sun et al. 1999), and the dimeric form has been reported to be approx. 130 kDa. However, since proteins separated using SDS-PAGE are applied to the gel and run under denaturing conditions, any secondary structures not connected by covalent bonds are interrupted. Therefore, if the dimer is linked by weaker interactions, only the monomeric form should have been observed. For the purpose of identifying the actual position of a GPI dimer on western blot, freshly prepared conditioned medium was cross-linked via glutaraldehyde to conserve any secondary structures and to preserve existing multimers. It was then concentrated using Amicon[®] concentration units and analyzed by western blotting for the presence of GPI (Fig. 8). While the concentrated but otherwise untreated conditioned medium contained GPI at both 63 and 130 kDa, the glutaraldehyde cross-linked sample showed only a single band at 130 kDa, showing that to be the actual position of the dimer.

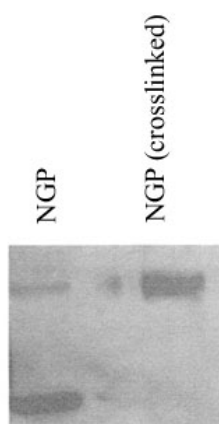


Fig. 8: Conditioned medium from NGP cells was concentrated by centrifugation through Amicon[®] concentration units and analyzed by western blotting with an antibody targeting GPI. The left lane shows the GPI protein in concentrated but otherwise untreated CM, the right lane shows GPI in the conditioned medium treated with glutaraldehyde before concentration to crosslink existing non-covalently bound multimers.

This experiment suggested that conditioned medium contained the dimeric form of GPI. The persistence of the dimer during denaturing SDS-PAGE could be due to a mechanical formation of bonds or steric conformations that formed during the concentration process. New conditioned medium was prepared and concentrated via evaporation at 39 °C instead of Amicon[®] concentration units. Only the 63 kDa GPI monomers were detected in medium concentrated by evaporation (data not shown), confirming that the persistent dimer formation was artefact of the concentration process. Taken together, GPI was detected in various amounts in conditioned medium from all NB cell lines in the panel examined. Extracellular GPI was elevated in cisplatin-resistant and TrkA-overexpressing cells compared to the parental cell lines. At least some of the extracellular GPI was present as dimers, the active form of the protein (Yanagawa et al. 2005), other than the persistent dimers produced as an artifact of concentration. Confirmation of extracellular GPI in NB cell cultures and published reports associating extracellular GPI with migration and invasion (Yanagawa et al. 2004; Torimura et al. 2001) indicated GPI could be an interesting target for future research.

4.1.3 YB-1 is expressed in neuroblastoma cells

YB-1 has also been shown to be involved in different aspects of tumorigenesis, as described in the introduction, making it an interesting candidate. Autoantibodies directed against YB-1 were detected in patient sera from all NB stages on the protein array, and these autoantibodies recognized different regions of the YB-1 protein. As the next step, YB-1 expression was evaluated in a panel of NB cell lines. The panel included cell lines with a single copy of *MYCN* as well as *MYCN*-amplified cell lines to represent both important NB phenotypic subgroups. Whole-cell extracts were prepared in RIPA buffer, and YB-1 was detected via western blotting (Fig. 9), YB-1

was expressed in similar amounts by all cell lines in the panel. No significant correlation between the amounts of YB-1 protein expression and *MYCN* status was observed

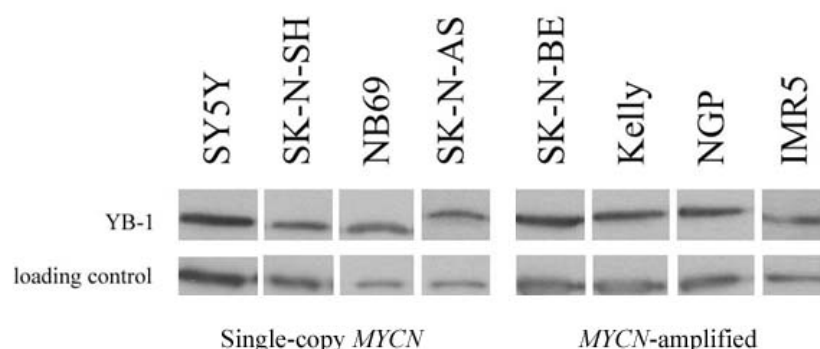


Fig. 9: Whole-cell extracts of NB cell lines were prepared in RIPA buffer and analyzed by western blotting using an antibody to YB-1. GAPDH was used as loading control. Single-copy and *MYCN*-amplified cell lines were included in the panel, a list of *MYCN* amplified cells can be found in the method section.

4.1.4 Use of a reverse ELISA to detect and quantify YB-1 autoantibodies in patient serum

4.1.4.1 Development of a YB-1 reverse ELISA

To verify the presence of autoantibodies against YB-1 in NB patient sera on an independent technological platform and to create a way to quantify YB-1 autoantibodies in serum samples from individual patients, a reverse ELISA was developed. Glutathione-coated 96-well ELISA plates and recombinant YB-1 protein (Abnova) N-terminally tagged with glutathione S-transferase (GST) were used. ELISA wells were incubated with 30 μ l of 0.05 M Tris-HCl containing 0.3 ng GST-tagged YB-1 protein as described in the materials and methods section (section 3.13). Through binding of the GST-tag to the glutathione on the well floor, the plates were evenly coated with YB-1 protein via a short tether and allowing better access to the protein for antibody binding. Unbound protein was removed in three rounds of washing and blocking of unspecific binding, as described in the method section.

4.1.4.2 Evaluation of the YB-1 reverse ELISA

In the process of developing the assay, its sensitivity was tested by addition of spiked-in amounts of murine YB-1 antibody (Abnova). The antibody was added to serum of healthy adults at a dilution of 1:100, then serial dilutions were performed with adult serum to reach YB-1 antibody dilution of 1:2000. For each well, 1 μ l of spike-in control serum dilution was then mixed with 29 μ l of blocking solution to a total volume of 30 μ l yielding final dilutions of 1:3000 up to 1:60,000. GST-tagged Galectin-1 protein in a final dilution of 1:3000 was used as a negative control to

exclude unspecific binding. Detection of bound antibody was achieved via a biotin-coupled polyclonal goat anti-mouse antibody (1:4000, Dako), followed by streptavidin-biotin complex (1:1000, GE Healthcare). Incubation and washing steps were performed as described in section 3.13. Quantification followed addition of 100 μ l BioFX® TMB Microwell Substrate (SurModics Inc.), which was converted by the horseradish peroxidase in the immune complexes. The conversion was stopped at 35 min, using 100 μ l BioFX® Stop Solution (SurModics Inc.). The graph shows a linear correlation of light emission and amounts of spiked-in YB-1 antibody. Strong signal detection was possible up to a dilution of 1:45,000 and the negative control showed very low unspecific binding. This experiment showed the possibility to detect and quantify low amounts of YB-1 antibody using the reverse ELISA.

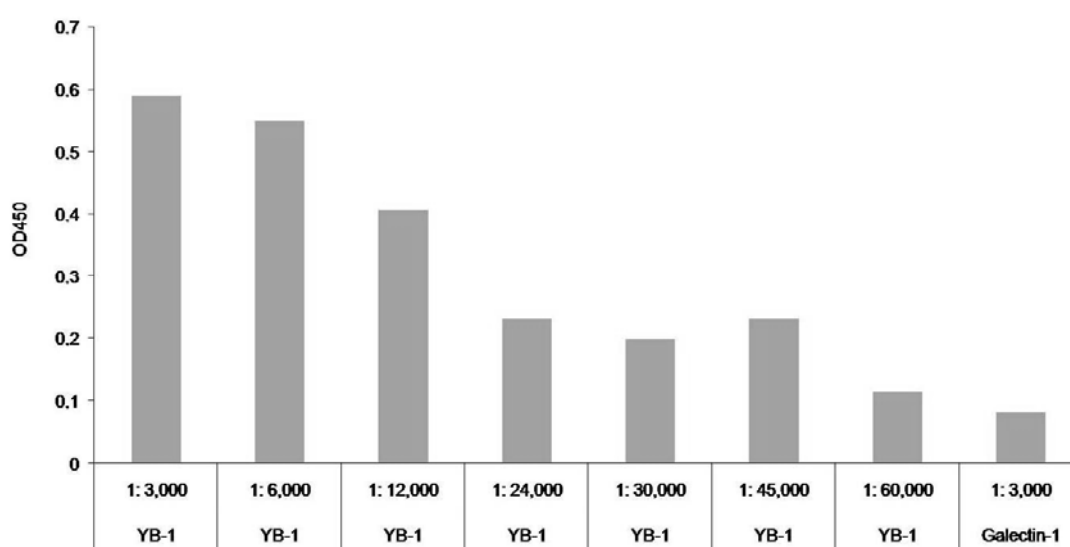


Fig. 10: Reverse ELISA detection of serum of healthy adults with spiked-in murine YB-1 antibody. Glutathione-coated plates were incubated with GST-tagged recombinant YB-1 protein to allow binding of the GST to the plate and presentation of the YB-1 protein as the ELISA target without steric hindrance by the plastic surface. To assess the sensitivity of the reverse ELISA, murine antibody was diluted in 100 μ l of serum from healthy adult volunteers, and 1 μ l of this dilution was further diluted in 29 μ l of blocking solution, yielding the final dilutions shown in the graph above. Antibody amounts were then detected via a secondary biotinylated anti-mouse antibody, as well as a streptavidin-coupled horseradish peroxidase for enzymatic quantification.

4.1.4.3 *Testing on clinical samples*

To detect YB-1 autoantibodies in NB patients, 3 μ l of patient serum diluted with 24 μ l of blocking solution to a total volume of 27 μ l was incubated per well. Blocking solution was used as a negative control. Control sera of healthy children were used as an additional negative control to detect only NB-specific autoantibodies. The pooled NB patient and control sera used in the protein array experiments were tested initially to confirm the results of the protein array. Detection of

bound YB-1 antibody was achieved via the same secondary anti-human antibody used in the protein array experiments and streptavidin-biotin-conjugated horseradish peroxidase as described in section 3.13. BioFX® TMB Microwell Substrate (SurModics Inc.) was used for quantification. It was converted by the horseradish peroxidase in the immune complexes within 10-60 min. The reaction was stopped and fixed by addition of 100 µl BioFX® Stop Solution (SurModics Inc.) and the absorbance at 450 nm was measured.

Serum samples from NB patients obtained at diagnosis were kindly provided by the serum bank at the University Hospital Göttingen, where samples were stored in a retrospective collection spanning more than 30 years of NB patient treatment in Germany. Considering the long time-span of collection and changing regard for standard collection procedures for patient samples, retrospectively collected samples were not collected or shipped using standard procedures to protect quality and comparability of protein samples. In the course of this project, new samples were collected at the University Hospital Essen, according to a standard operating procedure, developed to minimize protein degradation and allow better comparison between serum samples. Due to the rarity of this disease, however, these prospectively collected samples are few. Because of the possible differences in serum handling and quality, it was important to normalize individual serum samples in order to compare relative YB-1 antibody levels. YB-1 antibody levels were normalized to two different values representative for the total protein content of the serum. Initially, a prominent band was quantified in Coomassie brilliant blue R-stained gels on a gel documentation system, and later the amount of serum albumin was quantified using a commercially available ELISA (Human Albumin ELISA Kit; Assaypro). Standard spectrophotometric protein quantification was not feasible due to the small volumes of patient sera available. Initially, 3 µl of each serum sample were separated on continuous gradient (4 % to 12 %) SDS-PAGE. Electrophoresis is described in section 3.11. One specific band at approx. 100 kDa was chosen because it was well defined and strong enough for colorimetric measurement in all samples, but not such an abundant protein that differences in intensity were not detectable. Intensity of this protein band was measured in all lanes and used for normalization of antibody concentrations (Fig. 11). All serum samples used in this study were later analyzed using a commercially available ELISA for human serum albumin. Due to higher reproducibility and easier comparison of samples, the albumin ELISA was superior to the Coomassie brilliant blue R gel-based quantification method for normalizing YB-1 antibody levels in serum samples.

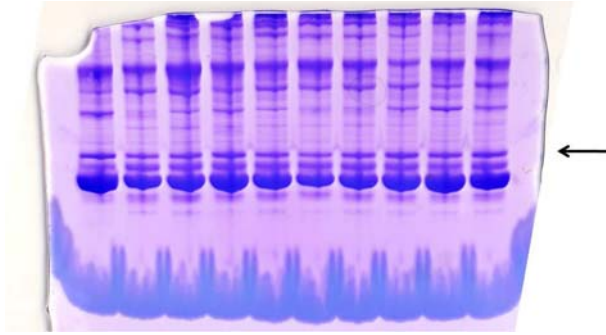


Fig. 11: Example of one gel used to determine total protein concentration of patient sera. Total protein content was stained with Coomassie brilliant blue R, and 3 μ l serum was loaded per lane onto a 4-12 % continuous gradient SDS-PAGE precast gel. Band intensity of the reference protein band (arrow) was colorimetric measured on the BioDoc system, and used to normalize antibody levels.

In the initial experiments analyzing the serum pools used in the protein array experiments, YB-1 antibodies were detected in all the serum pools from NB patients (Fig. 12). Highest levels were detected in serum from patients with stages 4 NB, the most prognostically unfavorable stage. All serum pools from NB patients, regardless of tumor stage, contained significantly higher levels of YB-1 antibody than the serum pool from age- and gender-matched healthy children. This validates the results from the protein array, where YB-1 autoantibodies were also detected in serum from all NB stages compared to healthy controls. While quantification of the array results was not possible, the reverse ELISA detected an approximately 9-fold elevation of YB-1 antibody in stage 4, 4-fold elevation in stage 4S and 5-fold elevation in stage 1 compared to control serum.

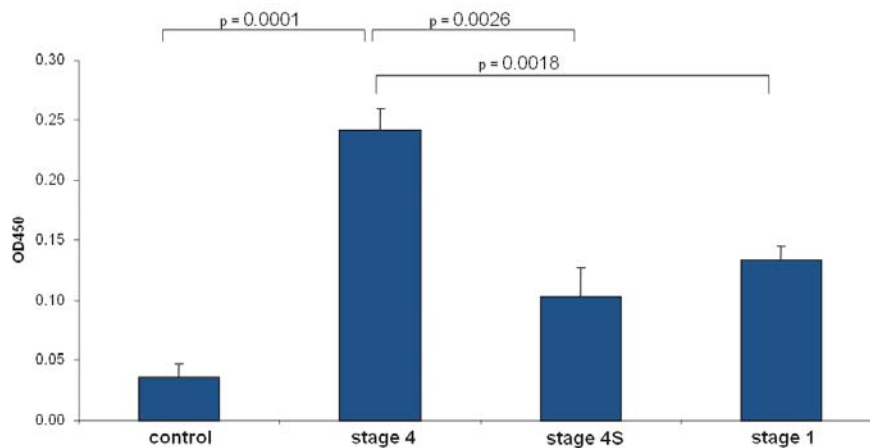


Fig. 12: Reverse ELISA detection of YB-1 antibody in pooled serum from NB patients with different tumor stages and healthy controls. Glutathione-coated plates were incubated with GST-tagged recombinant YB-1 protein to allow binding of the GST to the plate and present the YB-1 protein as the ELISA target. NB patient sera pooled according to stage and serum from healthy controls were incubated in wells overnight to allow binding of YB-1 antibodies in the serum. Antibody amounts were then detected via a secondary anti-human antibody coupled to horseradish peroxidase for enzymatic quantification. The experiment was performed in

duplicates, p-values were calculated using the student's unpaired t-test and light emission is shown as bar graphs of the mean value with whiskers representing the standard deviation.

Since the reverse ELISA was capable of detecting as low as a 1:45000 dilution of murine YB-1 antibody, was therefore shown to be sensitive enough (Fig. 10) and required only 3 μ l of serum, serum samples from individual patients could be analyzed. Fig. 13 shows YB-1 antibody levels of all tested single patient sera, normalized to human serum albumin concentration. Serum samples from two healthy adult volunteers were also included as negative controls and to assess possible age-specific differences for YB-1 antibody variability. YB-1 antibody levels in the adult sera were comparable to those in the healthy children.

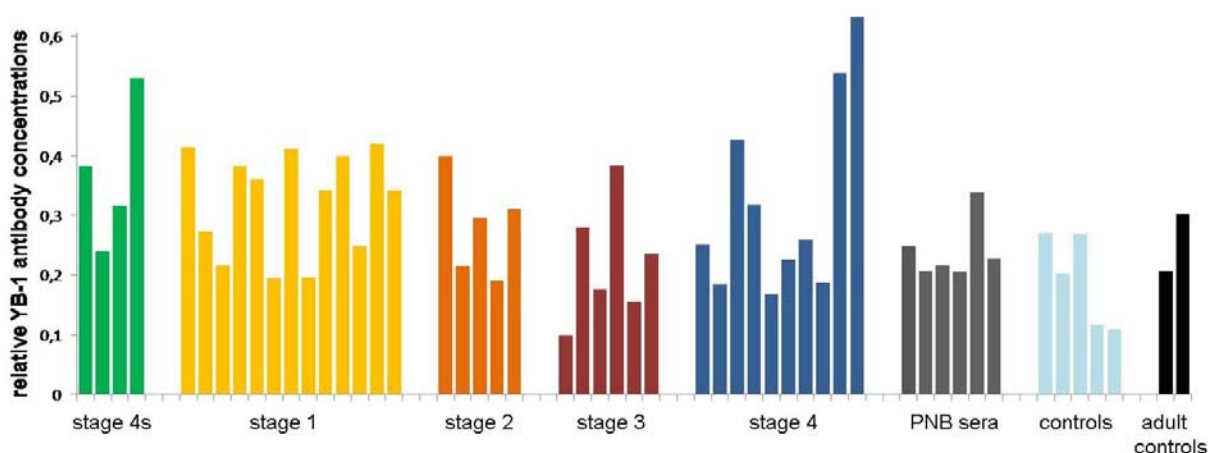
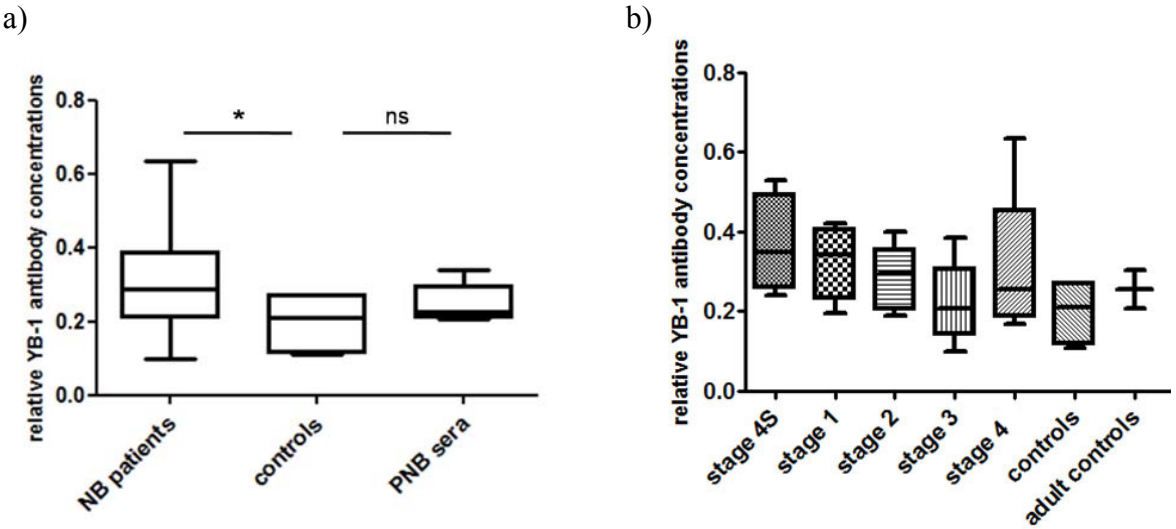


Fig. 13: YB-1 antibody concentrations in individual serum samples were analyzed using the YB-1 reverse ELISA. Stage 4s, stage 1, stage 2, stage 4 and stage 4 were retrospectively collected serum samples from NB patients. PNB sera included all serum samples collected prospectively from NB patients treated at the University Hospital Essen according to an SOP. Controls include serum samples from all healthy children and adult controls include serum samples from two healthy adults. Concentration of serum albumin was measured using a commercially available ELISA for human albumin and HSA concentration was used to normalize samples for comparison. YB-1 antibody levels in the individual sera are shown as bars representing the mean value.

Detected YB-1 antibody levels varied both between and within the NB stage groups. Statistical analysis was not conducted for differences between NB stages because of the limited sample number available for some groups and the lack of an obvious trend for elevated YB-1 antibodies in patients from a single stage. However, highest YB-1 antibody levels were detected in two serum samples from stage 4 NB patients as well as in one sample of a stage 4s patient and two of the three lowest levels were detected in serum samples from healthy controls. For further statistical analysis of the single patient sera, samples from NB patients were further divided into two subgroups based on the collection method of the sera as a quality control. Retrospectively collected samples from NB patients and serum samples prospectively collected from NB patients for this study using a

standard protocol were compared to controls in a box plot analysis (Fig. 14a). The group of NB patients showed significantly higher levels of YB-1 antibody in comparison to the controls, although the large range of the whiskers represents strong variation between individual patient samples within each group. Levels of YB-1 antibody in prospectively collected NB patient sera were not significantly different from antibody levels in the control sera although very few prospectively collected samples were available. Fig. 14b shows an alternative analysis of the data. Normalized YB-1 antibody levels of individual NB sera were now grouped by stage of disease and compared to controls. In addition to the control sera from healthy children, two adult controls were included in this analysis to assess the possible effect of patient age on YB-1 antibody levels. An unpaired t-test showed that significantly higher YB-1 antibody levels were detected in stage 4S and stage 1 patients in comparison to the controls. No significant difference was seen for the remaining stages or the adult controls. Overall, YB-1 antibody levels were significantly higher in serum from NB patients when data of all retrospectively collected NB sera was combined. The breakdown into individual stages showed that this increase is mostly due to high antibody levels in stage 4S and 1 sera while stage 4 sera showed the most statistical spread.



Unpaired t-tests for Fig. 14a

NB patients vs. controls:	$p = 0.0363$	significant
PNB sera vs. controls:	$p = 0.2298$	not significant
PNB sera vs. NB patients:	$p = 0.2885$	not significant

Unpaired t-tests for Fig. 14b

stage 4S NB vs. controls:	$p = 0.0233$	significant
stage 1 NB vs. controls:	$p = 0.0066$	significant
stage 2 NB vs. controls:	$p = 0.1018$	not significant

stage 3 NB vs. controls:	p = 0.6424	not significant
stage 4 NB vs. controls:	p = 0.1058	not significant

Fig. 14: YB-1 antibody concentrations in serum from groups of NB patients, healthy control children and healthy adults. Relative YB-1 antibody concentrations of individual sera were grouped and shown as a box plots in Fig. 14a and 14b. The results of unpaired t-tests are listed to compare all groups shown in the box-plots. NB patients included all retrospectively collected samples from NB patients with any stage. Controls include serum samples from all healthy children. PNB sera included all serum samples collected prospectively from NB patients treated at the University Hospital Essen according to an SOP.

4.1.5 YB-1 is present in medium conditioned by NB cell lines

Since autoantibodies were detected in serum from NB patients, it is possible that YB-1 was secreted by tumor cells or released by injured or dying tumor cells in amounts above what might normally be present in circulating serum, triggering an autoimmune response to this protein. It has been reported for monocytes and macrophages that YB-1 is actively secreted via a non-classical pathway where it acts as an extracellular mitogen for these cells (Frye et al. 2009). Medium conditioned by the NB cell line panel described above was analyzed for the presence of YB-1 protein using western blotting. Cell growth was monitored throughout the experiment to exclude unspecific protein release as a result of cell death resulting from overcrowded cultures. Various amounts of YB-1 protein were detected in conditioned medium from all NB cell lines analyzed (Fig.15). Highest levels were detected in conditioned medium from NB69 and SY5Y cell lines.

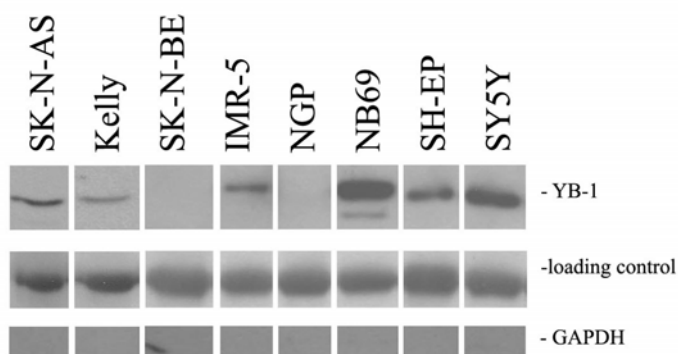


Fig. 15: Extracellular amounts of YB-1 protein, detected in conditioned medium of NB cells. Cells were cultivated in serum-free, supplemented RPMI for 72 h. Conditioned medium was then removed and centrifuged to remove nonadherent cells and cell debris. Conditioned medium was sterile filtered and protease inhibitors were added before concentrating it approx. 100-fold via centrifugation in Amicon® concentration units with a 5 kDa cut-off filter. Equal volumes were loaded onto SDS-PAGE, and western blot analysis was performed using an antibody against YB-1, followed by stripping the blot and detection of transferrin, a protein supplemented in equal amounts to the serum-free medium, and therefore, present in

roughly equal amounts in medium conditioned by every cell line. Transferrin was used as a loading control to assess differences in concentration between the samples. GAPDH was used as an additional control for unspecific release of protein.

The amount of extracellular YB-1 did not correlate with the presence of *MYCN*-amplification. Cell death and subsequent release of intracellular proteins was excluded via staining with methylene blue which can be taken up by dead or injured cells but leaves intact cells colorless (Bonora 1982). To stain the cells with methylene blue, the supernatant was removed first and used for analysis of extracellular protein as described in section 3.9. Trypsin was added to cover the cell layer and incubated with the cells for 3-5 min. Trypsinized cells were mixed with 10 ml of complete medium and 200 μ l methylene blue was added. After 1 min incubation, blue cells were counted under the microscope and a ratio of dead cells and overall cell number was calculated. Additionally, western blot analysis for the cytosolic protein GAPDH was performed for all conditioned media as an indicator for unspecific protein release from injured or dying cells. Low levels of GAPDH were only detected in conditioned medium from the SK-N-BE cell line. This cell line showed lowest amounts of extracellular YB-1, which renders unspecific release of YB-1 unlikely. Extracellular YB-1 levels were not correlated with indicators of increased nonspecific protein release. These data in addition to published reports that active secretion of YB-1 can occur indicate that extracellular protein most probably was a result of active and selective secretion of YB-1.

4.2 ASSOCIATION OF YB-1 WITH KNOWN NEUROBLASTOMA MARKER PROTEINS

4.2.1 YB-1 is associated with TrkA expression in the SY5Y cell line

The possible correlation between YB-1 and other proteins known to play a role in NB development and pathogenesis were next addressed in NB cell culture models. Neurotrophin receptors play an important role in the progression of neuroblastoma. While TrkA expression in the tumor is generally linked to disease stages with a better patient prognosis, TrkB expression is associated with an unfavorable prognosis (Ho et al. 2002). NB cell models stably overexpressing either the TrkA or the TrkB receptors are established in the laboratory. To examine a possible relationship between YB-1 and neurotrophin receptor expression, whole cell lysates of 3 NB cell lines stably expressing Trk-A were prepared in RIPA buffer, and YB-1 expression was compared to the parental cell lines using western blot analysis. YB-1 expression was significantly lower in TrkA-expressing SY5Y cells, but no significant differences in YB-1 expression between TrkA-expressing and parental cells were observed for the NB69 and IMR-5 cell lines (Fig.16). Additionally, expression of the YB-1 protein in a TrkB-overexpressing NB cell culture model of the NB cell line SY5Y was compared to expression the parental cell line. No differences in YB-1 protein

expression were observed here (data not shown). Taken together, while there may be some relationship in terms of an inverse correlation between YB-1 and TrkA expression in the SY5Y cell line, this correlation was not seen in the other two tested cell line models and more research is needed in order to assess this correlation.

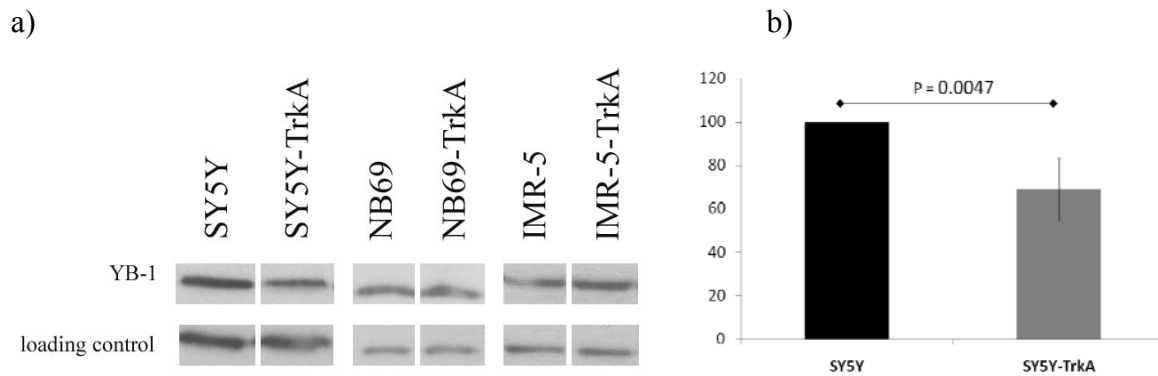


Fig. 16: YB-1 protein expression in TrkA-overexpressing NB cell culture models. **a)** Whole-cell lysates were prepared in RIPA buffer and analyzed by western blotting. GAPDH was used as loading control. **b)** Band intensity was measured for YB-1 expression in SY5Y-TrkA and parental cells and normalized to GAPDH expression from 3 independent experiments. Bars represent the mean relative YB-1 expression \pm standard deviation, and an unpaired t-test was performed to test for a significant difference in expression.

4.2.2 MYCN activates expression of YB-1 and promoter binding analysis confirms that both MYCN and c-Myc bind can the YB-1 promoter and activate transcription

MYCN amplification is one of the major prognostic factors for NB, and is associated with poor outcome. Members of the Myc protein family bind as heterodimers to the E-box motif, CACGTG, which is also found in the *YB-1* promoter (Norris et al. 1997). Although no clear association between YB-1 expression and MYCN amplification was observed for NB cell lines, many amplified cell lines did strongly express YB-1. Two different inducible NB cell culture models for MYCN were used to assess whether MYCN could affect YB-1 expression. The SH-EP-MYCN-ER cell line is an inducible system that holds transcriptionally inactive MYCN tethered in the cytoplasm to an engineered form of the estrogen receptor in the inactive state (Schulte et al. 2008). Treatment of the cells with 4-hydroxy-tamoxifen (4-OHT) binds the estrogen receptor allowing translocation of the fusion protein to the nucleus and activation of MYCN, which can be monitored via mRNA expression of the MYCN target gene, *ODC1*. Successful induction, resulting in a strong activation of MYCN and increased *ODC1* transcription was confirmed after 72 h treatment with 200 μ mol 4-OHT/l culture medium. *YB-1* expression was determined by semi-quantitative RT-PCR at this time, and a strong increase of *YB-1* expression was detected in the induced SH-EP-MYCN-ER cell line in comparison to the untreated control. (Fig.17).

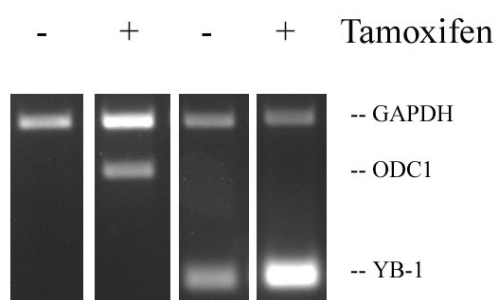
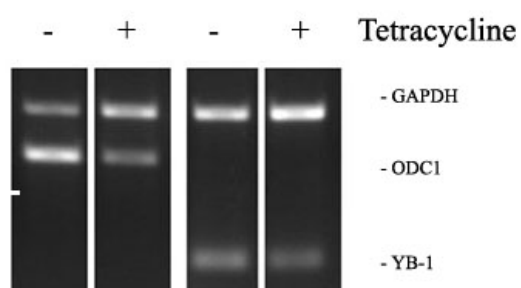


Fig. 17: Semi-quantitative RT-PCR showing mRNA expression levels of *YB-1* and *ODC1*. MYCN activation was induced by 72 h treatment with 200 μ mol 4-OHT/l culture medium, uninduced control cells were cultured in complete medium alone. Total RNA was isolated at 72 h and used for reverse transcription. *GAPDH* expression was used as an internal loading control.

The Tet-21/N cell line is a conditional expression system in which tetracycline treatment reduces *MYCN* expression at the transcript level by at least 15-fold (Lutz et al. 1996). Tet-21/N cells were cultured in the presence of 1 μ g/ml tetracycline for 72 h, MYCN activity was monitored by assessing levels of *ODC1* mRNA via semi-quantitative RT-PCR. At 72 h, *ODC1* expression was reduced by 70-80 %. Tetracycline treatment for 72 h also strongly decreased *YB-1* expression (Fig.18a). Western blot analysis of YB-1 and MYCN expression in whole-cell extracts from Tet-21/N cells treated for 72 h with tetracycline also showed reduced levels of both MYCN and YB-1 proteins (Fig. 18b). Fig.18c shows relative band intensities of YB-1 expression derived from the western blot in Fig. 18 b as a bar graph. YB-1 and GAPDH band intensities were measured and YB-1 expression was normalized to GAPDH expression. The data obtained using these two inducible model systems supports that MYCN expression or activity activates *YB-1* expression either directly or indirectly as a downstream target.

a)



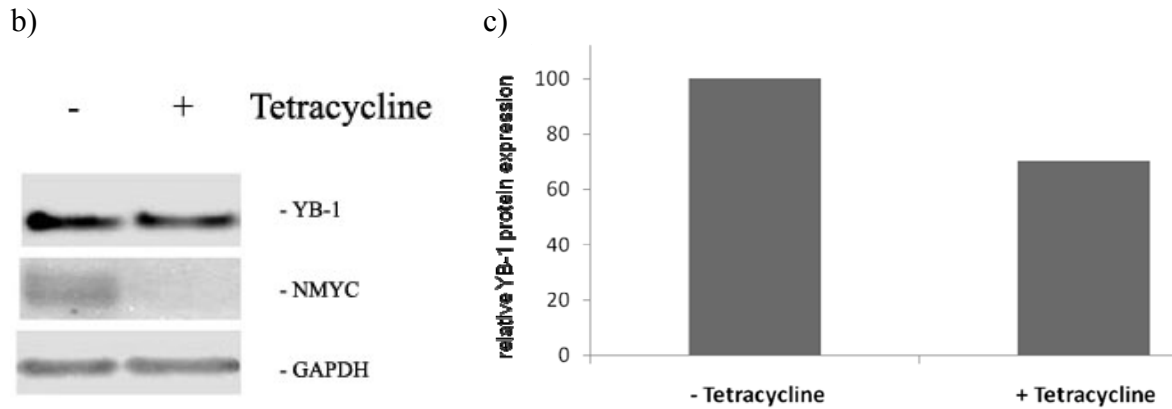


Fig. 18: Tetracycline-mediated repression of *MYCN* expression in Tet-21/N cells also reduced YB-1 expression on both mRNA and protein levels. a) Cells were cultured either with or without 1 μ g/ml tetracycline, and total RNA was isolated after 72 h then reverse transcribed. *OCD1* and *YB-1* expression were determined by semi-quantitative RT-PCR. GAPDH was used as an internal loading control. The experiment was performed three times. b) Whole-cell lysates were prepared in RIPA buffer after 72 h tetracycline treatment as in a, and analyzed via western blotting. YB-1 and MYCN proteins were detected, and GAPDH protein levels were used as a loading control. c) YB-1 and GAPDH band intensities of the western blot, shown in Fig. 18b were measured using the UVI chemi system (Biometra). YB-1 expression was normalized to GAPDH expression, and is shown as a bar graph.

Since MYCN induced *YB-1* transcription and the *YB-1* promotor contains an E-box binding motif for MYCN, we asked whether *YB-1* could be a direct target of MYCN. Binding of the MYCN or c-Myc proteins to gene promoters was analyzed using ChIP-chip technology in cooperation with F. Westermann (DKFZ, Heidelberg). Either the MYCN or c-Myc protein was immunoprecipitated from cell lysates of a panel of NB cell lines (Kelly, IMR-5, SH-EP and SH-SY5Y cell lines as well as the WAC2 cell line, which constitutively expresses the *MYCN* transgene) after cross-linking DNA-protein complexes with formamide. Binding to the YB-1 promoter was assessed in a chip format to confirm a direct interaction of Myc proteins with the YB-1 promoter. MYCN bound to the CpG region of the *YB-1* promoter region as well as to the canonical e-box in all cell lines examined (Fig. 19). Double binding peaks for H3K4me3 are characteristic for genes activated by Myc proteins using this methodology. The valley between the peaks is indicative of the area of transcriptional start. This type of curve indicates that Myc proteins bind to regions of the promoter to activate transcription, rather than distinctly to the canonical e-box. Marks for active transcription (H3K4me3), transcript elongation (H3K36me3) and transcriptional repression (H3K27me3) were also analyzed, showing that not only did Myc proteins bind to the promoter, but that transcription of the *YB-1* mRNA occurred. Marks for transcriptional activation of *YB-1* were strongly bound by Myc proteins relative to other promoters analyzed using this ChIP-chip platform. These data show that both MYCN and c-Myc can bind the *YB-1* promoter and activate transcription in NB cells.

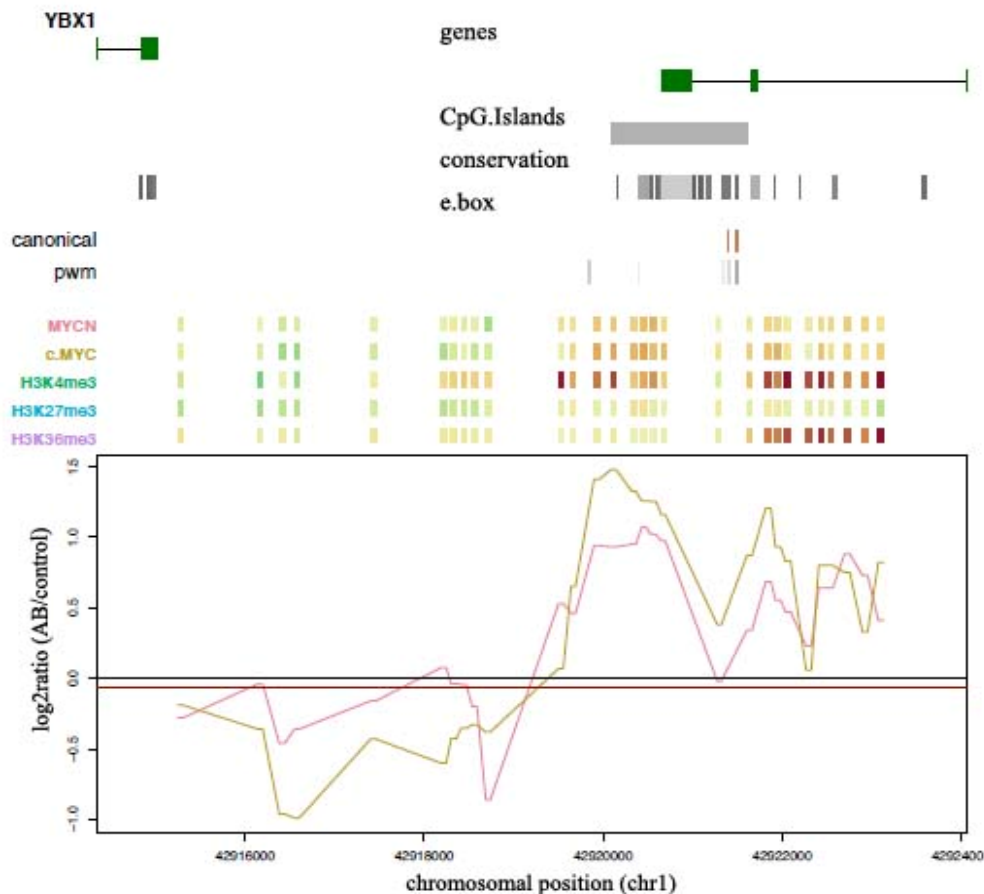


Fig. 19: Both MYCN and c-MYC proteins bind to the *YB-1* promoter in NB cell lines. Binding was analyzed using ChIP-chip technology, and included histone marks for active transcription (H3K4me3), transcript elongation (H3K36me3) and transcriptional repression (H3K27me3). Binding strength is shown in a color scale ranging from green tones (no binding) to red tones (strong binding). Binding for lysates from the Kelly cell line are shown as an example, and binding from other cell lines are shown in Appendix I.

4.3 INFLUENCE OF YB1 ON PROLIFERATION

4.3.1 Downregulation of YB-1 reduces cell viability

To further investigate the role of YB-1 for NB cells, YB-1 expression was downregulated by siRNA-mediated knockdown in NB cell lines. A role for YB-1 in proliferation has been described (Lu et al. 2005; Uchiyama et al. 2006) so proliferation and viability were assessed for NB cells after YB-1 downregulation. Since knockdown of YB-1 was shown to sensitize cells to cisplatin (Ohga et al. 1996), the cisplatin-resistant subline, SK-N-BEcp was included in the experiments as well. The SK-N-BE cell line and a cisplatin-resistant subline, SK-N-BEcp, were transfected with siRNA targeting YB-1 or mock control. Scrambled nonspecific control siRNAs were used as an additional control in initial experiments to exclude the possibility of nonspecific effects of siRNA transfection. mRNA expression of mock controls was comparable to expression in cells transfected

with scrambled control siRNA. *YB-1* expression was quantified 72 h after transfection using real-time RT-PCR and normalized against *GAPDH* expression. *YB-1* expression was reduced by 48 % in SK-N-BE cells and by 61 % in SK-N-BEcp cells in relation to the mock-transfected controls by siRNA transfection (Fig. 20a). To assess the timepoint of maximum protein reduction, YB-1 protein expression was analyzed via western blotting. The SK-N-BE and the SK-N-BEcp cell line were transfected with siRNA targeting YB-1 or mock control and whole-cell protein lysates were produced in RIPA buffer 48 h, 72 h and 96 h after siRNA transfection. Maximum reduction of YB-1 expression (by 70-80 %) was obtained 72 h after transfection for both cell lines (Fig. 20 b/c). Microscopic observation of the transfected and mock-transfected cultures throughout the experiments showed no obvious changes in cell morphology or adhesion as indication of increased cell death following YB-1 downregulation.

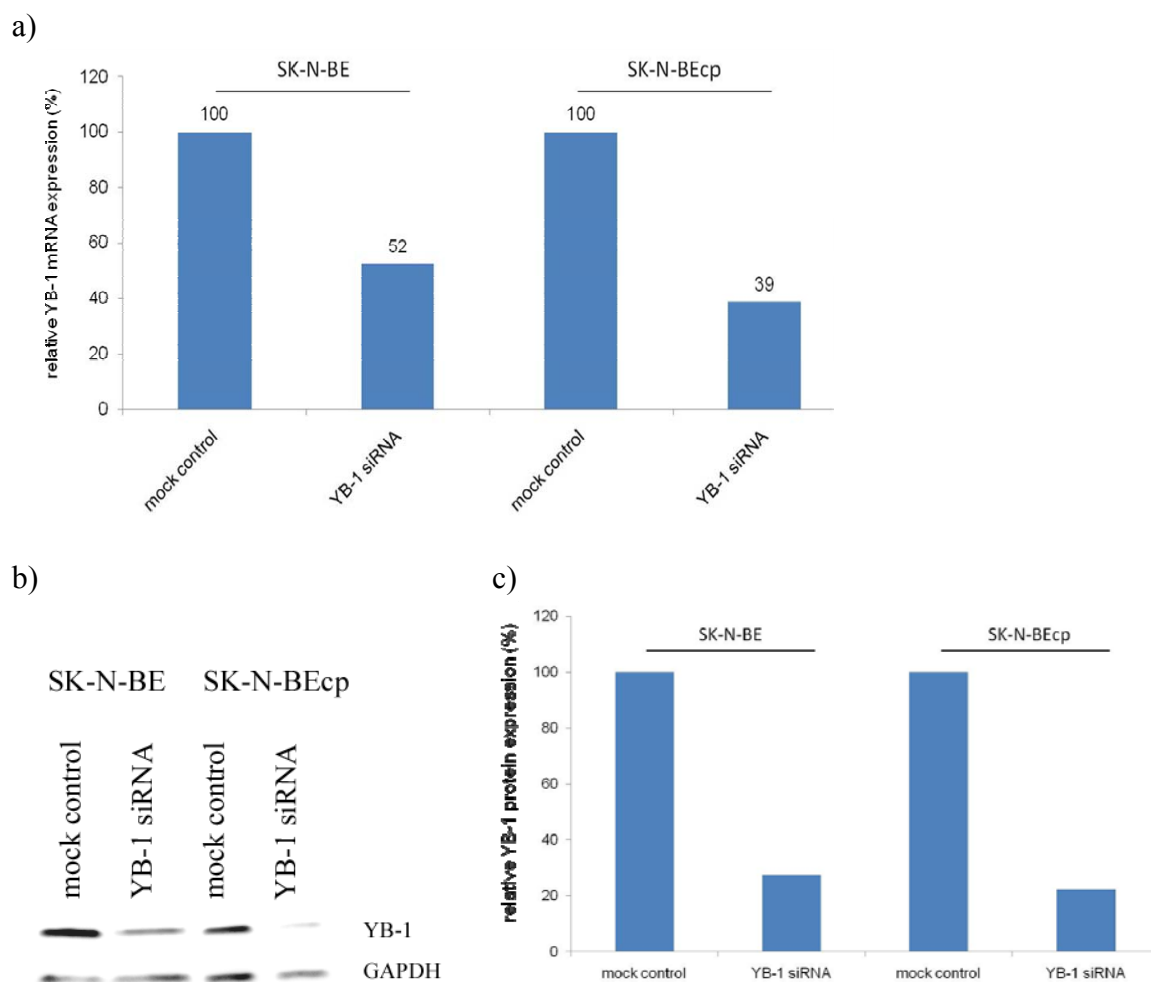


Fig. 20: Efficiency of siRNA-mediated knockdown of YB-1 expression on mRNA and protein level a) Cells were transfected with siRNA targeting YB-1 or mock-transfected. Total RNA was isolated and reverse transcribed for real-time PCR using the Applied Biosystems StepOnePlus™ system. YB-1 expression was normalized to the GAPDH housekeeping gene. Relative expression was set to 100 % in the mock-transfected controls and bars show relative YB-1 mRNA expression. b) To quantify downregulation once on protein

level, whole-cell lysates were made in RIPA buffer 72 h after transfection, and analyzed on western blot with antibodies targeting YB-1 and GAPDH (as a loading control) c) Band intensities of the western blot in Fig. 20b were measured, normalized against GAPDH protein expression. Bars show relative YB-1 expression.

Transient transfection with siRNA targeting YB-1 maximally reduced YB-1 expression at the protein level 72 h after transfection, but could not eliminate YB-1 protein expression entirely. However, with a 70-80 % reduction in protein, siRNA-mediated knockdown should be useful to assess the impact of YB-1 on cell viability after cytotoxic drug treatment. YB-1 knockdown has been reported to increase the sensitivity of human epidermoid cells to cytostatic drugs (Ohga et al. 1996), and it was of interest if this was also the case in NB cells. YB-1 was downregulated in SK-N-BE and SK-N-BEcp cells, and cell viability in the absence and presence of cisplatin was monitored. For this, cells were transfected with siRNA targeting YB-1 or mock transfected, then cisplatin was added to the medium of the treatment group 48 h after transfection. Viability was assessed using a MTT assay 24 h later. These timepoints were chosen so that maximal YB-1 protein downregulation occurred during cisplatin treatment. Knockdown of YB-1 significantly decreased viability of both SK-N-BE and SK-N-BEcp cells compared to the mock-transfected controls (Fig. 21). However, sensitivity of either cell line to cisplatin remained unchanged in cells with normal or repressed YB-1 expression. These results support a general involvement of YB-1 in proliferation, but no specific role in protection against cytostatic drug treatment.

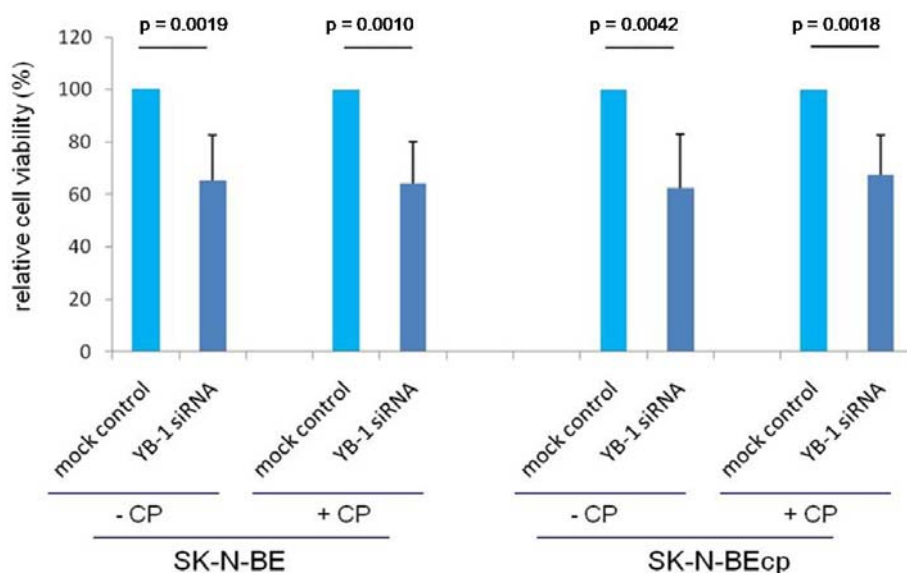


Fig. 21: YB-1 downregulation reduces cell viability in both parental and cisplatin-resistant SK-N-BE cells. Cells were transfected with siRNA targeting YB1 or mock-transfected, then treated with or without 12.5 µg/ml or 17.5 µg/ml (for SK-N-BE or cisplatin-resistant cells, respectively) for 4 h starting 48 h after transfection. Cells were incubated for another 24 h in regular medium until viability was assessed via MTT assay. The mean OD values for mock-transfected and untreated controls were set to 100 %, and bars show

mean viability relative to the controls \pm S.D. Significance was calculated using the unpaired t-test and p-values are shown above the comparison.

4.4 ASSOCIATION OF YB-1 WITH REPAIR AND DEVELOPMENT OF RESISTANCE IN NB

4.4.1 YB-1 is involved in the repair of double-strand breaks in NB

Double-strand breaks (DSBs) are a result of irradiation, but may also occur spontaneously during cell cycle progression. They are usually repaired fast, mainly through the repair pathway of non-homologous end joining (NHEJ). It has been described in human embryonic kidney cells that YB1 binds to various repair proteins of the NHEJ pathway, such as Ku80 (Gaudreault et al. 2004). To explore the role of YB-1 for repair mechanisms of DSBs in NB, cells were treated with siRNA targeting YB-1 and DSBs were counted per nucleus. Immunofluorescent labeling of γ -H2AX, a phosphorylated protein, which binds DNA at the site of DSB (Kuo et al. 2008) was used for detection of DSBs. γ -H2AX foci in the nucleus indicate the site of a DSB, and can be manually counted under the microscope. (Fig. 22a). In order to allow statistical analysis, 100 nuclei were counted for each sample. Cells were grown under standard conditions to observe the effect of YB-1 depletion on DSBs throughout the normal cell cycle. Knockdown of YB-1 led to a significant increase of the average number of DSBs per nucleus in SK-N-BE cells. This accumulation of DNA lesions shows that YB-1 downregulation hampers the cells capability to repair DSBs efficiently, and points towards a role of YB-1 in repair mechanisms of NB. Interestingly, knockdown of YB-1 did not lead to a significant increase of DSBs in the cisplatin-resistant SK-N-BEcp cells.

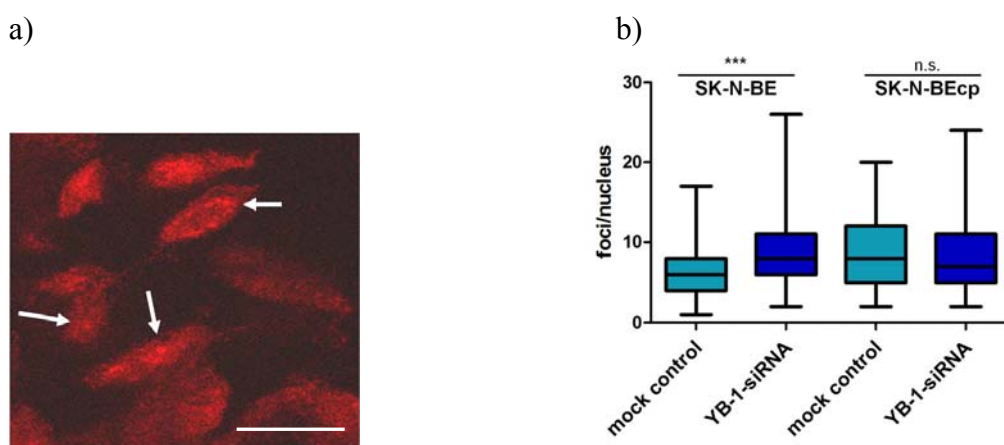


Fig. 22: YB-1 downregulation increases DSBs in SK-N-BE cells a) SK-N-BE and SK-N-BEcp cells were grown on coverslips, and transfected with YB-1 targeting siRNA or mock-transfected for a control. Cells were fixed using 4 % paraformaldehyde 72 h after transfection. An immunofluorescently labeled antibody against γ -H2AX was used to visualize DSBs in the nucleus, and γ -H2AX foci (white arrows) were counted.

A total of 100 nuclei were counted per sample from 3 independent experiments. Bar 25 μm b) Box-plots show the combined results from all experimental data and statistical analysis. Boxes represent the 25th to the 75th percentile of each group with the median of each group as the middle line; whiskers are drawn up to the minimum and maximum value of each group. *** $p < 0.0001$; n.s. $p = 0.1551$ Experiments was performed in cooperation with Steffi Kuhfittig-Kulle.

4.4.2 The effect of YB-1 downregulation on DNA adduct formation

YB-1 downregulation increased the number of γ -H2AX foci in NB cells and heightened susceptibility to cisplatin, observed by the decrease in cell viability. To address whether other repair pathways might be influenced by YB-1 depletion, effects of knockdown on nucleotide excision repair (NER) were studied. NER is the primary mechanism used for the repair of intrastrand cross-links, which is the major lesion caused by cisplatin-induced DNA damage (Basu et al. 2010). SK-N-BE and SK-N-BEcp cells were transfected with siRNA targeting YB-1, and were pulse-treated with cisplatin 48 h after transfection cells as in previous experiments for cisplatin treatment. After an additional 24 h, cells were fixed on coverslips and stained with an antibody against DNA-adducts for quantification. Downregulation of YB-1 did not lead to significantly altered adduct quantity in SK-N-BE or SK-N-BE cp cells.

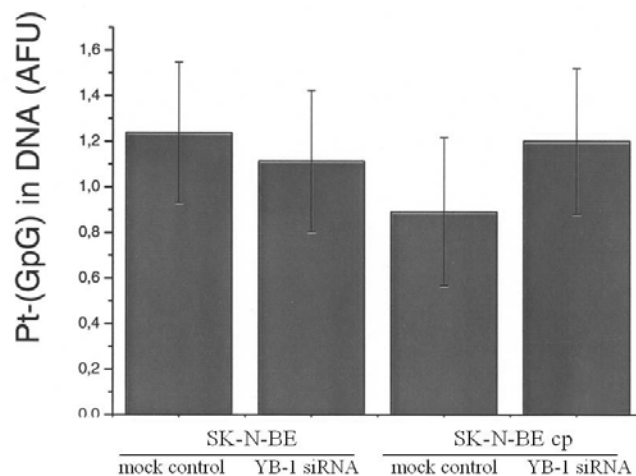


Fig. 23: Quantification of DNA adducts in NB cells after YB-1 downregulation in the presence of cisplatin treatment. Cells were transiently transfected with siRNA targeting YB-1 or mock-transfected as controls. All cultures were treated with cisplatin for 4 h (SK-N-BE cells with 12.5 $\mu\text{g/ml}$ and SK-N-BEcp with 17.5 $\mu\text{g/ml}$), 48 h after transfection. Cisplatin-induced DNA adducts (Pt-(GpG)) were detected by immunostaining. Antibody-derived signals were normalized for the total DNA content of a given cell, and expressed as arbitrary fluorescence units (AFU).

4.4.3 *YB-1 localization in response to cisplatin*

YB1 is linked to various mechanisms in the cytoplasm as well as in the nucleus. The process of shutteling within the cells compartments is strictly regulated and it has been shown for several tumor types, e.g. non small lung cancer (Shibahara et al. 2001), that the cellular localization of YB-1 is an important marker of prognostic stage or tumor malignancy. Since it has also been shown that translocation of YB-1 occurs in response to cytostatic agents (Koike et al. 1997; Stein et al. 2001), the intracellular localization of YB-1 in response cisplatin treatment was assed here for NB cells. SK-N-BE and SK-N-BEcp cells were grown on cover slips and then kept in medium containing cisplatin for 24 h. Microscopic controls showed that cells were attached and evenly spread after the incubation period. Cells were subsequently stained with an immunoflourescent antibody against YB-1 to monitor the intracellular location. Nuclei were stained with 4',6-diamidino-2-phenylindole (DAPI). A diffuse staining of the nucleus as well as a cytoplasmic signal was observed in SK-N-BE cells (Fig.24). Cisplatin treatment did not significantly alter the YB-1 distribution. However, a discrete formation of foci was observed in some regions but these changes could not be clearly allocated to the nucleus. The cisplatin-resistant subline, grown in regular medium, did show a more intensive, predominantly cytoplasmic, staining, Nuclei appeared larger and showed a grained structure of the immunoflourescent labeling. Addition of cisplatin did not significantly alter the distribution pattern but a minor increase of stained spots could be observed. Taken together, YB-1 showed a predominantly cytoplasmic localization in both cell lines analyzed. The grained and more intense staining of cisplatin-resistant cells might be because of increased YB-1 expression or may be due to accumulation of the protein. Cisplatin in the concentrations used in this experiment did not result in significant translocation but seemed to increase the overall amount of YB-1 protein levels in both cell lines.

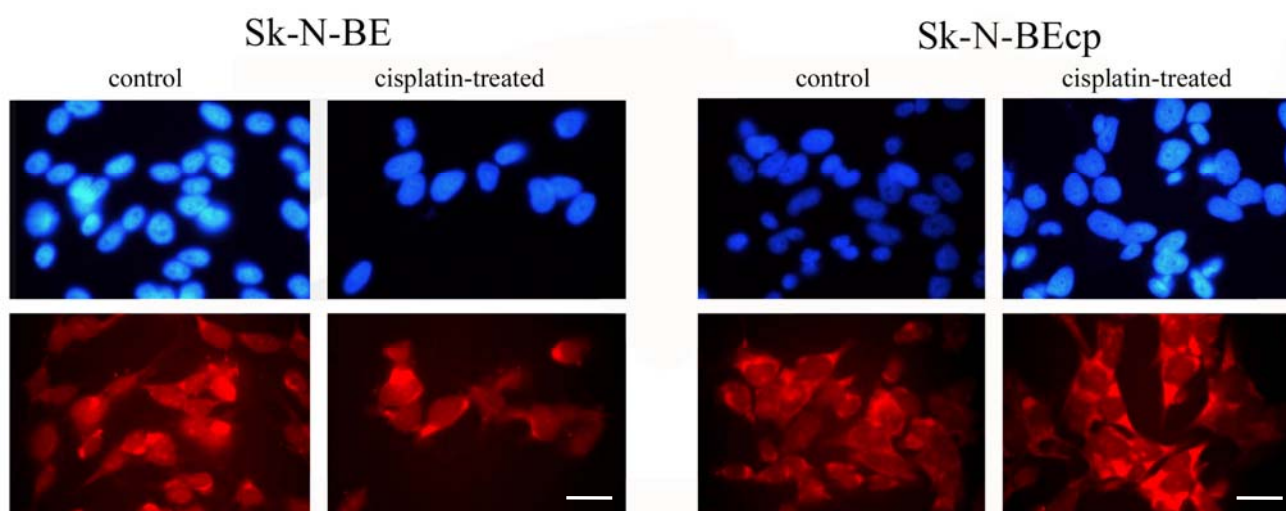


Fig. 24: Intracellular distribution of YB-1 protein in the absence and presence of cisplatin. Cells were grown on cover slips and incubated with cisplatin for 24 h. SK-N-BE cells kept in medium containing 7.5 $\mu\text{g/ml}$

cisplatin, cisplatin-resistant SK-N-BE were incubated with 12.5 $\mu\text{g/ml}$. Cells were fixed using 4 % paraformaldehyde and stained with a primary antibody targeting YB-1 as well as a secondary antibody, fluorescently labeled with Texas Red. 4',6-diamidino-2-phenylindole (DAPI) was used to stain the nuclei. Bars 25 μm .

4.4.4 *Cisplatin treatment increases YB-1 expression*

YB-1 downregulation has been reported to increase the sensitivity of human epidermoid cells to cytostatic drugs (Ohga et al. 1996), and the results of the immunofluorescent staining for YB-1 described in section 3.15 pointed towards increased expression of the protein in response to a cytostatic agent. While immunofluorescence is a good method to assess intracellular distribution, it is limited for quantifying changes in protein expression. Western blot analysis was performed using whole-cell RIPA extracts of SK-N-BE and SK-N-BEcp cells treated with cisplatin, and relative YB-1 protein expression was assessed. Western blot analysis showed a significant increase of YB-1 protein in cisplatin-treated cells in comparison to the untreated controls for both cell lines (Fig. 25). The upregulation of YB-1 in response to cisplatin in NB cells indicates a role for YB-1 in responding to cytostatic agents. YB-1 upregulation may help the cells to deal with DNA damage and improve repair capacities.

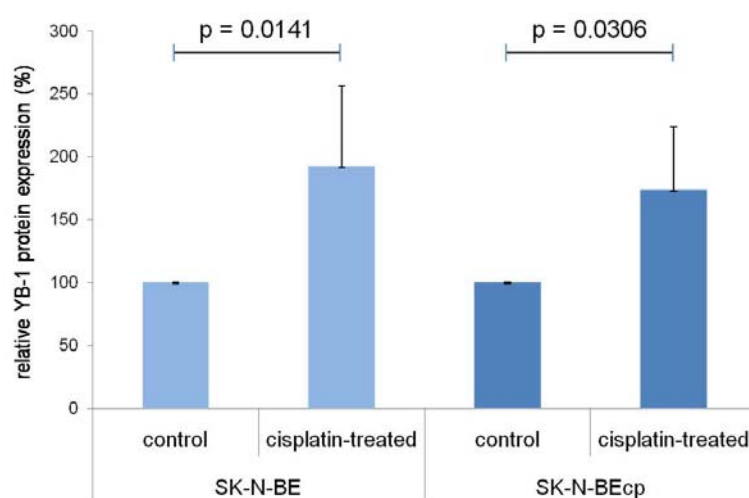


Fig. 25: Cisplatin treatment increased YB-1 protein expression in both parental and cisplatin-resistant SK-N-BE cells. Cells were treated with cisplatin (12.5 $\mu\text{g/ml}$ for the SK-N-BE cells and 17.5 $\mu\text{g/ml}$ for the cisplatin-resistant cells) for 2h. Whole-cell lysates were prepared in RIPA buffer. The YB-1 and GAPDH proteins were detected via western blot analysis. Band intensity of both proteins was quantified, and YB-1 expression was normalized to GAPDH expression. Relative YB-1 expression was set to 100 % for untreated controls of both cell lines to allow comparison. Bars represent the mean of at least 3 independent experiments with whiskers representing the standard deviation. Significance was assessed using an unpaired t-test.

4.4.5 *YB-1 binds to various repair proteins*

The results of the experiments presented above indicate that YB-1 participates in DNA repair mechanisms in NB cells. To further explore this involvement, co-immunoprecipitation (Co-IP) experiments were used to detect YB-1 interactions with repair proteins. Whole-cell lysates were prepared in RIPA buffer and were precleared with Preclearing Matrix F (ExactaCruz, Santa Cruz) to remove proteins that unspecifically bind the co-immunoprecipitation matrix. Formation of the antibody-IP matrix complex and incubation with the precleared cell lysate was performed as described in section 3.12. Rat IgG was used as a negative control. To develop the assay and to establish optimal binding conditions for each antibody, the washing of the matrix was performed three times with PBS and/or, for more stringent conditions, with RIPA buffer. Best results were obtained for all antibodies when washed twice with RIPA and then once with PBS, each washing step was performed for 15 min on a rotary shaker at 4 °C. Proteins bound to the matrix were eluted and separated on a NuPAGE® BisTRIS 4-12 % polyacrylamide gradient gel, and 20 µl aliquots of the supernatant at each step were also analyzed by western blotting to control for the removal of non-specifically bound proteins during the washing of the matrix. An example of the Co-IP with Ku80, including supernatants from all washing steps is shown in Fig. 26.

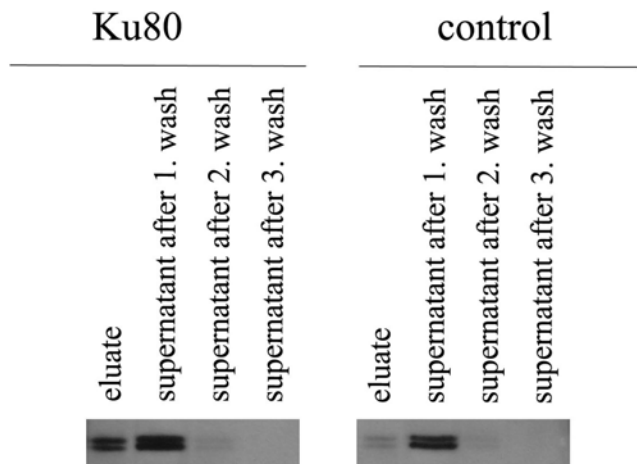


Fig. 26: Co-IP shows binding of YB-1 to the repair protein Ku80 in whole-cell NB lysate of NB cells. Whole-cell extracts of SK-N-BE cells were prepared in RIPA buffer. A preclearing step was performed as described in the methods section. Co-IP with a YB-1 antibody and a negative control (rat IgG) was performed with the precleared lysates. Bound YB-1 protein with its binding partners was eluted after several washing steps and YB-1 protein was detected in whole-cell lysates, the eluates and each supernatant using western blotting.

Ku80, is involved in the NHEJ repair pathway, and was reported to interact with YB-1 in human 293 embryonic kidney cells (Gaudreault et al. 2004). Ku80 was chosen as a positive control, and another protein from this pathway was selected, namely Rad51. In order to assess a second repair

pathway, XPC and ERCC1, which are involved in NER, were chosen. NER is the primary mechanism for the repair of cisplatin-induced damage, and even though YB-1 downregulation did not significantly abolish the repair of DNA adducts in NB cells, it was still shown that YB-1 was upregulated in response to cisplatin. Since a role of YB-1 in resistance to cisplatin has been described in literature for human epidermoid cancer cells (Ohga et al. 1996), binding of YB-1 to NER repair proteins may still be conceivable. Co-immunoprecipitations utilized Ku80, XPC and Rad51 antibody linked to beads (Immunoprecipitation Kit Santa Cruz Biotechnology) and whole-cell lysates of SK-N-BE cells in RIPA buffer. Binding of YB-1 to Ku80, was verified for the NB cells (Fig. 27a). More YB-1 protein was detected in the eluate from XPC-coated beads than the eluate from the rat IgG-coated beads used in the control co-immunoprecipitation (Fig. 27b), indicating that XPC was also bound to YB-1 in the whole-cell lysates. Binding of the Rad51 protein and YB-1 in whole-cell extracts was also detected compared to nonspecific binding to the control beads (Fig. 27c). To examine, whether binding of YB-1 to Ku80 is further enhanced in the presence of cytostatic agents, the co-immunoprecipitation was repeated using whole-cell lysates from NB cells treated 4 h with 12.5 μ g/ml cisplatin, however, enhanced binding was not observed here (data not shown).

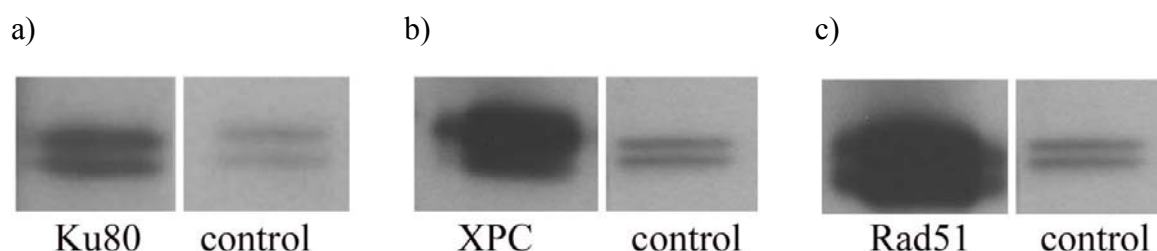


Fig. 27: Co-IP shows binding of YB-1 to the repair proteins Ku80, XPC and Rad51 in whole-cell NB lysate of NB cells. Whole-cell extracts of SK-N-BE cells were prepared in RIPA buffer. A preclearing step was performed as described in the methods section. Co-IP with Ku80, XPC and Rad51 antibody and a negative control (rat IgG) was performed with the precleared lysates. Bound YB-1 protein with its binding partners was eluted after several washing steps. Proteins were detected in whole-cell lysates and the eluates using western blotting.

5 DISCUSSION

NB is one of the most common cancers of childhood, and early detection as well as efficient treatment options are crucial for patient survival. This study describes the detection of potential novel markers of NB via utilization of serum-derived autoantibodies. It also shows that autoantibodies against the YB-1 protein are elevated in serum from NB patients, with highest abundance in sera from stage 4 patients. YB-1 is detectable in medium conditioned by NB cell lines, most probably due to active secretion. The extracellular presence of YB-1 in the area surrounding the tumor would expose the protein to the immune system, and might trigger the formation of autoantibodies. Knockdown of the YB-1 protein in NB cells increased DNA double-strand breaks and reduced cell viability. Co-immunoprecipitation experiments also showed that YB-1 was associated with proteins involved in various repair pathways, Ku80, Rad51 and XPC, in NB cells. YB-1 was shown to be a direct target of MYCN. Amplification of the *MYCN* gene is the strongest predictor of bad prognosis for NB known to date, and the fact that YB-1 is a MYCN target indicates that YB-1 could be an important factor in the development and progression on NB.

Patient serum autoantibodies can be used for detection of tumor markers

Autoantibodies in NB patient serum were used in this study to identify possible novel marker proteins for NB via protein array analysis. Antibodies against several proteins were specifically detected in serum from certain stages of NB. The two the most relevant candidate proteins were GPI, detected in serum from stage 1 NB patients, and YB-1, detected in serum from patients with all NB stages relative to healthy age- and gender-matched children. Multiple individual clones for YB-1 were detected in each analysis, and since these clones are directed against different parts of the YB-1 protein, it is highly unlikely to be a false negative. Based on this result, YB-1 was the best target identified using this methodology for further research. It has been previously reported that cancer patients sometimes show an immune response to self-proteins expressed by their tumors (Anderson et al. 2005), and that the level of antibody formation against an antigen varies according to tumor type, as shown for patients with non-small cell lung cancer (Bergqvist et al. 2003). Autoantibodies have also been detected in NB patients. Rodolfo et al. reported that 10 % of patients with stage III and stage IV tumors had evidence of antibodies to the NY-ESO-1 antigen (Rodolfo et al. 2003). Since a protein must be exposed to the immune system, cell surface or secreted proteins may be more apt to become targets of autoantibodies, and it is likely that proteins against which antibodies were detected on the array, are present outside the tumor cells. However, it is unclear what causes the immune system to react to some proteins while most of the others are still recognized as “self”. It has been described that self-proteins triggering an immune response are mostly altered in some form, rendering them immunogenic (Anderson et al. 2005). A structural

mutation of all proteins detected on the array seems unlikely since it would strongly hamper cell survival, so alternative triggers of autoantibody formation must be taken into consideration. It has been described that autophagy, a pathway which degrades and recycles proteins, promotes peptide transfer from autophagic vacuoles to the cell surface and subsequent MHC class II presentation (Dengjel et al. 2005). This, together with other autophagy actions, such as cytokine regulation, is thought to play a role in the loss of self-tolerance to molecules and may also provide an explanation for the formation of autoantibodies against intracellular proteins (Lleo et al. 2007). Autophagy is not only required for the normal turnover of cellular components, but is also associated with tumor development, where it assists the tumor to survive nutrient-limiting conditions, especially in the poorly vascularized internal region of the tumor (Shintani et al. 2004). The process of apoptosis has also been linked to formation of autoantibodies. Allina et al., have shown in biliary epithelial cells that intracellular molecules cleaved by caspases can generate cell-surface expressed autoantigens that may jeopardize self tolerance (Allina et al. 2006). Taken together, several possible pathways for the development of autoantibodies have been described and probably involve alteration or degradation of the proteins as part of the process. Intracellular proteins can also become immunogenic via transport to the surface, either through secretion of the entire protein or through vesicular transport of peptides following autophagy.

NB cells secrete GPI

Antibodies against GPI were detected via protein array analysis in sera from patients with stage 1 NBs. GPI, although mainly known as an enzyme in the glycolysis pathway, has been previously linked to cancer progression since, for example, it is upregulated in gastric cancer tissue and colorectal cancer and associated with poor prognosis for these specimens (Gong et al. 2005; Nakamori et al. 1994). Selective secretion of GPI by fibrosarcoma cells via a nonclassical active secretory mechanism has been reported (Niinaka et al. 1998). Antibodies against GPI have also been found in serum from patients with rheumatoid arthritis (Schaller et al. 2001), further supporting the possibility of autoantibody formation against principally intracellular proteins in disease states. Surprisingly, antibodies against GPI were detected in only stage 1 NB patients in this study, a stage associated with good patient prognosis, contrary to the association with poor outcome described in literature. However, detection of an autoantibody may indicate enhanced secretion of the protein or an unspecific release of at least a portion of the protein as a result of cell necrosis or autophagy. Both of which must not be associated with total protein expression in the tumor, and may also be a result of spontaneous tumor regression with subsequent protein release as well as immune response against the tumor. Both scenarios are likely for stage 1 NB. Extracellular GPI protein was detected in conditioned medium of all NB cell lines used in this study. During the course of collecting the conditioned medium, cultured cells appeared adherent and did not reach 100 % confluency. Cultures were trypsinized after medium collection and both adherent cells as

well as cells from the conditioned medium were assessed by trypan blue. There was no correlation between the percentage of nonviable cells and the amount of GPI in the conditioned medium, so an unspecific release of cytoplasmic contents due to necrotic cell death was an unlikely reason for GPI in the medium. One report demonstrated active secretion of GPI by human umbilical vein endothelial cells, and showed that secreted GPI promoted tumor growth via angiogenesis (Yanagawa et al. 2004). Taken together, GPI can be secreted by some cell types and has been shown to trigger the formation of autoantibodies in humans. In this work, GPI was detected extracellularly in cultured NB cells, and autoantibodies were detected in the serum from patients with stage 1 NBs, hinting towards an active secretion of GPI by NB cells and a possible role in NB tumor immune response. Whether GPI secreted by NB cells stimulates angiogenesis could be assessed in a preclinical xenograft model where extracellular GPI is selectively blocked via an antibody and xenograft tumor growth as well as angiogenesis is monitored. According to the report by Anderson et al. (2005), a protein alteration may trigger the immune response. Therefore, whole genome sequencing analysis of larger tumor cohorts could additionally provide data on whether GPI is a target for mutation in specific subsets.

NB patients show elevated YB-1 antibody concentrations

Autoantibodies against the YB-1 protein were detected in serum from all NB stages in comparison to control serum. Detection of these autoantibodies was highly relevant due to the representation by many independent clones. Subsequent quantification via reverse ELISA confirmed elevated antibody levels in pooled NB sera in comparison to controls and also showed that highest levels were detectable in serum from patients with stage 4 NB. Further analysis of individual patient sera by reverse ELISA showed a high variability within the single patients. Median antibody concentrations of NB patients were significantly elevated in comparison to controls, further demonstrating the possible use of YB-1 as a marker for this disease. Interestingly, YB-1 antibody levels in the serum from individual NB patients varied largely, reflecting strong interindividual differences in antibody concentrations, also within the groups. Hypothetically, these differences could be caused by differences in tumor size or could also be a sign of enhanced autophagy, possibly due to tumor starvation and subsequent release of YB-1 peptides. Highest levels of YB-1 antibody were detected in serum from two stage 4 patients; however, the median value was not elevated in comparison to the other NB stages. It might be possible that these two sera were responsible for the high antibody levels of stage 4 serum pools, detected in the initial experiment. These results show strong antibody expression of some stage 4 tumors which may provide evidence that YB-1 is more important for these highly aggressive stages. Analysis of a larger, prospectively collected patient cohort would allow a better statistical analysis and assumption about this. Additionally, it would then be possible to further break down the patient groups with different tumor stages, and correlate the antibody levels to other patient data, such as tumor size or age at

diagnosis. Taken together, YB-1 antibody concentrations are elevated in sera of NB patients in comparison to controls. Although a significant difference for stage 4 tumors was only observed in pooled sera, some individual patients with stage 4 tumors did show very strong YB-1 antibody expression.

The majority of the serum samples available were retrospectively collected. Six samples were prospectively collected using a standardized protocol designed to limit differences based on sample processing and storage. YB-1 antibody levels were less variable in prospectively collected sera. Although it did not reach statistical significance, the median YB-1 antibody level was slightly higher in prospectively collected serum samples from NB patients compared to controls. The small sample size is probably the reason why this difference did not reach significance. A recent publication described the detection and potential use of p53 autoantibodies as a biomarker for serous ovarian cancer, and the authors suggested that detection of autoantibodies might be affected by storage length (Anderson et al. 2010). Varying transport and storage times and conditions of the retrospectively collected serum samples might have affected the antibody concentrations, since measurable antibody concentrations in retrospectively collected sera could have been reduced by degradation. Although antibodies have a long half-life in serum and are relatively stable proteins (Anderson et al. 2008; Zhang et al. 2010), a standardized collection and storage protocol is crucial to reduce variability between samples and, thus, specificity of detection and comparability of results.

What could the presence of YB-1 autoantibodies in patient serum tell us about the NB? On the one hand, elevated levels of YB-1 antibody might indicate a strong, possibly protective, immune response as proposed for high titers of her2/neu antibodies in breast cancer patients (Jager et al. 1999). On the other hand, they could also be a useful surrogate biomarker for differences in tumor biology. It was shown that the presence of p53 autoantibodies is correlated with tumor burden and p53 mutation in breast cancer patients (Anderson et al. 2008). The presence of YB-1 antibodies might reflect characteristics of tumor progression in NB patients as well. Since very strong levels of YB-1 antibodies were found predominantly in stage 4 patient sera, an association of these antibodies with progression and bad prognosis appears possible. As discussed before, autophagy is a possible mechanism, leading to immunogenic responses against intracellular proteins (Lleo et al. 2007). Since autophagy is used to maximize nutrition resources and associated with tumor development (Shintani et al. 2004) this would further point towards autoantibodies being a marker for malignancy. Further research on a larger patient cohort would be needed to find common patterns of YB-1 antibody formation in NB, but this research points towards YB- antibodies being a marker for prognostically bad tumor features found in some NB patients.

NB cell lines secrete YB-1 protein

All NB cell lines tested expressed the YB-1 protein. YB-1 protein was also detected in the medium of cultured cells, and the amount present extracellularly was not correlated with cell death in the cultures, rendering active secretion as the most likely mechanism responsible for the extracellular presence. Active secretion of the YB-1 protein via a non-classical, vesicle-mediated pathway has been described for mesangial and monocytic cells (Frye et al. 2009), where extracellular YB-1 stimulated migration and proliferation. YB-1 protein has also been previously detected in serum of healthy adults (Krings 2008), and the presence of autoantibodies in the tested NB sera in this work indicate that the protein is present extracellularly in vivo as well. It is as yet unclear whether increased levels of antibody in NB patients reflect larger extracellular YB-1 protein amounts. A highly sensitive detection method, such as a protein ELISA would be useful for this analysis. Since extracellular YB-1 is associated with proliferation, an active secretion of YB-1 from NB cells in order to stimulate tumor development may be possible. In conclusion, YB-1 is present in NB cells, secreted from them and is likely to also be present in human serum. Since extracellular YB-1 stimulates tumor progression of mesangial and monocytic cells (Frye et al. 2009), it may play a similar role for NB tumor cells, and this aspect should be further investigated.

Assessment of a possible correlation between neurotrophin receptors and YB-1

The neurotrophin receptors TrkA and TrkB play a major role in the development of NB and NB cell models stably overexpressing Trk receptors (Eggert et al. 2002) were also examined in this study in order to assess a possible correlation to YB-1. While TrkA promotes growth inhibition, neuronal differentiation and inhibits angiogenesis in a NB xenograft model, TrkB is associated with biologically unfavorable NB (Nakagawara et al. 1994; Eggert et al. 2000). An inverse correlation of YB-1 to TrkA was observed in cell lysates of SH-SY5Y cells, one of the NB cell lines used in the research presented here. Since YB-1 is expressed in angiogenic endothelial cells of various tumors, such as glioblastoma, gastric or colon cancers, as well as in cultured tumor cells and YB-1 knockdown inhibited growth of human umbilical vein endothelial cells (Takahashi et al. 2010), it might be possible that low levels of YB-1 is part of the mechanism involved to cause growth inhibition in tumors strongly expressing TrkA. It is tempting to speculate that downregulation of YB-1, as a result of enhanced TrkA receptor expression, could at least in part mediate the decrease in angiogenic activity in TrkA-expressing tumors, and consequently, contribute to the more favorable prognosis. However, so far data to support this hypothesis has only been derived from one cell line while the two other tested cell lines did not show a significant inverse correlation. Further research, especially from experiments utilizing in vivo models, is necessary to explore a possible relationship. Xenografts of SY5Y-TrkA cells, as compared with the parental SY5Y or SY5Y-TrkB cells, injected into nude mice have shown that tumor growth was remarkably repressed in SY5Y-TrkA xenografts (Eggert et al. 2002). To explore a possible involvement of YB-1 in this

signal-response cascade, an additional vector overexpressing YB-1 could be inserted in the SY5Y-TrkA cell line to restore high YB-1 levels and possibly promote subsequent tumor growth. Since TrkB receptor expression is associated with biologically unfavorable NB, and YB-1 also seems to be associated with unfavorable tumor features, a correlation of both proteins was explored as well. Interestingly no such correlation was seen on protein level in the tested cell lines. In conclusion, YB-1 expression was inversely correlated to TrkA receptor expression in one of the cell lines examined here but no significant correlation was seen in the other tested cell lines. Further analysis will be needed to investigate if repression of the YB-1 protein contributes to TrkA-mediated processes that result in better patient prognosis.

Assessment of a possible correlation between MYCN proteins and YB-1

Genomic amplification of *MYCN*, causing overexpression of the MYCN protein, is the genetic aberration most consistently associated with poor outcome and tumor progression in NB (Brodeur et al. 1984; Seeger et al. 1985). It is also known that transgenic overexpression of MYCN is sufficient to induce NB in mice (Weiss et al. 1997). Therefore, a possible association with YB-1, which has also been previously linked to cancer progression, e.g. in breast cancer or glioblastoma (Janz et al. 2002, Faury et al. 2007), is of major interest for further research. NB cell lines with single-copy and amplified *MYCN* were examined in this dissertation research. They all expressed YB-1, but YB-1 expression levels were not correlated to the *MYCN* status of the cell line. However, protein expression is dependent on multiple features and difficult to compare across various cell lines. It has been shown in cancers without amplified *MYCN* and low MYCN expression levels that expression of c-MYC is often elevated (Sadee et al. 1987; Breit et al. 1989). A repression of c-MYC by MYCN, was also observed for *MYCN*-amplified stage 4S tumors showing an inverse correlation between MYCN and c-MYC as part of an autoregulatory loop, controlled via repression of each other at defined promoter sites. (Sadee et al. 1987; Breit et al. 1989; Westermann et al. 2008). MYCN and c-MYC have common target genes (Westermann et al. 2008), therefore, it is not possible to draw a conclusion for the relationship between YB-1 expression based only on the *MYCN* amplification status. In order to examine the interaction between YB-1 and MYCN under defined conditions, inducible model systems were utilized in this work. It was shown that YB-1 is upregulated in response to MYCN induction and YB-1 downregulation follows MYCN repression, demonstrating a regulation of YB-1 by MYCN. MYCN is known to bind the E-box motif, and the promoter region of YB-1 contains an E-box motif (Wu et al. 2007), so that regulation via direct interaction is possible. Further experiments were conducted to determine whether MYCN directly bound the YB-1 promoter to activate transcription. ChIP-on-chip analyses not only showed binding of the MYCN, but also of the c-Myc protein to the promoter region of YB-1 as well as initiation and transcription of YB-1. These experiments show that c-MYC can also bind to the YB-1 promoter when MYCN protein levels are low and activate

transcription. These findings may explain why no correlation between YB-1 was observed with *MYCN* amplification in cell lines, although the two proteins share a common pathway. The discovery that Myc proteins can directly regulate YB-1 may be relevant for processes involved with NB progression. YB-1 is involved in various processes required for cancer progression, and it is possible that at least some of these processes may be ultimately initiated or driven by an overexpression of either c-Myc or *MYCN*, resulting from either gene amplification or other mechanisms maintaining high MYC protein levels in NB cells. Consistent with our findings, it has been shown for ovarian cancer that YB-1 knockdown led to downregulation of known downstream targets of *MYCN* and c-myc, such as *NDRG1*, a protein involved in cellular differentiation (Basaki et al. 2006; Pflueger et al. 2009). Since the results presented in this dissertation show YB-1 regulation through *MYCN* and Basaki et al. demonstrated a positive correlation between *NDRG1* expression and YB-1, it is possible that the effect of *MYCN* on *NDRG1* is mediated via a pathway involving YB-1, which would highlight the importance of YB-1 in the regulation of Myc-dependent proteins. It will be interesting to further investigate, if YB-1 knockdown also decreases expression of other known Myc-target genes, such as *MRP* (Norris et al. 1997) and thereby to assess if YB-1 is involved in other pathways of Myc-dependent gene regulation. In conclusion, it was shown here that both, *MYCN* and c-Myc, not only bind directly to the YB-1 promoter but also activate transcription. Additionally, a published report describes an effect on Myc-dependent proteins following YB-1 knockdown. Together this shows the importance of YB-1 as a downstream target of the Myc family of proteins and at least some involvement of YB-1 in Myc-dependent gene regulation.

Knockdown of YB-1 protein significantly decreased proliferation of SK-N-BE cells in normal medium as well in the presence of cisplatin. Equal results were obtained for the cisplatin-resistant SK-N-BEcp cells. Consistent with these findings, multiple publications have shown implications of YB1 in proliferation processes, namely that it activates genes associated with general pathways of proliferation, such as cyclin A, cyclin B1, matrix metalloproteinase-2 (MMP-2), and the *MDR1* gene (Jurchott et al. 2003; Uchiumi et al. 1993; Mertens et al. 1997). The decreased proliferation after YB-1 depletion is even more interesting in the cisplatin-resistant cell line, since YB-1 is involved in the development of resistance against cisplatin in human epidermoid cancer, mouse embryonic stem cells and melanoma cells (Schitteck et al. 2007; Shibahara et al. 2004; Ohga et al. 1996). All these publications describe increased sensitivity against cisplatin after YB-1 downregulation, suggesting that it has protective capacity against cytotoxic effects of DNA damaging agents. Whether the lower proliferation seen in this study is due to increased chemosensitivity or because of proliferation defects, remains to be elucidated. Knockdown of the YB-1 protein was most successful 72 h after siRNA transfection, reflecting a long turnover time of the protein. Even though downregulation reduced protein expression by 80 %, this long incubation time complicated experiments because cultures reached confluency before the experiment could be

completed and the residual YB-1 protein may have been enough to maintain YB-1 functionality. Future experiments would benefit from a cell line, stably transfected with an inducible YB-1 shRNA construct. However, knockdown of YB-1 has been published for multiple cell lines and it has been shown that even reductions of around 50 % are sufficient to strongly impair the chemoprotective properties of YB-1 protein (Ohga et al. 1996). In conclusion YB-1 is associated with multiple proteins involved in proliferation as well as in the development of resistance and it was shown here that YB-1 depletion reduces proliferation of cultured NB cells.

Association of YB-1 with cellular repair activity

Formation of double strand breaks (DSBs) is induced by irradiation, but also occurs spontaneously during cell cycle progression. DSBs are usually repaired fast, in higher eukaryotes, mostly via non-homologous end joining (NHEJ) (Gaudreault et al. 2004; Fattah et al. 2010). Defects in this repair pathway will, therefore, lead to accumulation of DSBs. DSBs were quantified in NB cells after YB-1 knockdown, and it was shown in this dissertation that YB-1 depletion significantly increased DSB accumulation. Similar effects were reported for breast cancer cell lines by Toulany et al, who showed that knockdown of YB-1 enhanced residual γ -H2AX foci after irradiation (Toulany et al. 2011). Interestingly, the authors describe an Akt-mediated phosphorylation of YB-1 at Ser102 in response to irradiation and propose that phosphorylated YB-1 is responsible for the development of radioresistant cells. C-terminal phosphorylation has been previously described as a major regulatory mechanism of YB-1 (Sutherland et al. 2005), and it has been shown that phosphorylation also influences translocation and transcriptional activity of YB-1 (Wu et al. 2006; Basaki et al. 2006). Additionally, it has been described that, in cells with oncogenic *K-RAS*, YB-1 is constitutively phosphorylated (Toulany et al. 2011). Although no *K-RAS* mutation has been described for the SK-N-BE cells used in this study, the cells do show a heterozygous point mutation of the *N-ras* gene (Moley et al. 1991). It has also been shown in another publication that the *N-ras* gene of SK-N-SH NB cells has transforming activity, while the normal *N-ras* gene does not (Taparowsky et al. 1983). However, as to this point, it is not clear, if YB-1 is constitutively phosphorylated in the cell lines used in this study and antibodies used here were not specific for phosphorylated YB-1 protein, but the finding that YB-1 knockdown led to significantly decreased proliferation strongly indicates functionally active YB-1 protein. In contrast to SK-N-BE cells, the cisplatin-resistant SK-N-BEcp did not show elevated levels of DSB after YB-1 downregulation. It was shown in breast cancer cells that cisplatin resistance is associated with overexpression of YB-1 (Garand et al. 2011), so a possible explanation for the resistance towards irradiation might be that YB-1 protein levels are elevated in the cisplatin-resistant SK-N-BEcp, leaving enough residual activity after knockdown to prevent a major accumulation of DSBs. A complete knockdown would be necessary to further explore this theory. However, transient transfection will not be sufficient here; again a stably transfected inducible vector containing YB-1 siRNA would be useful.

Additionally, development of resistance towards cytotoxic agents is a multifactorial event and it might be that the resistant cells have developed additional ways of repair efficiency, such as involvement of the tumor suppressor protein p53 to prevent DSB accumulation (Basu et al. 2010). Development of resistance is one of the greatest challenges in NB therapy. YB-1 has been associated with resistance against various DNA-damaging agents, among them cisplatin and UV light, since it was shown that knockdown of the protein sensitizes cells against these agents (Ohga et al. 1996, Shibahara et al. 2004) and that development of this resistance leads to YB-1 upregulation (Levenson et al. 2000). In this dissertation research, western blot analysis was performed from cell extracts of SK-N-AS and SK-N-AScp cells, and a significant increase of YB-1 protein following cisplatin treatment was observed for both cell lines. Additionally, immunofluorescent staining of both cell lines pointed towards increased overall amounts of YB-1 following cisplatin treatment. Taken together, YB-1 depletion leads to accumulation of DSBs, and cisplatin treatment increases YB-1 expression in NB cells. Both findings are consistent with published reports, and show the association of YB-1 expression with genotoxic stress in NB cells as well as the possible involvement of YB-1 in mechanisms of resistance and repair.

The influence of YB-1 depletion on the formation of cisplatin-induced DNA adducts was analyzed in this dissertation research as well. Although adduct formation slightly increased in SK-N-BEcp cells after YB-1 knockdown, no significant change was observed in either of the tested cell lines. Unfortunately, the experiment could only be successfully performed once, limiting the interpretation of the results. It has been described in melanoma cells that downregulation of YB-1 increased the sensitivity to cisplatin (Schitteck et al. 2007), but according to the experiment performed here, no significant change in adduct formation was observed for NB. It might be that YB-1 is involved in other proliferation processes but not directly in the repair of cisplatin damage, since its knockdown does reduce proliferation but is not able to influence adduct repair. Consistent with this finding is the publication by Uchiumi et al., where YB-1 knock-out mice were shown to be embryonic lethal due to incomplete neural tube closure. The authors proclaimed an involvement of YB-1 in cell proliferation, since its knock-out led to a failure in morphological transformation of cultured cells (Uchiumi et al. 2006). However, additional analysis of cisplatin adduct repair in YB-1 deficient cells would be necessary for a clear statement. Although literature describes that YB-1 is involved in repair of cisplatin-damaged DNA, initial experiments performed in this dissertation research could not validate this, and more research is needed to show if YB-1 knockdown impairs adduct-repair or if YB-1 depletion results in proliferation defects. While DSBs are mostly repaired through nonhomologous end joining (Critchlow et al. 1998), the repair of intrastrand cross-links, the major lesion caused by cisplatin, is performed via the nucleotide excision repair (NER) system (Basu et al. 2010). An influence of YB-1 depletion on adduct repair was not seen in NB cells, however it has been described in literature that YB-1 does bind cisplatin-modified DNA and

interacts with PCNA, a protein involved in the NER (Nichols et al. 1992; Ise et al. 1999). To target the question of how YB-1 is involved in the various repair pathways of NB cells, a set of repair proteins pathways was analyzed for a possible interaction with YB-1. Binding of YB-1 to XPC in NB cells was shown here. XPC is widely known to be involved in the NER pathway, the main pathway for DNA adduct repair, where it is needed for the recognition of bulky DNA adducts, caused by chemotherapeutics, such as cisplatin (Neher et al. 2010). It was shown in this dissertation research that cisplatin exposure enhanced YB-1 expression and YB-1 binds XPC. However, YB-1 knockdown did not impair the repair of cisplatin-caused DNA adducts. Therefore, an alternative explanation to involvement in the NER pathway, for the binding of YB-1 to XPC in NB must be considered. Recent studies show that XPC is not only involved in NER, but also plays a role in DSB repair or in base-excision repair (BER) tumor suppressor protein p53 to prevent DSB accumulation (D'Errico et al. 2006; Despras et al. 2007). An involvement of YB-1 via XPC in these repair mechanisms is, therefore, possible. Additionally, it was demonstrated that YB-1 binds the Ku80 and Rad51 repair proteins in NB cells. Binding of YB-1 to Ku80 was previously shown in human 293 embryonic kidney cells (Gaudreault et al. 2004), and this interaction was validated here for NB. The Ku70/Ku80 heterodimer, or Ku, is the central component of the nonhomologous end joining (NHEJ) pathway, responsible for the repair of DSBs (Postow et al. 2008). As shown above, YB-1 knockdown impairs the repair of spontaneously occurring DSBs in SK-N-BE cells and binding of YB-1 to Ku80 now additionally highlights the involvement of YB-1 in the NHEJ repair pathway. Rad51 is involved in the DSB repair via homologous recombination, where it binds to single- and double-stranded DNA and exhibits DNA-dependent ATPase activity (Benson et al. 1994; Li et al. 2007). The binding of YB-1 to XPC, Ku80 and Rad51 demonstrates the connection of YB-1 to various repair pathways, and although this is just the first step in the recognition of YB-1 involvement in repair mechanisms of NB, it indicates that YB-1 could be important for processes governing NB tumor progression or development of resistance. Assessment of the contribution of YB-1 in repair of NB cells has to be answered with further experiment such as *in vitro* NHEJ assays, where NHEJ efficiency can be assessed through conversion of monomeric linear substrate into multimers and circular products as shown in (Despras et al. 2007).

It has been shown in several other entities, such as lung or breast cancer that not just the overall amount, but also the intracellular location of YB-1 is of consequence for progression and prognosis of cancer (Bargou et al. 1997; Shibahara et al. 2001). And, although, YB-1 does not seem to be directly involved in the repair of cisplatin-derived DNA adducts in NB, it is known that it binds to cisplatin-modified DNA (Ise et al. 1999). Therefore, the intracellular localization of YB-1 in the absence and presence of cisplatin was monitored via immunofluorescence. Diffuse staining of nucleus and cytoplasm was observed in SK-N-BE cells, no significant change occurred after treatment with cisplatin besides slightly more prominent fluorescent spots. Similar results were

obtained for the cp-resistant sub-cell line; in both cell lines YB-1 was mainly localized in the cytoplasm. However, consistent with reports that overexpression of YB-1 in breast cancers causes cisplatin resistance (Garand et al. 2011) it was observed here that overall immunofluorescent staining appeared more pronounced in the SK-N-BEcp cell line, even in cell culture medium without cytostatics, hinting towards elevated protein levels. Additionally, cisplatin exposure led to elevated levels of YB-1 protein in both cell lines as described above. These observations strengthen the role of YB-1 in the reaction of cells towards treatment with cisplatin. However, contrary to several publications where nuclear translocation of YB-1 following genotoxic stress has been described, no such translocation was observed here. However, they report, e.g. for adenocarcinomic human alveolar basal epithelial cells that the translocation occurs in the presence of wild type p53 (Zhang et al. 2003). The SK-N-BE cell lines used in this study is known to contain wild type p53. It has been described as well that, while the p53 wild type SK-N-BE cells line was derived from a patient before therapy, another cell line SKNBE(2c), was taken from the same patient after relapse past cytotoxic therapy. These SKNBE(2c) cells showed a mutated and non-functional version of p53 (Tweddle et al. 2001). This observation raises the question, whether the SK-N-BEcp cells used here, which were made resistant in our lab, do still possess functional p53. Sequencing analysis of the p53 gene would be required to exclude a mutant p53 which would hamper translocation of YB-1. In addition, other factors, such as poor immunofluorescent staining, low YB-1 protein amounts or insufficient cisplatin treatment could be the reason, why no translocation could be observed here.

Patient autoantibodies led to the identification of GPI and YB-1 as possible players in NB progression and the development of resistance. Deeper investigation of the systems in which YB-1 is involved in NB cells identified that the protein is an important direct downstream target of Myc-proteins and that YB-1 depletion significantly decreased cell proliferation and led to DSB accumulation while cisplatin treatment increased YB-1 expression in NB cells. Additionally an interaction of YB-1 with various repair proteins, namely XPC, Rad51 and Ku80 was shown. These observations show the importance of YB-1 for NB. Further research and in vivo studies will be necessary to assess the role of YB-1 as a possible future target for treatment of resistant tumors. Additionally the inhibition of YB-1 as a new downstream target of Myc-proteins may provide new insights into the carcinogenesis and possible therapy of MYCN-amplified tumors.

6 SUMMARY

Neuroblastoma is one of the most common cancers of childhood, and early detection as well as efficient treatment options are crucial for patient survival. This study describes the detection of potential novel markers of neuroblastoma via utilization of serum-derived autoantibodies. It also shows that autoantibodies against the Y-box binding protein 1 (YB-1) are elevated in serum from neuroblastoma patients, with highest abundance in serum from stage 4 patients. YB-1 is detectable in medium conditioned by neuroblastoma cell lines, most probably due to active secretion. The extracellular presence of YB-1 in the area surrounding the tumor would expose the protein to the immune system, and might trigger the formation of autoantibodies. Knockdown of the YB-1 protein in neuroblastoma cells increased DNA double-strand breaks and reduced cell viability. Co-immunoprecipitation experiments also showed that YB-1 was associated with proteins involved in various repair pathways, Ku80, Rad51 and XPC, in neuroblastoma cells. YB-1 was shown to be a direct target of MYCN. Amplification of the *MYCN* gene is the strongest predictor of bad prognosis for neuroblastoma known to date, and the fact that YB-1 is a MYCN target indicates that YB-1 could be an important factor in the development and progression of neuroblastoma. Additionally the inhibition of YB-1 as a new downstream target of Myc-proteins may provide new insights into the carcinogenesis and possible therapy of MYCN-amplified tumors. Neuroblastoma is a very heterogeneous disease and early detection as well as consequent patient monitoring and staging is crucial to prevent patient over- or undertreatment. Results of this study may help with tumor staging and YB-1 may be a possible future target for treatment of resistant tumors.

7 REFERENCES

1. Aebi, S., Kurdi-Haidar, B., Gordon, R., Cenni, B., Zheng, H., Fink, F., Christen, R., Boland, R., Koi, M., Fishel, R., Howell, S.(1996): Loss of DNA mismatch repair in acquired resistance to cisplatin. *Cancer Res* 56(13), 3087-3090.
2. Allina, J., Hu, B., Sullivan, D., Fiel, M., Thung, S., Bronk, S., Huebert, R., van de Water J., LaRusso, N., Gershwin, M., Gores, G., Odin, J.A. (2006): T cell targeting and phagocytosis of apoptotic biliary epithelial cells in primary biliary cirrhosis. *J Autoimmun* 27(4), 232-241.
3. Ambros, P., Ambros, I., Brodeur, G., Haber, M., Khan, J., Nakagawara, A., Schleiermacher, G., Speleman, F., Spitz, R., London, W., Cohn, S., Pearson, A., Maris, J. (2009): International consensus for neuroblastoma molecular diagnostics: report from the International Neuroblastoma Risk Group (INRG) Biology Committee. *Br J Cancer* 100(9), 1471-1482.
4. Anderson, K. S. and LaBaer, J. (2005): The sentinel within: exploiting the immune system for cancer biomarkers. *J Proteome Res* 4(4), 1123-1133.
5. Anderson, K. S., Ramachandran, N., Wong, J., Raphael, J., Hainsworth, E., Demirkan, G., Cramer, D., Aronzon, D., Hodi, F., Harris, L., LaBaer, J. (2008): Application of protein microarrays for multiplexed detection of antibodies to tumor antigens in breast cancer. *J Proteome Res* 7(4), 1490-1499.
6. Anderson, K. S., Wong, J., Vitonis, A., Crum, C., Sluss, P., Labaer, J., Cramer, D. (2010): p53 autoantibodies as potential detection and prognostic biomarkers in serous ovarian cancer. *Cancer Epidemiol Biomarkers Prev* 19(3), 859-868.
7. Astanehe, A., Finkbeiner, M., Hojabrpour, P., To, K., Shadeo, A., Stratford, A., Lam, W., Berquin, I., Duronio, V., Dunn, S. (2009): The transcriptional induction of PIK3CA in tumor cells is dependent on the oncoprotein Y-box binding protein-1. *Oncogene* 28(25), 2406-2418.
8. Bader, A. G., Vogt, P. K. (2008): Phosphorylation by Akt disables the anti-oncogenic activity of YB-1. *Oncogene* 27(8), 1179-1182.
9. Bargou, R. C., Jurchott, K., Wagener, C., Bergmann, S., Metzner, S., Bommert, K., Mapara, M., Winzer, K.J., Dietel, M., Dörken, B., Royer, H. (1997): Nuclear localization and increased levels of transcription factor YB-1 in primary human breast cancers are associated with intrinsic MDR1 gene expression. *Nat Med* 3(4), 447-450.
10. Basaki, Y., Hosoi, F., Oda, Y., Fotovati, A., Maruyama, Y., Oie, S., Ono, M., Izumi, H., Kohno, K., Sakai, K., Shimoyama, T., Nishio, K., Kuwano, M.. (2006): Akt-dependent nuclear localization of Y-box-binding protein 1 in acquisition of malignant characteristics by human ovarian cancer cells. *Oncogene* 26(19), 2736-2746.
11. Basu, A., Krishnamurthy, S. (2010): Cellular responses to Cisplatin-induced DNA damage. *J Nucleic Acids* 2010.
12. Benson, F. E., Stasiak, A., West, S.C. 1994): Purification and characterization of the human Rad51 protein, an analogue of E. coli RecA. *EMBO J* 13(23), 5764-5771.
13. Bergmann, S., Royer-Pokora, B., Fietze, E., Jürchott, K., Hildebrandt, B., Trost, D., Leenders, F., Claude, J., Theuring, F., Bargou, R., Dietel, M., Royer, H.D. (2005): YB-1 provokes breast cancer through the induction of chromosomal instability that emerges from mitotic failure and centrosome amplification. *Cancer Res* 65(10), 4078-4087.
14. Bergqvist, M., Brattstrom, D., Lamberg, K., Wernlund, J., Larsson, A., Wagenius, G. (2003): The presence of anti-p53 antibodies in sera prior to thoracic surgery in non small cell lung

- cancer patients: its implications on tumor volume, nodal involvement, and survival. *Neoplasia* 5(4), 283-287.
15. Biedler, J. L., Helson, L., Spengler, B. (1973): Morphology and growth, tumorigenicity, and cytogenetics of human neuroblastoma cells in continuous culture. *Cancer Res* 33(11), 2643-2652.
 16. Boeckman, H. J., Trego, K. S., Turchi, J.J. (2005): Cisplatin sensitizes cancer cells to ionizing radiation via inhibition of nonhomologous end joining. *Mol Cancer Res* 3(5), 277-285.
 17. Boegsted, M., Holst, J. M., Fogd, K., Falgreen, S., Sørensen, S., Schmitz, A., Bukh, A., Johnsen, H.E., Nyegaard, M., Dybkaer, K. (2011): Generation of a predictive melphalan resistance index by drug screen of B-cell cancer cell lines. *PLoS One* 6(4), e19322.
 18. Bonora, D. M. A. (1982): A simple colorimetric method for detecting cell viability in cultures of eukaryotic microorganisms. *Curr. Microbiol.* 7 217–21.
 19. Bown, N., Cotterill, S., Lastowska, M., O'Neill, S., Pearson, A.D., Plantaz, D., Meddeb, M., Danglot, G., Brinkschmidt, C., Christiansen, H., Laureys, G., Speleman, F., Nicholson, J., Bernheim, A., Betts, D.R., Vandesompele, J., Van Roy, N. (1999): Gain of chromosome arm 17q and adverse outcome in patients with neuroblastoma. *N Engl J Med* 340(25), 1954-1961.
 20. Breit, S. and Schwab, M. (1989): Suppression of MYC by high expression of NMYC in human neuroblastoma cells. *J Neurosci Res* 24(1), 21-28.
 21. Brodeur, G. M. (2003): Neuroblastoma: biological insights into a clinical enigma. *Nat Rev Cancer* 3(3), 203-216.
 22. Brodeur, G. M., Goldstein, M. N. (1976): Histochemical demonstration of an increase in acetylcholinesterase in established lines of human and mouse neuroblastomas by nerve growth factor. *Cytobios* 16(62), 133-138.
 23. Brodeur, G. M., Look, A. T., Shimada, H., Hamilton, V.M., Maris, J.M., Hann, H.W., Leclerc, J.M., Bernstein, M., Brisson, L.C., Lemieux, B., Tuchman, M., Woods, W.G. (2001): Biological aspects of neuroblastomas identified by mass screening in Quebec. *Med Pediatr Oncol* 36(1), 157-159.
 24. Brodeur GM, M. J. (2006). Neuroblastoma. Principles and practice of pediatric oncology, 5th edn. P. D. Pizzo PA. Philadelphia, J B Lippincott Company, 933–970
 25. Brodeur, G. M., Pritchard, J., et al. (1993): Revisions of the international criteria for neuroblastoma diagnosis, staging, and response to treatment. *J Clin Oncol* 11(8), 1466-1477.
 26. Brodeur, G. M., Seeger, R. C., Schwab, M., Bishop, J.M. (1984): Amplification of N-myc in untreated human neuroblastomas correlates with advanced disease stage. *Science* 224(4653), 1121-1124.
 27. Cahill, D., Connor, B., Carney, J.P. (2006): Mechanisms of eukaryotic DNA double strand break repair. *Front Biosci* 11, 1958-1976.
 28. Chan, H. S., Gallie, B. L., DeBoer, G., Haddad, G., Ikegaki, N., Dimitroulakos, J., Yeger, H., Ling, V. (1997): MYCN protein expression as a predictor of neuroblastoma prognosis. *Clin Cancer Res* 3(10), 1699-1706.
 29. Chan, H. S., Haddad, G., Thorner, P.S., DeBoer, G., Lin, Y.P., Ondrusek, N., Yeger, H., Ling, V. (1991): P-glycoprotein expression as a predictor of the outcome of therapy for neuroblastoma. *N Engl J Med* 325(23), 1608-1614.
 30. Chattopadhyay, R., Das, S., Maiti, A.K., Boldogh, I., Xie, J., Hazra, T.K., Kohno, K., Mitra, S., Bhakat, K.K. (2008): Regulatory role of human AP-endonuclease (APE1/Ref-1) in YB-1-mediated activation of the multidrug resistance gene MDR1. *Mol Cell Biol* 28(23), 7066-7080.
 31. Chaudhary, P. and Roninson, I. (1993): Induction of multidrug resistance in human cells by transient exposure to different chemotherapeutic drugs. *J Natl Cancer Inst* 85(8), 632-639.

32. Chen, Y. R., Sekine, K., Yanai, H., Tanaka, M., Miyajima, A. (2009): Y-box binding protein-1 down-regulates expression of carbamoyl phosphate synthetase-I by suppressing CCAAT enhancer-binding protein-alpha function in mice. *Gastroenterology* 137(1), 330-340.
33. Chibi, M., Meyer, M., Skepu, A., G. Rees D., Moolman-Smook, J. C., Pugh, D. J. (2008): RBBP6 interacts with multifunctional protein YB-1 through its RING finger domain, leading to ubiquitination and proteosomal degradation of YB-1. *J Mol Biol* 384(4), 908-916.
34. Cobbold, L. C., Spriggs, K. A., Haines, S. J., Dobbyn, H. C., Hayes, C., de Moor, C. H., Lilley, K. S., Bushell, M., Willis, A. E. (2008): Identification of internal ribosome entry segment (IRES)-trans-acting factors for the Myc family of IRESs. *Mol Cell Biol* 28(1), 40-49.
35. Cohen, S. B., Ma, W., Valova, V. A., Algie, M., Harfoot, R., Woolley, A. G., Robinson, P. J., Braithwaite, A. W. (2009): Genotoxic stress-induced nuclear localization of oncoprotein YB-1 in the absence of proteolytic processing. *Oncogene* 29(3), 403-410.
36. Cohn, S. L., Pearson, A. D. et al. (2009): The International Neuroblastoma Risk Group (INRG) classification system: an INRG Task Force report. *J Clin Oncol* 27(2), 289-297.
37. Critchlow, S. E. and Jackson, S. P. (1998): DNA end-joining: from yeast to man. *Trends Biochem Sci* 23(10), 394-398.
38. D'Errico, M., Parlanti, E., Teson, M., de Jesus, B. M., Degan, P., Calcagnile, A., Jaruga, P., Bjoras, M., Crescenzi, M., Stefanini, M., Dizdaroglu, M., Dogliotti, E. (2006): New functions of XPC in the protection of human skin cells from oxidative damage. *EMBO J* 25(18), 4305-4315.
39. Dahl, E., En-Nia, A., Wiesmann, F., Krings, R., Djudjaj, S., Breuer, E., Fuchs, T., Wild, P. J., Hartmann, A., Dunn, S. E., Mertens, P. R. (2009): Nuclear detection of Y-box protein-1 (YB-1) closely associates with progesterone receptor negativity and is a strong adverse survival factor in human breast cancer. *BMC Cancer* 9, 410.
40. Das, S., Chattopadhyay, R., Bhakat, K. K., Boldogh, I., Kohno, K., Prasad, R., Wilson, S. H., Hazra, T. K. (2007): Stimulation of NEIL2-mediated oxidized base excision repair via YB-1 interaction during oxidative stress. *J Biol Chem* 282(39), 28474-28484.
41. Dengjel, J., Schoor, O., Fischer, R., Reich, M., Kraus, M., Muller, M., Kreymborg, K., Altenberend, F., Brandenburg, J., Kalbacher, H., Brock, R., Driessen, C., Rammensee, H. G., Stevanovic, S. (2005): Autophagy promotes MHC class II presentation of peptides from intracellular source proteins. *Proc Natl Acad Sci U S A* 102(22), 7922-7927.
42. Despras, E., Pfeiffer, P., Salles, B., Calsou, P., Kuhfittig-Kulle, S., Angulo, J. F., Biard, D. S. (2007): Long-term XPC silencing reduces DNA double-strand break repair. *Cancer Res* 67(6), 2526-2534.
43. Dhooze, C. R., De Moerloose, B. M., Philippe, Laureys, G. G. (1997): Expression of the MDR1 gene product P-glycoprotein in childhood neuroblastoma. *Cancer* 80(7), 1250-1257.
44. Didier, D. K., Schiffenbauer, J., Woulfe, S. L., Zacheis, M., Schwartz, B. D. (1988): Characterization of the cDNA encoding a protein binding to the major histocompatibility complex class II Y box. *Proc Natl Acad Sci U S A* 85(19), 7322-7326.
45. Eggert, A., Grotzer, M. A., Ikegaki, N., Liu, X. G., Evans, A. E., Brodeur, G. M. (2002): Expression of the neurotrophin receptor TrkA down-regulates expression and function of angiogenic stimulators in SH-SY5Y neuroblastoma cells. *Cancer Res* 62(6), 1802-1808.
46. Eggert, A., Ikegaki, N., Liu, X., Chou, T., Lee, V. M., Trojanowski, J. Q., Brodeur, G. M. (2000): Molecular dissection of TrkA signal transduction pathways mediating differentiation in human neuroblastoma cells. *Oncogene* 19(16), 2043-2051.
47. El-Badry, O. M., Romanus, J. A., Helman, L. J., Cooper, M. J., Rechler, M. M., Israel, M. A. (1989): Autonomous growth of a human neuroblastoma cell line is mediated by insulin-like growth factor II. *J Clin Invest* 84(3), 829-839.

48. el-Deiry, W. S., Tokino, T., Velculescu, V. E., Levy, D. B., Parsons, R., Trent, J. M., Lin, D., Mercer, W. E., Kinzler, K. W., Vogelstein, B. (1993): WAF1, a potential mediator of p53 tumor suppression. *Cell* 75(4), 817-825.
49. En-Nia, A., Yilmaz, E., Klinge, U., Stefanidis, I., Mertens, P. R. (2005): Transcription factor YB-1 mediates DNA polymerase alpha gene expression. *J Biol Chem* 280 (9), 7702-7711.
50. Evans, A. E., D'Angio, G. J., Randolph, J. (1971): A proposed staging for children with neuroblastoma. Children's cancer study group A. *Cancer* 27(2), 374-378.
51. Evdokimova, V., Ruzanov, P., Anglesio, M. S., Sorokin, A. V., Ovchinnikov, L. P., Buckley, J., Triche, T. J., Sonenberg, N., Sorensen, P. H. (2006): Akt-mediated YB-1 phosphorylation activates translation of silent mRNA species. *Mol Cell Biol* 26(1), 277-292.
52. Evdokimova, V., Ruzanov, P., Imataka, H., Raught, B., Svitkin, Y., Ovchinnikov, L. P. Sonenberg, N. (2001): The major mRNA-associated protein YB-1 is a potent 5' cap-dependent mRNA stabilizer. *EMBO J* 20(19), 5491-5502.
53. Evdokimova, V., Tognon, C., Ng, T., Ruzanov, P., Melnyk, N., Fink, D., Sorokin, A., Ovchinnikov, L. P., Davicioni, E., Triche, T. J., Sorensen, P. H. (2009): Translational activation of snail1 and other developmentally regulated transcription factors by YB-1 promotes an epithelial-mesenchymal transition. *Cancer Cell* 15(5), 402-415.
54. Fattah, F., Lee, E. H., Weisensel, N., Wang, Y., Lichter, N., Hendrickson, E. A. (2010): Ku regulates the non-homologous end joining pathway choice of DNA double-strand break repair in human somatic cells. *PLoS Genet* 6(2), e1000855.
55. Faury, D., Nantel, A., Dunn, S. E., Guiot, M. C., Haque, T., Hauser, P., Garami, M., Bogner, L., Hanzely, Z., Liberski, P. P., Lopez-Aguilar, E., Valera, E. T., Tone, L. G., Carret, A. S., Del Maestro, R. F., Gleave, M., Montes, J. L., Pietsch, T., Albrecht, S., Jabado, N. (2007): Molecular profiling identifies prognostic subgroups of pediatric glioblastoma and shows increased YB-1 expression in tumors. *J Clin Oncol* 25(10), 1196-1208.
56. Favrot, M., Combaret, V. et al. (1991): Expression of P-glycoprotein restricted to normal cells in neuroblastoma biopsies. *Br J Cancer* 64(2), 233-238.
57. Fink, D., Nebel, S., Aebi, S., Zheng, H., Nehme, A., Christen, R. D., Howell, S. B. (1996): The role of DNA mismatch repair in platinum drug resistance. *Cancer Res* 56(21), 4881-4886.
58. Frye, B. C., Halfter, S., Djudjaj, S., Muehlenberg, P., Weber, S., Raffetseder, U., En-Nia, A., Knott, H., Baron, J. M., Dooley, S., Mertens, P. R. (2009): Y-box protein-1 is actively secreted through a non-classical pathway and acts as an extracellular mitogen. *EMBO Rep* 10(7), 783-789.
59. Fujita, T., Ito, K., Izumi, H., Kimura, M., Sano, M., Nakagomi, H., Maeno, K., Hama, Y., Shingu, K., Tsuchiya, S., Kohno, K., Fujimori, M. (2005): Increased nuclear localization of transcription factor Y-box binding protein 1 accompanied by up-regulation of P-glycoprotein in breast cancer pretreated with paclitaxel. *Clin Cancer Res* 11(24 Pt 1), 8837-8844.
60. Fukuda, T., Ashizuka, M., Nakamura, T., Shibahara, K., Maeda, K., Izumi, H., Kohno, K., Kuwano, M., Uchiumi, T. (2004): Characterization of the 5'-untranslated region of YB-1 mRNA and autoregulation of translation by YB-1 protein. *Nucleic Acids Res* 32(2), 611-622.
61. Gadner H., G., Niemeyer C. (2005). *Pädiatrische Hämatologie und Onkologie*, Springer
62. Garand, C., Guay, D., Sereduk, C., Chow, D., Tsofack, S., Langlois, M., Perreault, E., Yin, H., Lebel, M. (2011): An integrative approach to identify YB-1-interacting proteins required for cisplatin resistance in MCF7 and MDA-MB-231 breast cancer cells. *Cancer Sci* 102(7), 1410-1417.
63. Gaudreault, I., Guay, D., (2004): YB-1 promotes strand separation in vitro of duplex DNA containing either mispaired bases or cisplatin modifications, exhibits endonucleolytic activities and binds several DNA repair proteins. *Nucleic Acids Res* 32(1), 316-327.

64. Gimenez-Bonafe, P., Fedoruk, M. N., Whitmore, T. G., Akbari, M., Ralph, J. L., Ettinger, S., Gleave, M. E., Nelson, C. C. (2004): YB-1 is upregulated during prostate cancer tumor progression and increases P-glycoprotein activity. *Prostate* 59(3), 337-349.
65. Gong, W., Jiang, Y., Wang, L., Wei, D., Yao, J., Huang, S., Fang, S., Xie, K. (2005): Expression of autocrine motility factor correlates with the angiogenic phenotype of and poor prognosis for human gastric cancer. *Clin Cancer Res* 11(16), 5778-5783.
66. Goodman, M., Gurney, J.G., Smith, M.A., Olshan, A.F. (1999). Sympathetic nervous system tumors. Cancer Incidence and Survival among Children and Adolescents: United States SEER Program. L. Ries, Smith, MA, Gurney, JG, et al, National Cancer Institute.
67. Graumann, P. and Marahiel, M. A. (1996): A case of convergent evolution of nucleic acid binding modules. *Bioessays* 18(4), 309-315.
68. Guay, D., Evoy, A. A., Paquet, E., Garand, C., Bachvarova, M., Bachvarov, D., Lebel, M (2008): The strand separation and nuclease activities associated with YB-1 are dispensable for cisplatin resistance but overexpression of YB-1 in MCF7 and MDA-MB-231 breast tumor cells generates several chemoresistance signatures. *Int J Biochem Cell Biol* 40(11), 2492-2507.
69. Hämatologie, G. f. P. O. u. (2008): Interdisziplinäre Leitlinie der Deutschen Krebsgesellschaft und der Gesellschaft f. Pädiatrische Onkologie und Hämatologie. A. online. AWMF-Leitlinien-Register Nr. 025/008.
70. Hann, H. W., Evans, A. E., Siegel, S. E., Wong, K. Y., Sather, H., Dalton, A., Hammond, D., Seeger, R. C. (1985): Prognostic importance of serum ferritin in patients with Stages III and IV neuroblastoma: the Childrens Cancer Study Group experience. *Cancer Res* 45(6), 2843-2848.
71. Hayakawa, H., Uchiumi, T., Fukuda, T., Kohno, K., Kuwano, M., Sekiguchi, M. (2002): Binding capacity of human YB-1 protein for RNA containing 8-oxoguanine. *Biochemistry* 41(42), 12739-12744.
72. Herxheimer, G. (1914): Ueber Turmören des Nebennierenmarkes, insbesondere das Neuroblastoma sympaticum. *Beitr Pathol Anat.*, 57:112.
73. Higashi, K., Inagaki, Y., Fujimori, K., Nakao, A., Kaneko, H., and Nakatsuka, I. (2003): Interferon-gamma interferes with transforming growth factor-signaling through direct interaction of YB-1 with Smad3. *J. Biol. Chem.* 278, 43470–43479.
74. Hiyama, E., Hiyama, K., Yokoyama, T., Matsuura, Y., Shay, J. W. (1995): Correlating telomerase activity levels with human neuroblastoma outcomes. *Nat Med* 1(3), 249-255.
75. Ho, R., Eggert, A., Hishiki, T., Minturn, J., Foster, P., Camoratto, A., Evans, A., Brodeur, G. (2002): Resistance to chemotherapy mediated by TrkB in neuroblastomas. *Cancer Res* 62(22), 6462-6466.
76. Hoehner, J. C., Gestblom, C., Hedborg, F., Sandstedt, B., Olsen, L., Pahlman, S. (1996): A developmental model of neuroblastoma: differentiating stroma-poor tumors' progress along an extra-adrenal chromaffin lineage. *Lab Invest* 75(5), 659-675.
77. Homer, C., Knight, D. A., Hananeia, L., Risk, J., Lasham, A., Royds, J. A., Braithwaite, A. W. (2005): Y-box factor YB1 controls p53 apoptotic function. *Oncogene* 24(56), 8314-8325.
78. Ise, T., Nagatani, G., Imamura, T., Kato, K., Takano, H., Nomoto, M., Izumi, H., Ohmori, H., Okamoto, T., Ohga, T., Uchiumi, T., Kuwano, M., Kohno, K. (1999): Transcription factor Y-box binding protein 1 binds preferentially to cisplatin-modified DNA and interacts with proliferating cell nuclear antigen. *Cancer Res* 59(2), 342-346.
79. Izumi, H., Imamura, T., Nagatani, G., Ise, T., Murakami, T., Uramoto, H., Torigoe, T., Ishiguchi, H., Yoshida, Y., Nomoto, M., Okamoto, T., Uchiumi, T., Kuwano, M., Funa, K., Kohno, K. (2001): Y box-binding protein-1 binds preferentially to single-stranded nucleic acids and exhibits 3'>5' exonuclease activity. *Nucleic Acids Res* 29(5), 1200-1207.
80. Izycka-Swieszevska, E., Wozniak, A., Kot, J., Grajkowska, W., Balcerska, A., Perek, D.

- Dembowska-Baginska, B., Klepacka, T., Drozynska, E. (2010): Prognostic significance of HER2 expression in neuroblastic tumors. *Mod Pathol* 23(9), 1261-1268.
81. Jager, E., Stockert, E., Zidianakis, Z., Chen, Y. T., Karbach, J., Jager, D., Arand, M., Ritter, G., Old, L. J., Knuth, A. (1999): Humoral immune responses of cancer patients against "Cancer-Testis" antigen NY-ESO-1: correlation with clinical events. *Int J Cancer* 84(5), 506-510.
 82. Janz, M., Harbeck, N., Dettmar, P., Berger, U., Schmidt, A., Jurchott, K., Schmitt, M., Royer, H. D. (2002): Y-box factor YB-1 predicts drug resistance and patient outcome in breast cancer independent of clinically relevant tumor biologic factors HER2, uPA and PAI-1. *Int J Cancer* 97(3), 278-282.
 83. Jones, P., Inouye, M. (1994): The cold-shock response-a hot topic. *Mol Microbiol* 11(5), 811-818.
 84. Jurchott, K., Bergmann, S., Stein, U., Walther, W., Janz, M., Manni, I., Piaggio, G., Fietze, E., Dietel, M., Royer, H. D. (2003): YB-1 as a cell cycle-regulated transcription factor facilitating cyclin A and cyclin B1 gene expression. *J Biol Chem* 278(30), 27988-27996.
 85. Kamura, T., Yahata, H., Amada, S., Ogawa, S., Sonoda, T., Kobayashi, H., Mitsumoto, M., Kohno, K., Kuwano, M., Nakano, H. (1999): Is nuclear expression of Y box-binding protein-1 a new prognostic factor in ovarian serous adenocarcinoma? *Cancer* 85(11), 2450-2454.
 86. Kaneko, Y., Kanda, N., Maseki, N., Sakurai, M., Tsuchida, Y., Takeda, T., Okabe, I. (1987): Different karyotypic patterns in early and advanced stage neuroblastomas. *Cancer Res* 47(1), 311-318.
 87. Keshelava, N., Seeger, R. C., Reynolds, C. P. (1997): Drug resistance in human neuroblastoma cell lines correlates with clinical therapy. *Eur J Cancer* 33(12), 2002-2006.
 88. Knoepfler, P. S., Cheng, P. F., Eisenman, R. N. (2002): N-myc is essential during neurogenesis for the rapid expansion of progenitor cell populations and the inhibition of neuronal differentiation. *Genes Dev* 16(20), 2699-2712.
 89. Knudson, A. G., Jr. and Strong, L. C. (1972): Mutation and cancer: neuroblastoma and pheochromocytoma. *Am J Hum Genet* 24(5), 514-532.
 90. Kohno, K., Izumi, H., Uchiumi, T., Ashizuka, M., Kuwano, M. (2003): The pleiotropic functions of the Y-box-binding protein, YB-1. *Bioessays* 25(7), 691-698.
 91. Koike, K., Uchiumi, T., Ohga, T., Toh, S., Wada, M., Kohno, K., Kuwano, M. (1997): Nuclear translocation of the Y-box binding protein by ultraviolet irradiation. *FEBS Lett* 417(3), 390-394.
 92. Kotchetkov, R., Cinatl, J., Blaheta, R., Vogel, J. U., Karaskova, J., Squire, J., Hernaiz Driever, P., Klingebiel, T., Cinatl, J., Jr. (2003): Development of resistance to vincristine and doxorubicin in neuroblastoma alters malignant properties and induces additional karyotype changes: a preclinical model. *Int J Cancer* 104(1), 36-43.
 93. Krebsgesellschaft, D. (2010). "Neuroblastom."
 94. Krings, R. (2008): Herstellung monoklonaler Antikörper gegen YB-1 und Charakterisierung ihrer Bindungseigenschaften. Dissertation Med. Fakultät, Hochschule Aachen.
 95. Kudo, S., Mattei, M., Fukuda, M. (1995): Characterization of the gene for dbpA, a family member of the nucleic-acid-binding proteins containing a cold-shock domain. *Eur J Biochem* 231(1), 72-82.
 96. Kunkel, T. A.; Erie, D. A. (2005): DNA mismatch repair. *Annu Rev Biochem* 74, 681-710.
 97. Kuo, L. J., Yang, L. X. (2008): Gamma-H2AX - a novel biomarker for DNA double-strand breaks. *In Vivo* 22(3), 305-309.
 98. Kuwano, M., Oda, Y., Izumi, H., Yang, S. J., Uchiumi, T., Iwamoto, Y., Toi, M., Fujii, T., Yamana, H., Kinoshita, H., Kamura, T., Tsuneyoshi, M., Yasumoto, K., Kohno, K. (2004): The

role of nuclear Y-box binding protein 1 as a global marker in drug resistance. *Mol Cancer Ther* 3(11), 1485-1492.

99. Lasham, A., Moloney, S., Hale, T., Homer, C., Zhang, Y. F., Murison, J. G., Braithwaite, A. W., Watson, J. (2003): The Y-box-binding protein, YB1, is a potential negative regulator of the p53 tumor suppressor. *J Biol Chem* 278(37), 35516-35523.

100. Lee, C., Dhillon, J., Wang, M. Y., Gao, Y., Hu, K., Park, E., Astanehe, A., Hung, M. C., Eirew, P., Dunn, S. E. (2008): Targeting YB-1 in HER-2 overexpressing breast cancer cells induces apoptosis via the mTOR/STAT3 pathway and suppresses tumor growth in mice. *Cancer Res* 68(21), 8661-8666.

101. Levenson, V. V., Davidovich, I. A., Roninson, I. B. (2000): Pleiotropic resistance to DNA-interactive drugs is associated with increased expression of genes involved in DNA replication, repair, and stress response. *Cancer Res* 60(18), 5027-5030.

102. Li, X., Zhang, X. P., Solinger, J. A., Kiiianitsa, K., Yu, X., Egelman, E. H., Heyer, W. D. (2007): Rad51 and Rad54 ATPase activities are both required to modulate Rad51-dsDNA filament dynamics. *Nucleic Acids Res* 35(12), 4124-4140.

103. Lieber, M. R. (2010): The mechanism of double-strand DNA break repair by the nonhomologous DNA end-joining pathway. *Annu Rev Biochem* 79, 181-211.

104. Liedert, B., Pluim, D., Schellens, J., Thomale, J. (2006): Adduct-specific monoclonal antibodies for the measurement of cisplatin-induced DNA lesions in individual cell nuclei; *Nucleic Acids Res.* 2006; 34(6): e47

106. Liu, Y., Prasad, R., Beard, W. A., Hou, E. W., Shock, D. D., Wilson, S. H. (2007): Coordination of steps in single-nucleotide base excision repair mediated by apurinic/apyrimidinic endonuclease 1 and DNA polymerase beta. *J Biol Chem* 282(18), 13532-13541.

107. Lleo, A., Invernizzi, P., Selmi, C., Coppel, R. L., Alpini, G., Podda, M., Mackay, I. R. Gershwin, M. E. (2007): Autophagy: highlighting a novel player in the autoimmunity scenario. *J Autoimmun* 29(2-3), 61-68.

108. Look, A. T., Hayes, F. A., Douglass, E. C., Castleberry, R. P., Bowman, L. C., Smith, E. I., Brodeur, G. M. (1991): Clinical relevance of tumor cell ploidy and N-myc gene amplification in childhood neuroblastoma: a Pediatric Oncology Group study. *J Clin Oncol* 9(4), 581-591.

109. Lu, Z. H., Books, J. T., Ley, T. (2005): YB-1 is important for late-stage embryonic development, optimal cellular stress responses, and the prevention of premature senescence. *Mol Cell Biol* 25(11), 4625-4637.

110. Lutz, M., Wempe, F., Bahr, I., Zopf, D., von Melchner, H. (2006): Proteasomal degradation of the multifunctional regulator YB-1 is mediated by an F-Box protein induced during programmed cell death. *FEBS Lett* 580(16), 3921-3930.

111. Lutz, W., Stohr, M., Schurmann, J., Wenzel, A., Lohr, A., Schwab, M. (1996): Conditional expression of N-myc in human neuroblastoma cells increases expression of alpha-prothymosin and ornithine decarboxylase and accelerates progression into S-phase early after mitogenic stimulation of quiescent cells. *Oncogene* 13(4), 803-812.

112. Mahoney, N. R., Liu, G. T., Menacker, S. J., Wilson, M. C., Hogarty, M. D., Maris, J. M. (2006): Pediatric horner syndrome: etiologies and roles of imaging and urine studies to detect neuroblastoma and other responsible mass lesions. *Am J Ophthalmol* 142(4), 651-659.

113. Marchand, F. (1891): Beitrage zur Kenntniss der normalen und pathologischen Anatomie der Glandula carotica und der Nebennieren. . *Vichows Arch* (5), 578.

114. Marenstein, D. R., Ocampo, M. T., Chan, M. K., Altamirano, A., Basu, A. K., Boorstein, R. J., Cunningham, R. P., Teebor, G. W. (2001): Stimulation of human endonuclease III by Y box-binding protein 1 (DNA-binding protein B). Interaction between a base excision repair enzyme and a transcription factor. *J Biol Chem* 276(24), 21242-21249.

115. Maris, J. M., Matthay, K. K. (1999): Molecular biology of neuroblastoma. *J Clin Oncol* 17(7), 2264-2279.
116. Maris, J. M., Weiss, M. J., Guo, C., Gerbing, R. B., Stram, D. O., White, P. S., Hogarty, M. D., Sulman, E. P., Thompson, P. M., Matthay, K. K., Seeger, R. C., Brodeur, G. M. (2000): Loss of heterozygosity at 1p36 independently predicts for disease progression but not decreased overall survival probability in neuroblastoma patients: a Children's Cancer Group study. *J Clin Oncol* 18(9), 1888-1899.
117. Martin, L. P., Hamilton, T. C., Schilder, R. J. (2008): Platinum resistance: the role of DNA repair pathways. *Clin Cancer Res* 14(5), 1291-1295.
118. Matthay, K. K., Villablanca, J. G., Seeger, R., Stram, D., Harris, R. E., Swift, P., Shimada, H., Black, C., Brodeur, G. M., Reynolds, C. (1999): Treatment of high-risk neuroblastoma with intensive chemotherapy, radiotherapy, autologous bone marrow transplantation, and 13-cis-retinoic acid. Children's Cancer Group. *N Engl J Med* 341(16), 1165-1173.
119. Mertens, P. R., Harendza, S., Pollock, A. S., Lovett, D. H. (1997): Glomerular mesangial cell-specific transactivation of matrix metalloproteinase 2 transcription is mediated by YB-1. *J Biol Chem* 272(36), 22905-22912.
120. Mittal, V. (2004): Improving the efficiency of RNA interference in mammals. *Nat Rev Genet* 5(5), 355-365.
121. Miyazaki, M., Kohno, K., Uchiumi, T., Tanimura, H., Matsuo, K., Nasu, M., Kuwano, M. (1992): Activation of human multidrug resistance-1 gene promoter in response to heat shock stress. *Biochem Biophys Res Commun* 187(2), 677-684.
122. Moley, J. F., Brother, M. B., Wells, S. A., Spengler, B. A., Biedler, J. L., Brodeur, G. M. (1991): Low frequency of ras gene mutations in neuroblastomas, pheochromocytomas, and medullary thyroid cancers. *Cancer Res* 51(6), 1596-1599.
123. Moore, J. K., Haber, J. E. (1996): Cell cycle and genetic requirements of two pathways of nonhomologous end-joining repair of double-strand breaks in *Saccharomyces cerevisiae*. *Mol Cell Biol* 16(5), 2164-2173.
124. Mosmann, T. (1983): Rapid colorimetric assay for cellular growth and survival: application to proliferation and cytotoxicity assays. *J Immunol Methods* 65(1-2), 55-63.
125. Mujoo, K., Cheresch, D. A., Yang, H. M., Reisfeld, R. A. (1987): Disialoganglioside GD2 on human neuroblastoma cells: target antigen for monoclonal antibody-mediated cytotoxicity and suppression of tumor growth. *Cancer Res* 47(4), 1098-1104.
126. Mullis, K. B. and Faloona, F. A. (1987): Specific synthesis of DNA in vitro via a polymerase-catalyzed chain reaction. *Methods Enzymol* 155, 335-350.
127. Nakagawara, A., Arima-Nakagawara, M., Scavarda, N. J., Azar, C. G., Cantor, A. B., Brodeur, G. M. (1993): Association between high levels of expression of the TRK gene and favorable outcome in human neuroblastoma. *N Engl J Med* 328(12), 847-854.
128. Nakagawara, A., Azar, C. G., Scavarda, N. J., Brodeur, G. M. (1994): Expression and function of TRK-B and BDNF in human neuroblastomas. *Mol Cell Biol* 14(1), 759-767.
129. Nakagawara, A., Kadomatsu, K., Sato, S., Kohno, K., Takano, H., Kuwano, M. (1991): Inverse expression of MYCN and mdr-1 in human neuroblastoma. *Prog Clin Biol Res* 366, 11-19.
130. Nakamori, S., Watanabe, H., Kameyama, M., Imaoka, S., Furukawa, H., Ishikawa, O., Sasaki, Y., Kabuto, T., Raz, A. (1994): Expression of autocrine motility factor receptor in colorectal cancer as a predictor for disease recurrence. *Cancer* 74(7), 1855-1862.
131. Neher, T. M., Rechkunova, N. I., Lavrik, O. I., Turchi, J. J. (2010): Photo-cross-linking of XPC-Rad23B to cisplatin-damaged DNA reveals contacts with both strands of the DNA duplex and spans the DNA adduct. *Biochemistry* 49(4), 669-678.

132. Nichols, A. F. and Sancar, A. (1992): Purification of PCNA as a nucleotide excision repair protein. *Nucleic Acids Res* 20(13), 2441-2446.
133. Nickerson, H. J., Matthay, K. K., Seeger, R. C., Brodeur, G. M., Shimada, H., Perez, Atkinson, J. B., Selch, M., Gerbing, R. B., Stram, D. O., Lukens, J. (2000): Favorable biology and outcome of stage IV-S neuroblastoma with supportive care or minimal therapy: a Children's Cancer Group study. *J Clin Oncol* 18(3), 477-486.
134. Niinaka, Y., Paku, S., Haga, A., Watanabe, H., Raz, A. (1998): Expression and secretion of neuroleukin/ phosphohexose isomerase/maturation factor as autocrine motility factor by tumor cells. *Cancer Res* 58(12), 2667-2674.
135. Norbury, C. J. and Hickson, I. D. (2001): Cellular responses to DNA damage. *Annu Rev Pharmacol Toxicol* 41, 367-401.
136. Norris, M. D., Bordow, S. B., Haber, P. S., Marshall, G. M., Kavallaris, M., Madafiglio, J., Cohn, S. L., Hipfner, D. R., Cole, S. P., Deeley, R., Haber, M. (1997): Evidence that the MYCN oncogene regulates MRP gene expression in neuroblastoma. *Eur J Cancer* 33(12), 1911-1916.
137. Norris, M. D., Bordow, S. B., Marshall, G. M., Haber, P. S., Cohn, S. L., Haber, M. (1996): Expression of the gene for multidrug-resistance-associated protein and outcome in patients with neuroblastoma. *N Engl J Med* 334(4), 231-238.
138. Oda, Y., Ohishi, Y., Saito, T., Hinoshita, E., Uchiumi, T., Kinukawa, N., Iwamoto, Y., Kohno, K., Kuwano, M., Tsuneyoshi, M. (2003): Nuclear expression of Y-box-binding protein-1 correlates with P-glycoprotein and topoisomerase II alpha expression, and with poor prognosis in synovial sarcoma. *J Pathol* 199(2), 251-258.
139. Ohga, T., Koike, K., Ono, M., Makino, Y., Itagaki, Y., Tanimoto, M., Kuwano, M., Kohno, K. (1996): Role of the human Y box-binding protein YB-1 in cellular sensitivity to the DNA-damaging agents cisplatin, mitomycin C, and ultraviolet light. *Cancer Res* 56(18), 4224-4228.
140. Ohga, T., Uchiumi, T., Makino, Y., Koike, K., Wada, M., Kuwano, M., Kohno, K. (1998): Direct involvement of the Y-box binding protein YB-1 in genotoxic stress-induced activation of the human multidrug resistance 1 gene. *J Biol Chem* 273(11), 5997-6000.
141. Okamoto, T., Izumi, H., Imamura, T., Takano, H., Ise, T., Uchiumi, T., Kuwano, M., Kohno, K. (2000): Direct interaction of p53 with the Y-box binding protein, YB-1: a mechanism for regulation of human gene expression. *Oncogene* 19(54), 6194-6202.
142. Pauly, M., Ries, F., Dicato, M. (1992): The genetic basis of multidrug resistance. *Pathol Res Pract* 188(6), 804-807.
143. Pflueger, D., Rickman, D. S., Sboner, A., Perner, S., LaFargue, C. J., Svensson, M. A., Moss, B. J., Kitabayashi, N., Pan, Y., de la Taille, A., Kuefer, R., Tewari, A. K., Demichelis, F., Chee, M. S., Gerstein, M. B., Rubin, M. A. (2009): N-myc downstream regulated gene 1 (NDRG1) is fused to ERG in prostate cancer. *Neoplasia* 11(8), 804-811.
144. Plantaz, D., Vandesompele, J., Van Roy, N., Lastowska, M., Bown, N., Combaret, V., Favrot, M. C., Delattre, O., Michon, J., Benard, J., Hartmann, O., Nicholson, J. C., Ross, F. M., Brinkschmidt, C., Laureys, G., Caron, H., Matthay, K. K., Feuerstein, B. G., Speleman, F. (2001): Comparative genomic hybridization (CGH) analysis of stage 4 neuroblastoma reveals high frequency of 11q deletion in tumors lacking MYCN amplification. *Int J Cancer* 91(5), 680-686.
145. Postow, L., Ghenoiu, C., Woo, E. M., Chait, B. T., Funabiki, H. (2008): Ku80 removal from DNA through double strand break-induced ubiquitylation. *J Cell Biol* 182(3), 467-479.
146. Quinn, J. J. and Altman, A. J. (1979): The multiple hematologic manifestations of neuroblastoma. *Am J Pediatr Hematol Oncol* 1(3), 201-205.
147. Rabik, C. A. and Dolan, M. E. (2007): Molecular mechanisms of resistance and toxicity associated with platinating agents. *Cancer Treat Rev* 33(1), 9-23.

148. Raguz, S. and Yague, E. (2008): Resistance to chemotherapy: new treatments and novel insights into an old problem. *Br J Cancer* 99(3), 387-391.
149. Rauen, T., Raffetseder, U., Frye, B. C., Djudjaj, S., Muhlenberg, P. J., Eitner, F., Lendahl, U., Bernhagen, J., Dooley, S., Mertens, P. R. (2009): YB-1 acts as a ligand for Notch-3 receptors and modulates receptor activation. *J Biol Chem* 284(39), 26928-26940.
150. Reed, M., Woelker, B., Wang, P., Wang, Y., Anderson, M. E., Tegtmeier, P. (1995): The C-terminal domain of p53 recognizes DNA damaged by ionizing radiation. *Proc Natl Acad Sci U S A* 92(21), 9455-9459.
151. Rodolfo, M., Luksch, R., Stockert, E., Chen, Y. T., Collini, P., Ranzani, T., Lombardo, C., Dalerba, P., Rivoltini, L., Arienti, F., Fossati-Bellani, F., Old, L. J., Parmiani, G., Castelli, C. (2003): Antigen-specific immunity in neuroblastoma patients: antibody and T-cell recognition of NY-ESO-1 tumor antigen. *Cancer Res* 63(20), 6948-6955.
152. Rogakou, E. P., Pilch, D. R., Orr, A. H., Bonner, W. M. (1998): DNA double-stranded breaks induce histone H2AX phosphorylation on serine 139. *J Biol Chem* 273(10), 5858-5868.
153. Sabath, D. E., Podolin, P. L., Prystowsky, M. B. (1990): cDNA cloning and characterization of interleukin 2-induced genes in a cloned T helper lymphocyte. *J Biol Chem* 265(21), 12671-12678.
154. Sadee, W., Yu, V. C., Richards, M. L., Preis, P. N., Schwab, M. R., Brodsky, F. M., Biedler, J. L. (1987): Expression of neurotransmitter receptors and myc protooncogenes in subclones of a human neuroblastoma cell line. *Cancer Res* 47(19), 5207-5212.
155. Saiki, R. K., Gelfand, D. H., Stoffel, S., Scharf, S. J., Higuchi, R., Horn, G. T., Mullis, K. B., Erlich, H. A. (1988): Primer-directed enzymatic amplification of DNA with a thermostable DNA polymerase. *Science* 239(4839), 487-491.
156. Sambrook J., F. E. F. u. M. T. (1989). *Molecular cloning: A laboratory manual*. 2nd Ed., Cold Spring Harbor Laboratory Press, NY, USA.
157. Sancar, A. (2003): Structure and function of DNA photolyase and cryptochrome blue-light photoreceptors. *Chem Rev* 103(6), 2203-2237.
158. Sassanfar, M., Dosanjh, M. K., Essigmann, J. M., Samson, L. (1991): Relative efficiencies of the bacterial, yeast, and human DNA methyltransferases for the repair of O6-methylguanine and O4-methylthymine. Suggestive evidence for O4-methylthymine repair by eukaryotic methyltransferases. *J Biol Chem* 266(5), 2767-2771.
159. Sawada, T., Kidowaki, T., Sakamoto, I., Hashida, T., Nakagawa, M., Kusunoki, T. (1984): Neuroblastoma. Mass screening for early detection and its prognosis. *Cancer* 53(12), 2731-2735.
160. Schaller M., Burton D., Ditzel H. (2001): Autoantibodies to GPI in rheumatoid arthritis: linkage between an animal model and human disease. *Nat Immunol* 2001, 2, 746-753.
161. Schilling, F. H., Spix, C., Berthold, F., Erttmann, R., Fehse, N., Hero, B., Klein, G., Sander, J., Schwarz, K., Treuner, J., Zorn, U., Michaelis, J. (2002): Neuroblastoma screening at one year of age. *N Engl J Med* 346(14), 1047-1053.
162. Schitteck, B., Psenner, K., Sauer, B., Meier, F., Iftner, T., Garbe, C. (2007): The increased expression of Y box-binding protein 1 in melanoma stimulates proliferation and tumor invasion, antagonizes apoptosis and enhances chemoresistance. *Int J Cancer* 120(10), 2110-2118.
163. Schulte, J. H., Horn, S., Otto, T., Samans, B., Heukamp, L. C., Eilers, U. C., Krause, M., Astrahantseff, K., Klein-Hitpass, L., Buettner, R., Schramm, A., Christiansen, H., Eilers, M., Eggert, A., Berwanger, B. (2008): MYCN regulates oncogenic MicroRNAs in neuroblastoma. *Int J Cancer* 122(3), 699-704.
164. Schwab, M., Alitalo, K., Klempnauer, K. H., Bishop, J., Gilbert, F., Brodeur, G., Goldstein, M., Trent, J. (1983): Amplified DNA with limited homology to myc cellular oncogene is shared by human neuroblastoma cell lines and a neuroblastoma tumour. *Nature* 305(5931), 245-248.

165. Sedletska, Y., Fourrier, L., Malinge, J. M. (2007): Modulation of MutS ATP-dependent functional activities by DNA containing a cisplatin compound lesion (base damage and mismatch). *J Mol Biol* 369(1), 27-40.
166. Seeger, R. C., Brodeur, G. M., Sather, H., Dalton, A., Siegel, S. E., Wong, K. Y., Hammond, D. (1985): Association of multiple copies of the N-myc oncogene with rapid progression of neuroblastomas. *N Engl J Med* 313(18), 1111-1116.
167. Seeger, R. C., Rayner, S. A., Banerjee, A., Chung, H., Laug, W. E., Neustein, H. B., Benedict, W. F. (1977): Morphology, growth, chromosomal pattern and fibrinolytic activity of two new human neuroblastoma cell lines. *Cancer Res* 37(5), 1364-1371.
168. Shibahara, K., Sugio, K., Osaki, T., Uchiumi, T., Kohno, K., Yasumoto, K., Sugimachi, K., Kuwano, M. (2001): Nuclear expression of the Y-box binding protein, YB-1, as a novel marker of disease progression in non-small cell lung cancer. *Clin Cancer Res* 7(10), 3151-3155.
169. Shibahara, K., Uchiumi, T., Fukuda, T., Kura, S., Tominaga, Y., Maehara, Y., Kohno, K., Nakabeppu, Y., Tsuzuki, T., Kuwano, M. (2004): Targeted disruption of one allele of the Y-box binding protein-1 (YB-1) gene in mouse embryonic stem cells and increased sensitivity to cisplatin and mitomycin C. *Cancer Sci* 95(4), 348-353.
170. Shibao, K., Takano, H., Nakayama, Y., Okazaki, K., Nagata, N., Izumi, H., Uchiumi, T., Kuwano, M., Kohno, K., Itoh, H (1999): Enhanced coexpression of YB-1 and DNA topoisomerase II alpha genes in human colorectal carcinomas. *Int J Cancer* 83(6), 732-737.
171. Shimada, H., Ambros, I. M., Dehner, L. P., Hata, J., Joshi, V., Roald, B., Stram, D. O., Gerbing, R. B., Lukens, J. N., Matthay, K. K., Castleberry, R. P. (1999): The International Neuroblastoma Pathology Classification (the Shimada system). *Cancer* 86(2), 364-372.
172. Shimada, H., Chatten, J., Sachs, N., Chiba, T., Misugi, K (1984): Histopathologic prognostic factors in neuroblastic tumors: definition of subtypes of ganglioneuroblastoma and an age-linked classification of neuroblastomas. *J Natl Cancer Inst* 73(2), 405-416.
173. Shimodaira, H., Yoshioka-Yamashita, A., Kolodner, R. D., Wang, J. Y. (2003): Interaction of mismatch repair protein PMS2 and the p53-related transcription factor p73 in apoptosis response to cisplatin. *Proc Natl Acad Sci U S A* 100(5), 2420-2425.
174. Shintani, T. and Klionsky, D. J. (2004): Autophagy in health and disease: a double-edged sword. *Science* 306(5698), 990-995.
175. Shiota, M., Izumi, H., Tanimoto, A., Takahashi, M., Miyamoto, N., Kashiwagi, E., Kidani, A., Hirano, G., Masubuchi, D., Fukunaka, Y., Naito, S., Nishizawa, S., Sasaguri, Y., Kohno, K. (2009): Programmed cell death protein 4 down-regulates Y-box binding protein-1 expression via a direct interaction with Twist1 to suppress cancer cell growth. *Cancer Res* 69(7), 3148-3156.
176. Sorokin, A. V., Selyutina, A. A., Skabkin, M. A., Guryanov, S. G., Nazimov, I. V., Richard, C., Th'ng, J., Yau, J., Sorensen, P. H., Evdokimova, V. (2005): Proteasome-mediated cleavage of the Y-box-binding protein 1 is linked to DNA-damage stress response. *EMBO J* 24(20), 3602-3612.
177. Stein, U., Jurchott, K., Walther, W., Bergmann, S., Schlag, P. M., Royer, H. D. (2001): Hyperthermia- induced nuclear translocation of transcription factor YB-1 leads to enhanced expression of multidrug resistance-related ABC transporters. *J Biol Chem* 276(30), 28562-28569.
178. Stenina, O. I., Poptic, E. J., DiCorleto, P. E. (2000): Thrombin activates a Y box-binding protein (DNA-binding protein B) in endothelial cells. *J Clin Invest* 106(4), 579-587.
179. Sun, Y. J., Chou, C. C., Chen, W. S., Wu, R. T., Meng, M., Hsiao, C. D. (1999): The crystal structure of a multifunctional protein: phosphoglucose isomerase/autocrine motility factor/neuroleukin. *Proc Natl Acad Sci U S A* 96(10), 5412-5417.
180. Sutherland, B. W., Kucab, J., Wu, J., Lee, C., Cheang, M. C., Yorida, E., Turbin, D., Dedhar, S., Nelson, C., Miller, K., Badve, S., Huntsman, D., Blake-Gilks, C., Chen, M., Pallen, C.

- J., Dunn, S. E. (2005): Akt phosphorylates the Y-box binding protein 1 at Ser102 located in the cold shock domain and affects the anchorage-independent growth of breast cancer cells. *Oncogene* 24(26), 4281-4292.
181. Suzuki, K. and Matsubara, H. (2011): Recent advances in p53 research and cancer treatment. *J Biomed Biotechnol* 2011, 978312.
182. Swamynathan, S. K., Nambiar, A., Guntaka, R. V. (1998): Role of single-stranded DNA regions and Y-box proteins in transcriptional regulation of viral and cellular genes. *FASEB J* 12(7), 515-522.
183. Takahashi, M., Shimajiri, S., Izumi, H., Hirano, G., Kashiwagi, E., Yasuniwa, Y., Wu, Y., Han, B., Akiyama, M., Nishizawa, S., Sasaguri, Y., Kohno, K. (2010): Y-box binding protein-1 is a novel molecular target for tumor vessels. *Cancer Sci* 101(6), 1367-1373.
184. Taparowsky, E., Shimizu, K., Goldfarb, M., Wigler, M. (1983): Structure and activation of the human N-ras gene. *Cell* 34(2), 581-586.
185. Tekur, S., Pawlak, A., Guellaen, G., Hecht, N. (1999): Contrin, the human homologue of a germ-cell Y-box-binding protein: cloning, expression, and chromosomal localization. *J Androl* 20(1), 135-144.
186. To, K., Fotovati, A., Reipas, K. M., Law, J. H., Hu, K., Wang, J., Astanehe, A., Davies, A. H., Lee, L., Stratford, A. L., Raouf, A., Johnson, P., Berquin, I. M., Royer, H. D., Eaves, C. J., Dunn, S. E. (2010): Y-box binding protein-1 induces the expression of CD44 and CD49f leading to enhanced self-renewal, mammosphere growth, and drug resistance. *Cancer Res* 70(7), 2840-2851.
187. Toh, S., Nakamura, T., Ohga, T., Koike, K., Uchiumi, T., Wada, M., Kuwano, M., Kohno, K. (1998): Genomic organization of the human Y-box protein (YB-1) gene. *Gene* 206(1), 93-97.
188. Torimura, T., Ueno, T., Kin, M., Harada, R., Nakamura, T., Harada, M., Watanabe, H., Avraham, R., Sata, M. (2001): Autocrine motility factor enhances hepatoma cell invasion across the basement membrane through activation of beta1 integrins. *Hepatology* 34(1), 62-71.
189. Toulany, M., Schickfluss, T. A., Eicheler, W., Kehlbach, R., Schitteck, B., Rodemann, H. P. (2011): Impact of oncogenic K-RAS on YB-1 phosphorylation induced by ionizing radiation. *Breast Cancer Res* 13(2), R28.
190. Tumilowicz, J. J., Nichols, W. W., Cholon, J. J., Greene, A. E. (1970): Definition of a continuous human cell line derived from neuroblastoma. *Cancer Res* 30(8), 2110-2118.
191. Tweddle, D., Malcolm, A., Pearson, A., Lunec, J. (2001): Evidence for the development of p53 mutations after cytotoxic therapy in a neuroblastoma cell line. *Cancer Res* 61(1), 8-13.
192. Uchiumi, T., Fotovati, A., Sasaguri, T., Shibahara, K., Shimada, T., Fukuda, T., Nakamura, T., Izumi, H., Kuwano, M., Kohno, K. (2006): YB-1 is important for an early stage embryonic development: neural tube formation and cell proliferation. *J Biol Chem* 281(52), 40440-40449.
193. Uchiumi, T., Kohno, K., Tanimura, H., Matsuo, K., Sato, S., Uchida, Y., Kuwano, M. (1993): Enhanced expression of the human multidrug resistance 1 gene in response to UV light irradiation. *Cell Growth Differ* 4(3), 147-157.
194. Valsesia-Wittmann, S., Magdeleine, M., Dupasquier, S., Garin, E., Jallas, A. C., Combaret, V., Krause, A., Leissner, P., Puisieux, A. (2004): Oncogenic cooperation between H-Twist and N-Myc overrides failsafe programs in cancer cells. *Cancer Cell* 6(6), 625-630.
195. Virchow, R. (1864-65). Hyperplasie der Zirbel und der Nebennieren. Hyperplasie der Zirbel und der Nebennieren. In: *Die Krankhaften Geschwulste*. Vol 2.
196. Wachowiak, R., Thielges, S., Rawnaq, T., Kaifi, J. T., Fiegel, H., Metzger, R., Quaas, A., Mertens, P. R., Till, H., Izbicki, J. R. (2010): Y-box-binding protein-1 is a potential novel tumour marker for neuroblastoma. *Anticancer Res* 30(4), 1239-1242.
197. Wargalla-Plate, U., Hero, B., Berthold, F. (1995): Neuroblastoma: diagnosis and therapy. *Praxis (Bern 1994)* 84(41), 1152-1157.

198. Watanabe, H., Takehana, K., Date, M., Raz, A. (1996): Tumor cell autocrine motility factor is the neuroleukin/phosphohexose isomerase polypeptide. *Cancer Res* 56(13), 2960-2963.
199. Weiss, W. A., Aldape, K., Mohapatra, G., Feuerstein, B. G., Bishop, J. M. (1997): Targeted expression of MYCN causes neuroblastoma in transgenic mice. *EMBO J* 16(11), 2985-2995.
200. Westermann, F., Muth, D., Benner, A., Bauer, T., Henrich, K. O., Oberthuer, A., Brors, B., Beissbarth, T., Vandesompele, J., Pattyn, F., Hero, B., Konig, R., Fischer, M., Schwab, M. (2008): Distinct transcriptional MYCN/c-MYC activities are associated with spontaneous regression or malignant progression in neuroblastomas. *Genome Biol* 9(10), R150.
201. Wolffe, A. P. (1994): Structural and functional properties of the evolutionarily ancient Y-box family of nucleic acid binding proteins. *Bioessays* 16(4), 245-251.
202. Woods, W. G., Gao, R. N., Shuster, J. J., Robison, L. L., Bernstein, M., Weitzman, S., Bunin, G., Levy, I., Brossard, J., Dougherty, G., Tuchman, M., Lemieux, B. (2002): Screening of infants and mortality due to neuroblastoma. *N Engl J Med* 346(14), 1041-1046.
203. Wu, J., Lee, C., Yokom, D., Jiang, H., Cheang, M. C., Yorida, E., Turbin, D., Berquin, I. M., Mertens, P. R., Iftner, T., Gilks, C. B., Dunn, S. E. (2006): Disruption of the Y-box binding protein-1 results in suppression of the epidermal growth factor receptor and HER-2. *Cancer Res* 66(9), 4872-4879.
204. Wu, J., Stratford, A. L., Astanehe, A., Dunn, S. E. (2007): YB-1 is a Transcription/Translation Factor that Orchestrates the Oncogenome by Hardwiring Signal Transduction to Gene Expression. *Translational Oncogenomics* 2007:2 49-65
205. Xu, W., Zhou, L., Qin, R., Tang, H., Shen, H. (2009): Nuclear expression of YB-1 in diffuse large B-cell lymphoma: correlation with disease activity and patient outcome. *Eur J Haematol* 83(4), 313-319.
206. Yanagawa, T., Funasaka, T., Tsutsumi, S., Raz, T., Tanaka, N., Raz, A. (2005): Differential regulation of phosphoglucose isomerase/autocrine motility factor activities by protein kinase CK2 phosphorylation. *J Biol Chem* 280(11), 10419-10426.
207. Yanagawa, T., Funasaka, T., Watanabe, H., Raz, A. (2004): Novel roles of the autocrine motility factor/phosphoglucose isomerase in tumor malignancy. *Endocr Relat Cancer* 11(4), 749-759.
208. Yang, W. H. and Bloch, D. B. (2007): Probing the mRNA processing body using protein macroarrays and "autoantigenomics". *RNA* 13(5), 704-712.
209. Zeltzer, P., Marangos, P., Evans, A., Schneider, S. L. (1986): Serum neuron-specific enolase in children with neuroblastoma. Relationship to stage and disease course. *Cancer* 57(6), 1230-1234.
210. Zhang, J. Y., Tan, E. M. (2010): Autoantibodies to tumor-associated antigens as diagnostic biomarkers in hepatocellular carcinoma and other solid tumors. *Expert Rev Mol Diagn* 10(3), 321-328.
211. Zhang, Y. F., Homer, C., Edwards, S. J., Lasham, A., Royds, J., Sheard, P., Braithwaite, A. W. (2003): Nuclear localization of Y-box factor YB1 requires wild-type p53. *Oncogene* 22(18), 2782-2794.
212. Zhu, Q. and Center, M. S. (1994): Cloning and sequence analysis of the promoter region of the MRP gene of HL60 cells isolated for resistance to adriamycin. *Cancer Res* 54(16), 4488-4492.

8 APPENDIX

8.1 LIST OF ABBREVIATIONS

%	percentage
°C	degree celsius
bp	base pairs
BSA	bovine serum albumine
cDNA	complementary DNA
CpG	cytosine-phosphatidyl-guanosine dinukleotide
ddH ₂ O	double distilled water
dil.	diluted
DMSO	dimethylsulfoxide
DNA	deoxyribonucleic acid
dNTP	deoxyribonucleoside triphosphate
DTT	dithiothreitol
EDTA	ethylenediaminetetraacetic acid
ELISA	Enzyme-linked immunosorbent assay
et al.	and others
FCS	fetal calf serum
Fig.	figure
FITC	fluorescein isothiocyanate
g	gravity
h	hour
Ig	Immunoglobuline
Kb	kilo bases
kDa	kilo dalton
MRI	magnetic resonance imaging
NB	neuroblastoma
ng	nanogramm
PAA	polyacylamide
PBS	phosphate buffered saline
PCR	polymerase chain reaction
RNA	ribonucleic acid
RNase	ribonuclease
RNP	ribonucleoprotein particle
RT	room temperature
SDS	sodium dodecyl sulfate
siRNA	small interfering RNA
Tab.	table
TAE	tris-Acetate-EDTA-buffer
Taq Polymerase	Thermophilus aquaticus Polymerase
Tris	tris(hydroxymethyl)-aminomethane
µg	mikrogramm

8.2 LIST OF FIGURES

Fig. 1:	Hypothetical model of the genetic origin of neuroblastoma
Fig. 2:	INRG Consensus Pretreatment Classification schema
Fig. 3:	Schematic representation of the structure of Y-box binding proteins
Fig. 4:	Schematic diagram of the functional domains of YB-1
Fig. 5:	The fetal brain protein array used for the detection of autoantibodies
Fig. 6:	Graphical breakdown of the 20 most significant targets of autoantibodies detected
Fig. 7:	GPI protein in conditioned media from cell lines
Fig. 8:	Conditioned medium from NGP cells
Fig. 9:	Whole-cell extracts of NB cell lines
Fig. 10:	Reverse ELISA detection of serum with spiked-in murine YB-1 antibody
Fig. 11:	Example of one gel used to determine total protein concentration of patient sera
Fig. 12:	Reverse ELISA detection of YB-1 antibody in pooled serum from NB patients
Fig. 13:	YB-1 antibody concentrations in individual serum samples
Fig. 14:	YB-1 antibody concentrations in serum from groups of NB patients and controls
Fig. 15:	Extracellular amounts of YB-1 protein
Fig. 16:	YB-1 protein expression in TrkA-overexpressing NB cell culture models
Fig. 17:	Semi-quantitative RT-PCR showing mRNA expression levels of <i>YB-1</i> and <i>ODC1</i>
Fig. 18:	Tetracycline-mediated repression of <i>MYCN</i> expression in Tet-21/N cells
Fig. 19:	Both <i>MYCN</i> and c-MYC proteins bind to the <i>YB-1</i> promoter in NB cell lines
Fig. 20:	Efficiency of siRNA-mediated knockdown of YB-1 expression
Fig. 21:	YB-1 downregulation reduces cell viability in SK-N-BE cells
Fig. 22:	YB-1 downregulation increases DSBs in SK-N-BE cells
Fig. 23:	Quantification of DNA adducts
Fig. 24:	Intracellular distribution of YB-1 protein in the absence and presence of cisplatin
Fig. 25:	Cisplatin treatment increased YB-1 protein expression in SK-N-BE cells
Fig. 26:	Co-IP shows binding of YB-1 to the repair protein Ku80
Fig. 27:	Co-IP shows binding of YB-1 to the repair proteins Ku80, XPC and Rad51
Fig. 28:	<i>MYCN</i> and c-MYC proteins bind to the <i>YB-1</i> promoter in the IMR5 NB cell line
Fig. 29:	<i>MYCN</i> and c-MYC proteins bind to the <i>YB-1</i> promoter in the SH-EP NB cell line
Fig. 30:	<i>MYCN</i> and c-MYC proteins bind the <i>YB-1</i> promoter in the SH-SY5Y NB cell line
Fig. 31:	<i>MYCN</i> and c-MYC proteins bind to <i>YB-1</i> promoter in the WAC2 NB cell line

8.3 LIST OF TABLES

Tab. 1:	General chemicals
Tab. 2:	Chemicals for western blotting, ELISA and Co-IP
Tab. 3:	Chemicals for cell culture
Tab. 4:	Chemicals for PCR
Tab. 5:	Primary Antibodies
Tab. 6:	Secondary Antibodies
Tab. 7:	General plasticware
Tab. 8:	Plasticware for cell culture
Tab. 9:	Technical Equipment
Tab. 10:	Cell lines used in this dissertation
Tab. 11:	Antibodies and corresponding dilutions used in this dissertation project
Table 12:	Autoantibody target proteins selected for further investigation

8.4 SUPPLEMENTARY DATA FOR BINDING ANALYSIS

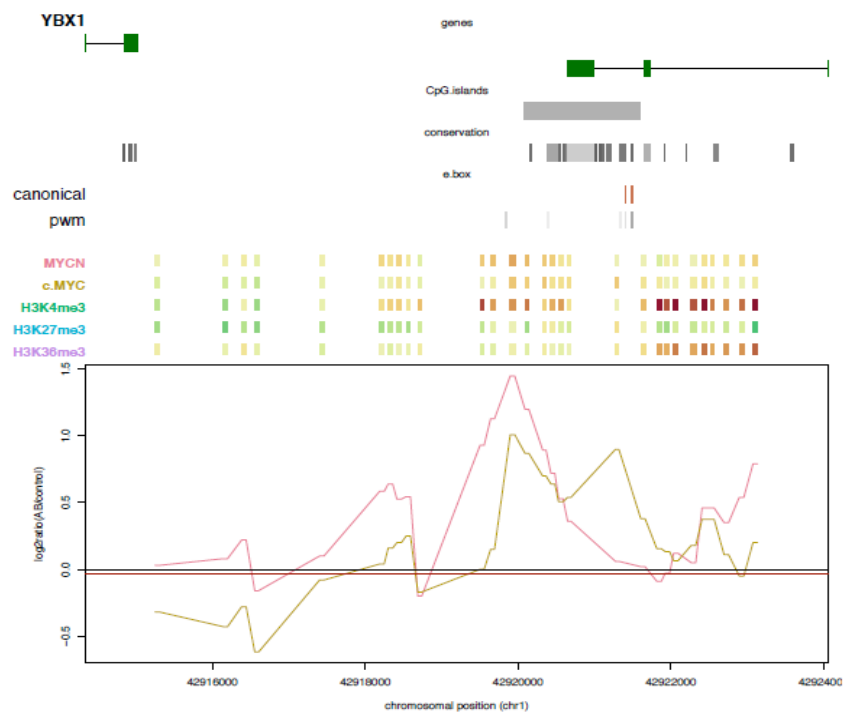


Fig. 28: Both MYCN and c-MYC proteins bind to the *YB-1* promoter in the IMR5 NB cell line. Binding was analyzed using ChIP-chip technology, and included histone marks for active transcription (H3K4me3), transcript elongation (H3K36me3) and transcriptional repression (H3K27me3). Binding strength is shown in a color scale ranging from green tones (no binding) to red tones (strong binding).

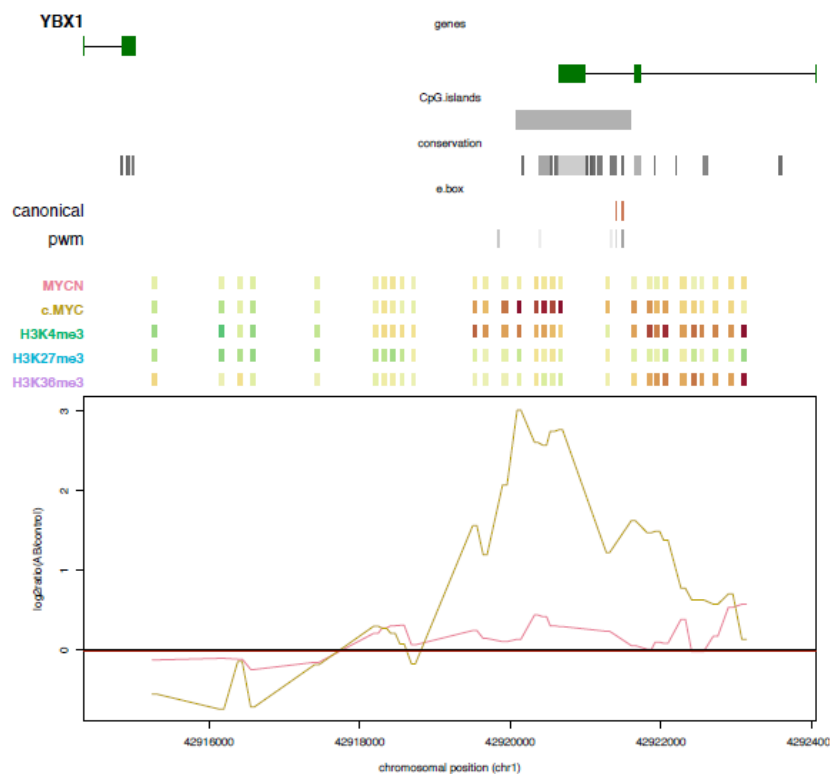


Fig. 29: Both MYCN and c-MYC proteins bind to the *YB-1* promoter in the SH-EP NB cell line. Binding was analyzed as described above.

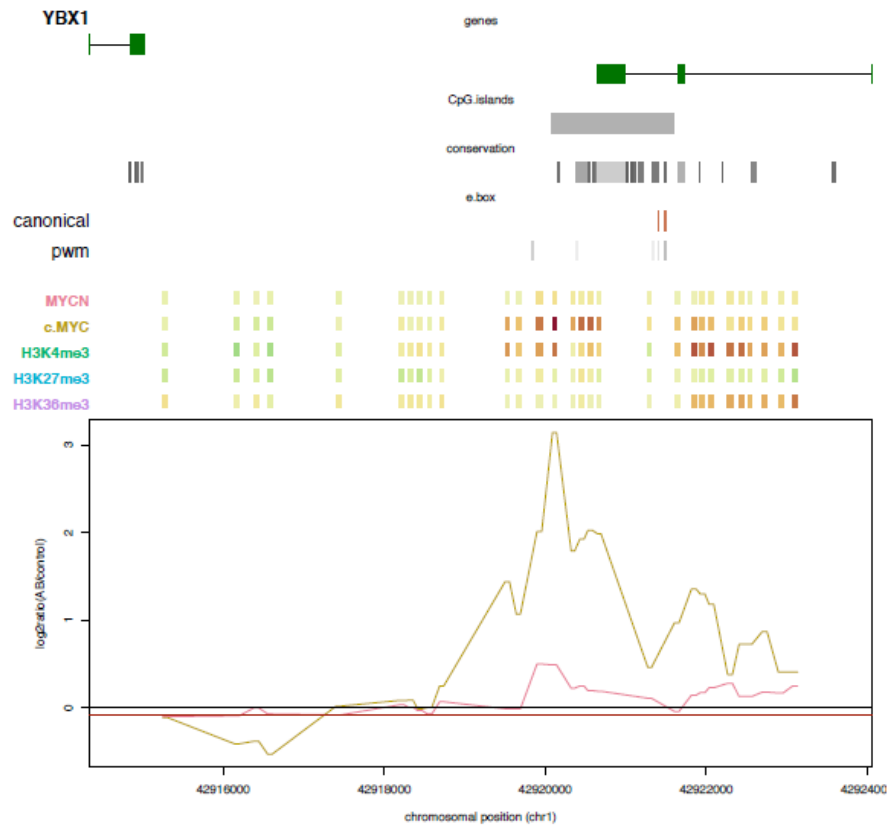


Fig. 30: Both MYCN and c-MYC proteins bind to the *YB-1* promoter in the SH-SY5Y NB cell line. Binding was analyzed as described above.

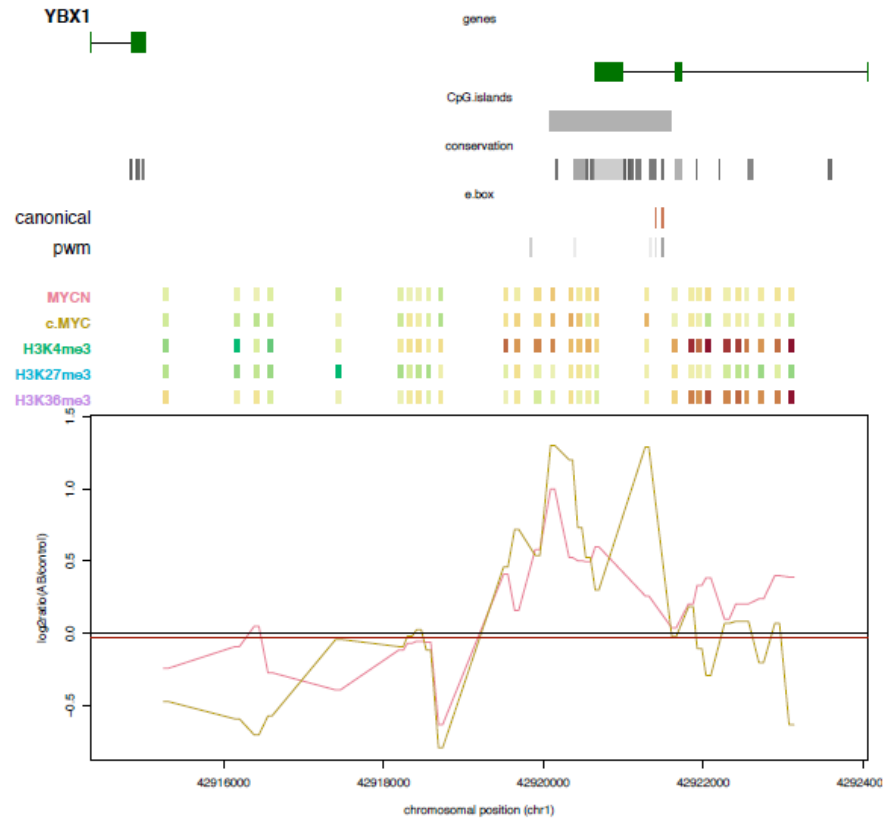


Fig. 31: Both MYCN and c-MYC proteins bind to the *YB-1* promoter in the WAC2 NB cell line. Binding was analyzed as described above.

9 ACKNOWLEDGEMENTS

Es war ein langer, aber zumeist sehr schöner Weg bis zur Fertigstellung dieser Arbeit und es gibt viele Personen, denen ich dafür danken möchte, dass sie mich auf diesem Weg begleitet haben. Durch sie wurden diese Jahre zu einem besonderen Erlebnis, an das ich immer gern zurückdenken werde.

Zunächst möchte ich Frau Prof. Dr. Angelika Eggert für die Möglichkeit danken, diese Arbeit in ihrem Labor anfertigen zu dürfen. Ihre guten Ideen waren immer sehr willkommen und sie gibt jungen Wissenschaftlern die Möglichkeit sich im Labor und auf Kongressen auszuprobieren und so ihren Weg zu finden. Sie hat es in einzigartiger Weise geschafft, ein wunderbares und buntes Team um sich herum aufzubauen, dem es weder an wissenschaftlichem Forscherdrang noch an Lebensfreude mangelt.

Ebenfalls danken möchte ich Frau Dr. Kathy Astrahantseff, die mich mit viel Geduld, Spaß an der Arbeit, kleinen Stößen in die richtige Richtung und dem ein oder anderen Glas Rotwein sehr unterstützt hat. Ich hätte mir keine bessere Betreuung wünschen können.

Ich möchte auch allen anderen Mitarbeitern des Onkolabors danken, die immer für eine lebendige und angenehme Stimmung gesorgt haben und nicht nur in wissenschaftlichen Fragen immer die richtige Antwort fanden. Da ich mich hier auf eine Seite beschränken muss, bleibt es leider bei einer kurzen Nennung. Trotzdem hoffe ich, ihr fühlt euch alle angesprochen. Danke an Alex, Harald, Ellen, die Andreas, Anjas und Steffis, Johannes, Melanie, Sabine, Gabi und alle Anderen. Besonders hervorheben möchte ich Frau Dr. Kuhfittig-Kulle, die mir bei der Planung und Durchführung der Untersuchungen zu Reparaturmechanismen sehr geholfen hat und auch sonst stets ein offenes Ohr für meine Fragen hatte.

Nicht zu vergessen sind auch die Mitglieder der Arbeitsgruppen der E.E.T.-Pipeline, denen ich viele schöne Kongresse und eine gute Zusammenarbeit verdanke. Vor allem wäre da die AG Frank Westermann für ihre Zusammenarbeit bei den Promotorbindungsanalysen hervorzuheben.

Ein ganz herzliches Dankschön gilt meinen Eltern. Sie haben mir dies alles ermöglicht und, auch wenn ihnen mein Weg nicht immer ganz gradlinig vorgekommen sein mag, haben sie mich dennoch begleitet und immer unterstützt. Ihr seid die Besten!

Zuletzt möchte ich noch einem ganz besonderen Menschen in meinem Leben danken. Rhett war immer für mich da und, obwohl er auch gelegentlich den Frust des Forschens abfangen musste, hat er mir stets geholfen, das Positive zu sehen und wird dies hoffentlich auch in Zukunft weiter tun.

10 CURRICULUM VITAE

Der Lebenslauf ist in der Online-Version aus Gründen des Datenschutzes nicht enthalten